PHOTOACTIVE MOLECULAR PROBES FOR PROTEIN KINASES: DEVELOPMENT OF SELECTIVE PHOTOLIGANDS FOR LYMPOCYTE SPECIFIC KINASE (LCK)

by

SAGIT HINDI

A dissertation submitted to the Graduate Faculty in Chemistry in partial fulfillment of the requirements for the degree of Doctor of Philosophy in the City University of New York

2007

UMI Number: 3284487

ProQuest Information and Learning Company
300 North Zeeb Road
P.O. Box 1346
Ann Arbor, MI 48106-1346

This manuscript has been read and accepted for the Graduate Faculty in Chemistry in satisfaction of the dissertation requirement for the degree of Doctor of Philosophy.

Dr. Akira Kawamura

Date — Chair of Examining Committee

Dr. Gerald Koeppl

Date — Executive Officer

Dr. David R. Mootoo

Dr. Fred Naider

Dr. Klaus Grohmann

Dr. Koji Nakanishi
Supervisory Committee

THE CITY UNIVERSITY OF NEW YORK

Abstract

Photoactive Molecular Probes for Protein Kinases:

Development of Selective Photoligands for Lymphocyte Specific Kinase

by

Sagit Hindi

Advisor: Dr. Akira Kawamura

This thesis describes the development of a chemical approach for selective labeling of protein kinases, regardless of their chemical reactivities, using photoactive molecular probes. Selectivity toward target proteins was attained based on the well-known fact that two modest-affinity ligands, when tethered through an appropriate linker, can make a bidentate ligand with high affinity and selectivity. Our probes were designed as bidentate ligands containing adenine, which targets the catalytic site of protein kinases, and benzophenone, which targets hydrophobic pockets in the vicinity of the catalytic site. In addition to its role as a recognition unit, benzophenone serves as a photocrosslinker to covalently label target proteins. Binding selectivity studies revealed that our probes, despite their simple structure, selectively tag certain proteins out of crude protein mixtures. In addition, it was shown that probe's selectivity can be modulated via modifications of the probe's chirality as well as the distance between adenine and benzophenone.

Our methodology was successfully employed for the development of a library of photoactive probes for selective tagging of Src-family of kinases. During this study, we

identified a selective photoactive probe for Lck, a Src-family kinase involved in lymphocyte proliferation and differentiation. This probe exhibited selectivity toward Lck both in a mixture of commercial kinases and in lysate from Jurkat cells, and was shown to interact with Lck through both its adenine and benzophenone units. Structural motifs crucial for the recognition by Lck were identified as the chirality of the probe's peptidic backbone as well as the distance between adenine and benzophenone and their locations within the probe. The probe-Lck complex was characterized by a series of photolabeling and mass spectrometric analyses, which showed that the benzophenone covalently binds to Leu384 residue located near the catalytic site of Lck. A structural model of probe-Lck complex was subsequently obtained and utilized for structure-affinity relationship studies. These studies resulted in improved labeling of Lck and revealed the importance of linker flexibility for efficient labeling by our probe. Further studies are required to fully characterize the affinity and selectivity of our probes and understand the recognition process in probe-Lck complex.

To My Precious Daughter,

Jordan Eden Jacoel,

Wishing you a lifetime of joy and happiness.

Acknowledgements

I would like to thank my mentor, Dr. Akira Kawamura, for his guidance and assistance during my doctoral studies and throughout the process of writing my thesis. He taught me how to work as an independent researcher and was steady source of wise encouragement and support.

I am also grateful to Dr. Klaus Grohmann, Dr. David Mootoo, Dr. Fred Naider, and Dr. Koji Nakanishi for serving on my doctoral committee. I am very grateful to them for meeting with me annually and providing me with valuable advice and suggestions given their individual areas of expertise. In particularly I would like to thank Dr. Fred Naider who spent many hours reviewing my dissertation. Dr. Klaus Grohmann not only served on my doctoral committee, but also granted me with valuable professional and personal advice.

I would like to thank my colleagues and friends at the Chemistry Department at Hunter College for turning my journey through graduate school into a pleasure. Special thanks go to Tal and Sagit Hasson for their kind friendship and support throughout this challenge. Additional thanks go to Stephanie Wolf for her help with proof reading my thesis and to Doina Mihai, James Laurence, Olga Aminova, and Cha Kwang Won for their help with my research project.

I also wish to express my warmest thanks to my parents in law, Lea and Richard Jacoel, for their support and appreciation for my studies. I am sincerely thankful to my mother in law for her valuable assistance during the last year of my Ph.D.

A debt of gratitude goes to my wonderful family in Israel, my parents Sara and Yair, my brother Gil, and my sisters, Vered and Mor. They have been by my side, with their unconditional love and support, throughout my entire life. Most of all, my mother deserves a lifetime of gratitude for her tremendous help and encouragement during my doctoral studies.

Finally, and most importantly, I am deeply grateful to my husband, David Jacque Jacoel, for sharing his life with me throughout the second half of my studies. David spiced up my life with his amazing personality and was a great source of fun, encouragement, and support. David, you are truly one of a kind, being handsome, smart, funny, a good cook, and a great father to Jordan. I love you and I wish you a full and fast recovery.

"There will come a time when you believe everything is finished.
That will be the beginning."
Louis L'Amour

Table of contents

List of Figures

List of Schemes and Tables

List of Abbreviations

Å	angstrom
ABP	adenine binding protein
Ac	acetyl
AEG	*N*-(2-aminoethylglycyl)
AMBER	assisted model building and energy refinement
ATP	adenosine triphosphate
Bhoc	benzhydryloxycarbonyl
Bn	benzyl
Boc	*tert*-butyloxycarbonyl
Bpa	*p*-benzoyl-phenylalanine
C	carbon
CD4	cluster of differentiation 4
CD8	cluster of differentiation 8
Cbz	carbobenzyloxy
COSY	correlation spectroscopy
DCC	*N*,*N*'-dicyclohexylcarbodimide
DCM	dichloromethane
DCU	dicyclohexylurea
DEPC	3,3-dimethylethylaminopropylcarbiimide
DMF	dimethylsulfoxide
DTT	dithiothreitol

ECL	enhanced chemiluminescence
ESI	electrospray ionization
Fmoc	9-fluorenylmethoxycarbonyl
H	proton
HOBT	1-hydroxybenzotriazole
H_2O	water
HPLC	high performance liquid chromatography
HRP	horseradish peroxidase
HSQC	heteronuclear multiple quantum correlation
K_{PAL}	photoaffinity labeling constant
LC	liquid chromatography
min	minutes
M^+	molecular ion
M	multiplet
MALDI-TOF	matrix assisted laser desorption ionization time-of-flight
MDR-MB-231	MDR-MB-231 breast cancer cell line
MeOH	methanol
MMFF94	Merck molecular force field 94
MHz	megahertz
mL	milliliter
mm	millimeter
MOE	molecular operating environment
MS	mass spectroscopy

NMR	nuclear magnetic resonance
PLG	photoaffinity-labeling group
PNA	peptide nucleic acid
PDVF	polyvinylidene fluoride
RP-HPLC	reversed phase high performance liquid chromatography
SDS-PAGE	sodium dodecyl sulfate polyacrylamide gel electrophoresis
SH2	Src homology domain 2
SH3	Src homology domain 3
SFK	Src family of kinases
SK-N-SH NB	SK-N-SH neuroblastoma cell line
TBS	tris buffered saline
TCR	T-cell receptor
TBS-T	tris buffered saline with 1% tween 20
TFA	trifluoroacetic acid
TIS	triisopropylsilane
TLC	thin layer chromatography
UV	ultraviolet spectroscopy

Chapter I

Introduction:

Chemical Proteomics and Research Outlook

I.1. Proteomics Research

The completion of the human genome project has created much excitement due to the likely impact that this information might have on the process of drug discovery and development. However, proteins, rather than genes, are ultimately responsible for most biological processes occurring inside the cell.[1] By studying the whole array of proteins in a cell, tissue, or organism we can significantly improve our understanding of disease processes and identify proteins that are potential targets for therapeutics.[2,3] Thus, the study of proteins is considered the next step, after genomics, in the understanding of biological systems. Proteomics is the large-scale study of cellular proteins, and its major goal is to identify, characterize, and assign biological functions to all proteins expressed by the genome.[4,5]

One of the major challenges of proteomics research comes from the heterogeneity of cellular proteins.[4,6-8] Each gene can produce multiple proteins through alternative post transcriptional and post translational modifications. Thus, the actual number of proteins far exceeds the estimated number of genes in the human genome. The diversity of cellular proteins is further complicated by the fact that proteins have various isoforms and variants.[6] Another challenge in functional proteomics stems from the structural diversity of proteins. Proteins are three-dimensional entities, and their structures are critical for their functions.[4,8] This often requires not only correct folding of polypeptide but also appropriate post-translational modifications.

Proteomics approaches generally fall into two complementary categories: methods for the global analysis of protein expression and methods for the global analysis of protein function.[8-12] For protein expression analysis, several powerful proteomics

techniques have been developed during the last decade. One of these techniques, widely used for protein expression analysis, is two dimensional gel electrophoresis (2DE) coupled with mass spectrometry (MS).[13,14] In this methodology, proteins are first separated by their isoelectric point and then by their molecular weight. Next, the separated proteins are visualized using a variety of chemical stains or fluorescent markers. Once the proteins are separated and quantified, they are identified. Individual spots are cut out of the gel and cleaved into peptides with proteolytic enzymes. These peptides can then be identified by mass spectrometry, especially a matrix-assisted laser desorption-ionization time-of flight (MALDI-TOF) mass spectrometer.[6,14]

Despite noteworthy advances in the development of automated 2DE-MS systems for rapid analysis of complex proteomes,[13-17] the separation capacity of 2DE significantly limits the applicability of this method. For example, several types of proteins, including membrane-bound and low abundance proteins, have proven difficult to analyze by 2DE.[18] This method is also limited by the ability of current staining methods to differentiate the enormous dynamic range of protein abundance.

Protein mixtures can also be analyzed without prior separation on 2DE using High Performance Liquid Chromatography (HPLC) coupled with tandem mass spectrometry (MS/MS).[6] These procedures begin with proteolytic digestion of the proteins in a complex mixture. The resulting peptides are injected onto HPLC that separates them based on hydrophobicity. HPLC can be coupled directly to a time-of-flight mass spectrometer using electrospray ionization. Peptides eluting from the column can be identified by tandem mass spectrometry (MS/MS).[6] This method, however, is limited by the capability of HPLC to separate peptides with similar hydrophobicity.

Recently, another approach was developed for quantitative proteomic analysis. This method employs small molecular probes, named isotope-coded affinity tags (ICAT), to covalently modify proteins through their cysteine residues.[19] An attractive feature of the ICAT method is that through the combined use of this chemical probe and MS analysis, both the relative abundance and sequence identities of ICAT-labeled peptides can be determined in a single experimental operation. Additionally, by focusing on cysteine-containing peptides, a significant reduction in complexity can be achieved.[5] The limitation of the ICAT is that they monitor protein abundance, which does not necessarily correlate with activity.

Protein microarray systems ("chips") provides a functional proteomics approach to probe protein function in a high throughput manner.[3,20] The approach allows screening of protein-protein or receptor-ligand interactions by immobilizing proteins on a glass slide while retaining their original biological functions. Therefore, functions of various proteins can simultaneously be compared with this approach. In addition, this method can be used for screening of potential protein binders and inhibitors, leading to the discovery of potential therapeutic reagents.[3] The scope of this technology is limited to those proteins that can be immobilized without affecting their native functions.

Another approach for functional proteomics employs biotin-tagged suicide inhibitors to covalently tag enzymes with biotin. Biotin-tagged proteins are then identified through SDS-PAGE or purified through affinity chromatography with avidin. This method is conceptually simple and circumvents many problems associated with proteomic analyses. By focusing on a single class of enzymes, this method significantly reduces problems associated with protein heterogeneity.

I.2. Chemical Proteomics and Molecular Probes

Chemical proteomics is a promising new class of proteomic methods which unites the fields of synthetic chemistry, protein biochemistry, and cell biology to create powerful tools for global analysis of protein expression and function.[5,21-25] Chemical proteomics utilizes chemical probes to selectively tag a small fraction of proteins in complex proteomes, thus reducing the complexity of proteomic analysis.

The most commonly used chemical probes are activity-based probes which consist of three basic elements: (*i*) a reactive functional group able to covalently attach to active sites of specific classes of enzymes, (*ii*) a reporter group, such as a fluorophore or biotin, for identification and purification of modified proteins, and (*iii*) a linker unit to prevent steric congestion of the reactive and reporter units and to provide selective binding interactions with target proteins (Figure 1).[5,8,21,24,25]

A number of activity-based probes have been reported,[4,8,22,21-27] some of which have been used successfully in proteomic profiling of biomedically significant enzymes including cysteine proteases,[26] serine hydrolyses,[27] protein kinase C,[28] ubiquitin and ubiquitin-like proteins,[29] and protein tyrosine phosphatases.[30] For example, the cysteine proteases probe, DCG-04,[26] which employed an epoxide as an electrophile to selectively label cysteine proteases (Figure 1a). Another example is the biotinylated fluorophosphonate[27] (FP-biotin) chemical probes (Figure 1b). In these probes, fluorophosphonate, which is a general suicide inhibitor for serine hydrolases, is employed to selectively tag catalytically active serine hydrolases in complex proteomes.

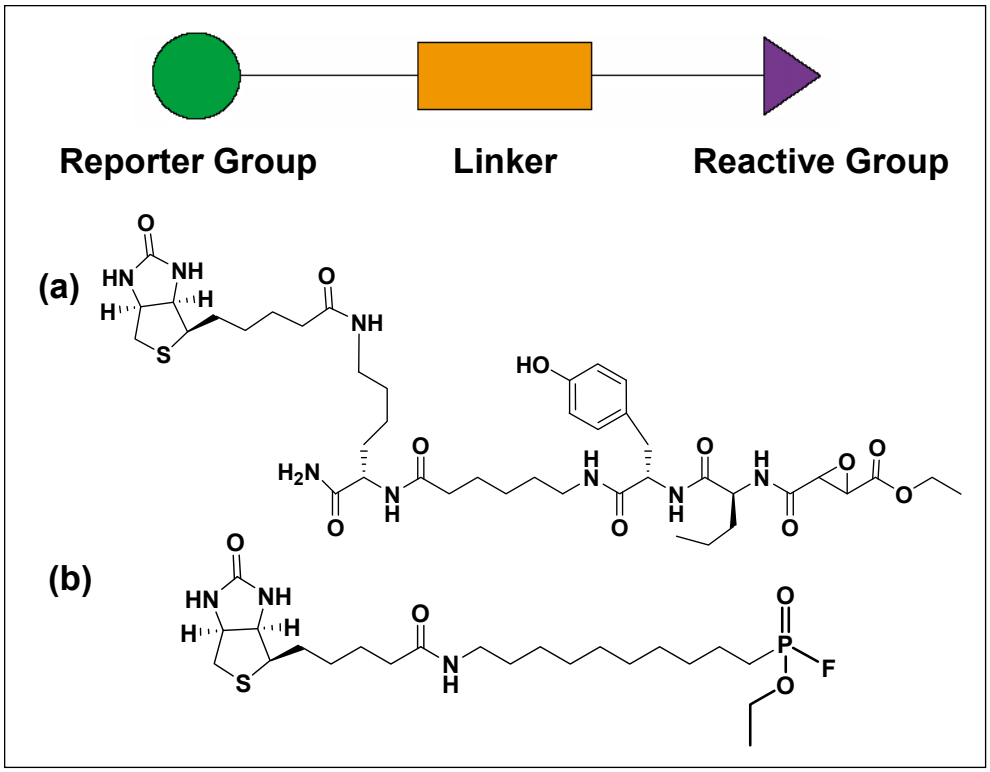

Figure 1. Anatomy of an activity-based chemical probe. Example of two probes that use different reactive groups and different linkers: (a) DCG-04 chemical probe,[26] (b) Biotinylated fluorophosphonate (FP-biotin) chemical probe.[27]

Although activity-based chemical probes provide novel insights for studying various proteins, their major limitation is that target proteins need to possess unique nucleophilic activity, such as catalytic activity of enzymes, to attain selective tagging. Therefore, a selective tagging strategy not relying on nucleophilic activity of functional side chain in proteins would greatly enhance our ability to carry out chemical proteomics studies on a wide variety of proteins.

Our study offers a complimentary approach that allows selective tagging of proteins regardless of their nucleophilic activity. Our approach utilizes an affinity group conjugated to a photo-labeling group (PLG)[31] (Figure 2). The affinity group binds in a non-covalent manner at the active site of the target protein, whereas the PLG covalently labels the target protein. Upon UV irradiation, the PLG modifies the target protein and forms a covalent protein-probe adduct. The photoligand must also contain a detectable tag which renders the modified protein distinguishable from unlabeled proteins and allows visualization and purification of tagged proteins.

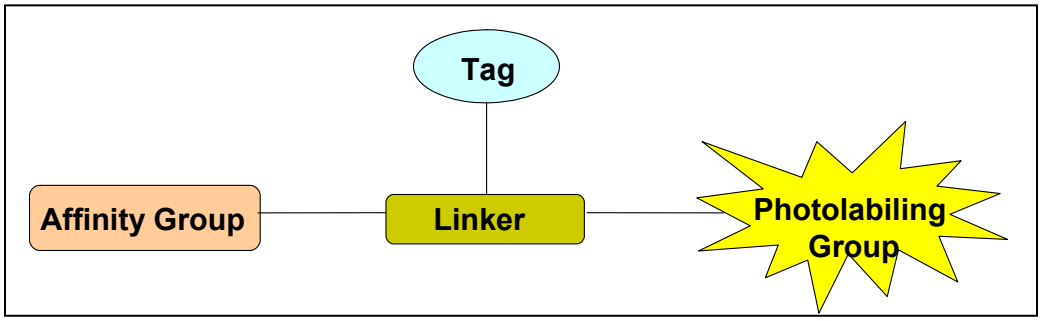

Figure 2. Anatomy of an affinity-based chemical probe.

Photoaffinity labeling has been used in many protein-ligand studies since it provides valuable information about the location and architecture of the ligand-binding site.[32-37] This information can be used to develop novel drug candidates that target proteins of therapeutic importance. For example, α-factor analogues containing benzophenone photophore were used to identify and characterize the ligand binding regions of the *Saccharomyces cervisiae* α-factor pheromone receptor.[32,33,38] Another

example is the development of highly specific photoaffinity labels for the investigation of the vasopressin receptor.[34]

The uniqueness of our approach, however, is the use of benzophenone not only as a photocrosslinker but also as an affinity group to search for protein surface hydrophobic pockets capable of molecular recognition. The most well studied protein surface pockets are enzyme active sites. For example, ATP-binding sites of many proteins are now understood at the atomic resolution. However, enzyme active sites are a small fraction of protein surface pockets. The vast majority of protein surfaces are still poorly defined, especially, in terms of their ability to recognize small molecules. Therefore, we decided to search for such pockets and utilize them for selective photolabeling of different proteins.

I.3. Research Summary

Our initial goal was to develop photoaffinity chemical probes for selective labeling of protein kinases, which are a group of biologically important proteins regulating complex cellular functions and pathways. Many kinases possess hydrophobic binding areas that can be targeted with hydrophobic PLGs, such as benzophenone. Our central hypothesis was that molecular probes containing both adenine and benzophenone can differentially bind to individual protein kinases due to differences in hydrophobic areas around the adenine binding site. We used adenine to target the adenine binding site on protein kinases and benzophenone to target nearby hydrophobic pockets.

At the onset of our study (Chapters II and III) we designed and synthesized photoactive chemical probes for selective labeling of protein kinases and evaluated the

probes' binding selectivity using two different cancer cell lines. Our probes, despite their simple structures, selectively labeled a small number of proteins out of a complex mixture, substantiating our central hypothesis. Furthermore, we showed that the chiral center in the *p*-benzoyl-phenylalanine (Bpa) linker unit plays an important role in the protein-binding selectivity.[31]

While the first part of our study proved the concept of using adenine-benzophenone conjugated probes for selective labeling of proteins, it presented two major concerns. First, blocking experiments showed that most proteins recognized our probes through the benzophenone moiety while adenine had no significant effect on binding selectivity. Second, difficulties in identification of tagged proteins disabled the verification that our probes tag adenine binding proteins. Therefore, in the second part of our study (Chapters IV and V), we decided to change our strategy and focus our attention on Src family of tyrosine kinases (SFKs).

We used the crystal structures of SFKs to determine the possible binding orientation of benzophenoe in hydrophobic pockets near the adenine binding site of SFKs. Then, we designed a new set of photoactive probes targeting the members of this family. Binding selectivity experiments revealed that a prototype probe, biotinyl-p-benzoyl-L-phenylalanyl-glycinyl-adenine-N^9-acetyl-(2-aminoethyl)glycinyl-glycine (**5-S**)**,** selectively labeled lymphocyte-specific kinase (Lck).[39] This discovery led us to further characterize the **5-S**-Lck complex and study the structural basis for the binding selectivity and affinity. Structural motifs crucial for the recognition of Lck by **5-S** were identified and the probe's binding site was located within the well-conserved region of Src-family kinases. Based on our finding we obtained a structural model for the **5-S**-Lck complex

and performed structure affinity relationship studies, in which we succeeded in improving the binding affinity toward Lck without impairing the binding selectivity.

Chapter II

Research Design and Methods

II.1. Probe Design

General Probe Structure

The goal of this study was to develop a simple chemical approach for profiling various kinases in cells. As an initial step toward this goal, we designed photoaffinity probes to target adenine binding proteins containing benzophenone binding pockets. We used adenine, as a first ligand, to target the catalytic site of protein kinases, and benzophenone, as a second ligand, to target hydrophobic areas near the substrate binding site (Figure 3). The uniqueness of this approach is that the benzophenone moiety also serves as a photo crosslinker to form a covalent bond at the binding site.

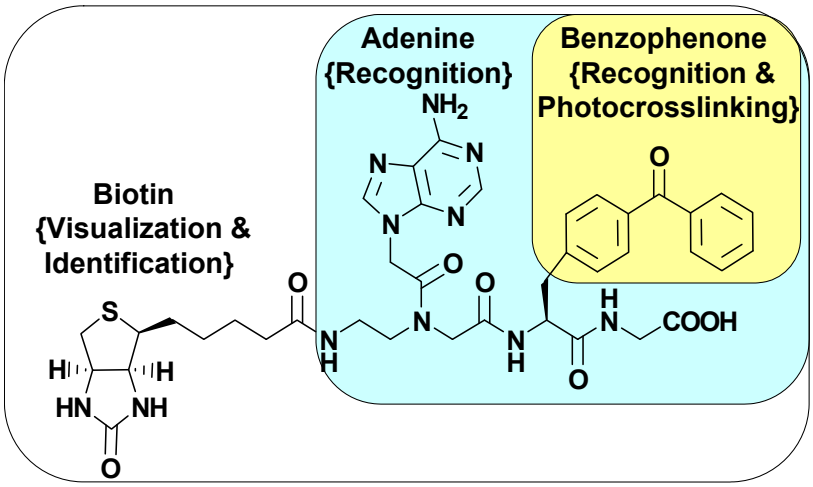

Figure 3. General structure of our prototype probe. The probe contains three functional units: adenine, benzophenone, and biotin. Adenine targets the catalytic site of kinases. Benzophenone, in addition to its role as photocrosslinker, targets hydrophobic pockets in the vicinity of the catalytic site. Biotin is used for visualization and purification of tagged kinases.

Our probes were expected to selectively label target proteins based on the principle of thermodynamic additivity, i.e., two modest-affinity ligands, when tethered through an appropriate linker, can make a bidentate ligand with high affinity and selectivity (Figure 4).[40-43] By tethering adenine and benzophenone it is possible to selectively photocrosslink kinases due to differences in hydrophobic areas around the adenine binding site.

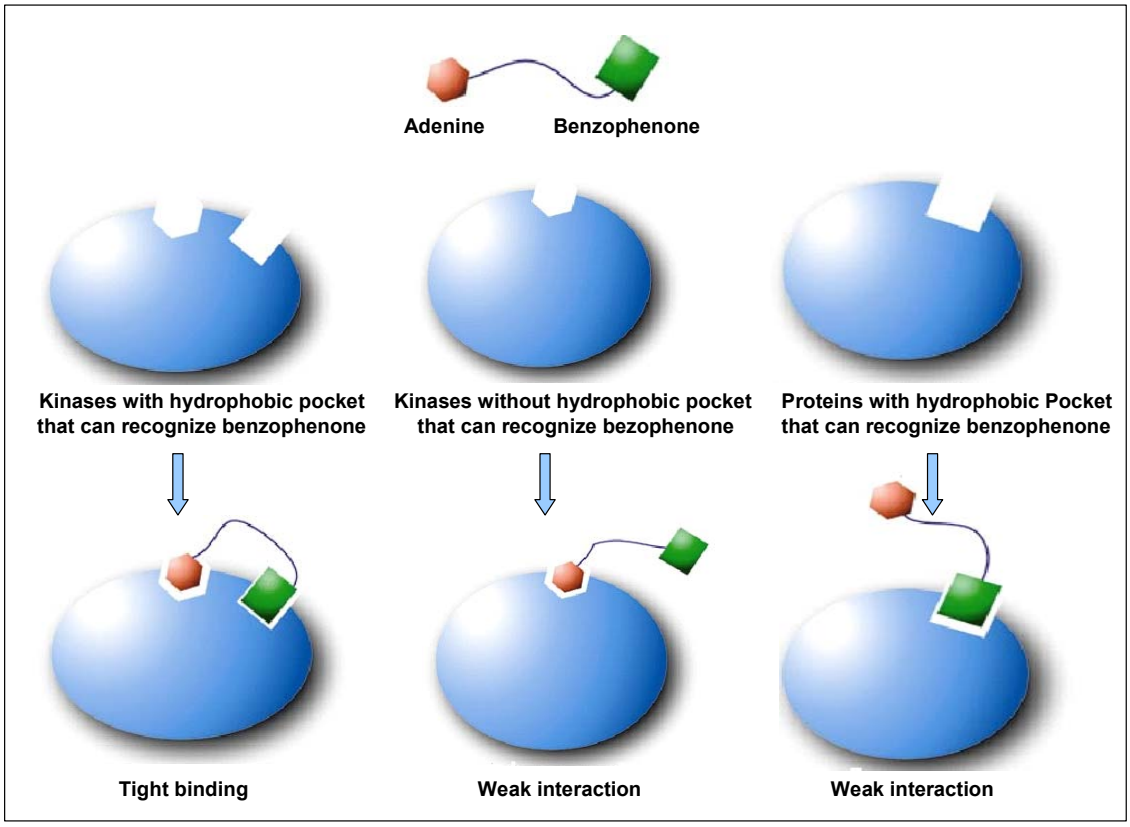

Figure 4. The principle of thermodynamic additivity. A tight binding bidentate ligand can be prepared from two modest ligands.

The probes also contain an N-terminal biotin unit, which allows the detection and purification of bound proteins. Biotin is the most commonly used tag for chemical probes,

due to its ability to provide both a gel-based method of detection and a method for purification of labeled enzymes using avidin-coated resins.[8,44,45]

We chose a peptidic backbone for our probes due to the ease of preparation and compatibility with solid-phase chemistry. Using standard solid-phase synthesis to assemble the probes, a diverse probe library can be readily generated to conduct detailed analyses on structure-activity relationships.[31] In addition, many enzymes have protein substrates and are, therefore, expected to bind probes with peptide character.[1]

Binding selectivity of individual probes can be modulated through modifications of the tethering region and recognition units.[41] For example, binding selectivity can be tuned by changing the length and flexibility of the linker between benzophenone and adenine.[36,41] This modification allows differential recognition by proteins with different distances between their adenine binding sites and hydrophobic pockets. Another way to modify binding selectivity is through alteration of their stereochemistry. This modification is expected to change the selectivity since chirality plays a central role in various biological recognition processes.[46,47]

Benzophenone as a Photocrosslinker

Many probe-protein interaction studies utilize benzophenone as a photoactive group[32-38,48] due to its three distinct advantages. First, benzophenone is chemically stable and can be incorporated into peptides by standard solid phase synthesis.[36,37,49] Second, benzophenone can be manipulated in ambient light and activated at 350-360 nm, avoiding protein-damaging wavelengths.[36] Third, benzophenone reacts preferentially with unreactive C-H bonds with high regio- and stereospecificity, which result from

geometrical and stereoelectronic preferences of the frontier molecular orbitals favoring certain angles and planes for the attack.[36,37,49]

Irradiation of benzophenone at 350 nm results in the promotion of one electron from a nonbonding n-orbital on oxygen to an antibonding л*-orbital of the carbonyl group forming a diradicaloid triplet state (Figure 5a). In the excited triplet state, the electron deficient oxygen n-orbital serves as an electrophilic center and abstracts hydrogen from weak C-H σ-bonds (Figure 5a).[36] The triplet state may last 80-120 μs in the absence of an abstractable H, but it may be much shorter in the presence of a suitably oriented C-H bond.[36]

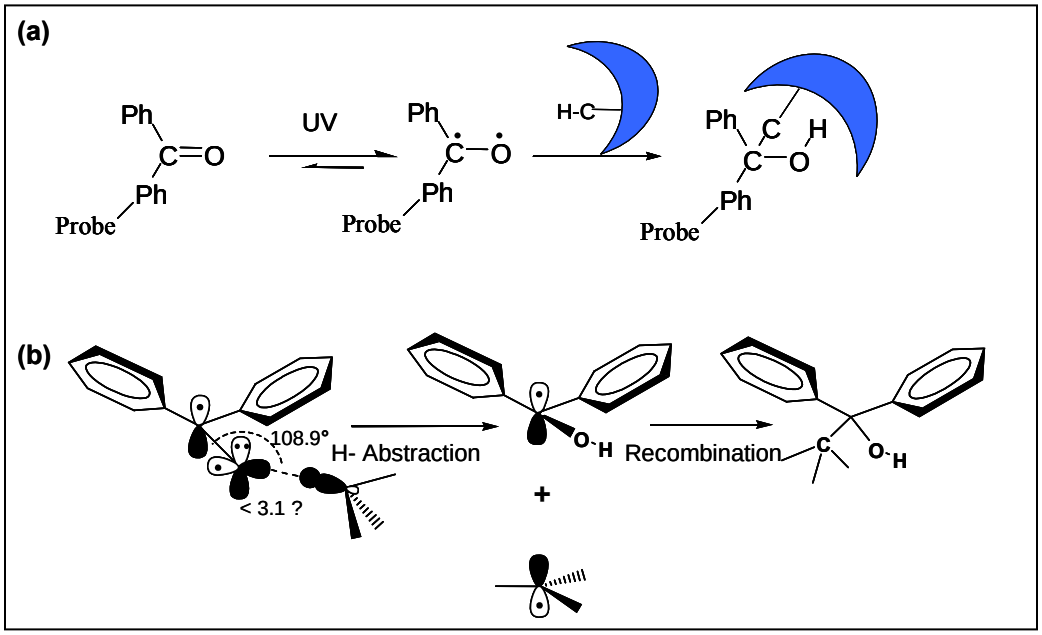

Figure 5. Photochemistry of benzophenone: (a) Radical formation and covalent attachment to target protein. (b) Regio- and stereoselectivity requirements for efficient H-abstraction and recombination reactions.[36]

The selectivity of this reaction is affected by several factors. First, the reactant and substrate must spend sufficient time at the reactive volume of benzophenone, which is a sphere with a radius of 3.1 Å, centered on the ketone oxygen. Second, in the excited state, the benzophenone ring system is required to be nearly planar, imposing significant rigidity. Third, the stereoselectivity of this reaction is affected by the preferred molecular orbital geometry of the excited triplet.[36] As shown in Figure 5b, the conformation of the n-л* triplet state is close to planarity, the half filled n-orbital lies in this plane, while the л* orbital is perpendicular to it. *Ab initio* calculations showed that the ideal C_{CO}-OH angle of the biradical attack is 108.9°, the O-H-C_{CH} is almost colinear, and the H-abstraction occurs in-plane.[50] Radical recombination may also affect the stereochemistry of this reaction, since it requires the p-orbitals to be collinear for maximum overlap.[36]

Finally, the reactivity and efficiency of the photocrosslinking by benzophenone depend on its environment. In biological systems, the most effective H-donors that can react with a benzophenone di-radical include backbone C-H bonds in amino acids, polypeptides, and carbohydrates. Particularly reactive sites include electron rich tertiary centers such as C_γ-H of leucine and C_β-H of valine as well as CH_2 groups next to heteroatoms in lysine, arginine, and methionine.[51]

II.2. Probe Synthesis

Since this study calls for a versatile synthetic method for rapid generation of various probes, a peptide backbone was selected as the tether. This permits convergent synthesis of various probes from simple building blocks, as shown in Figure 6. Probe syntheses can be performed either in solution by Boc/Cbz chemistry or on a solid-phase support using Fmoc/Bhoc chemistry. Probe synthesis is described in detail in Chapters III and IV (pages 27-28 and 58-59).

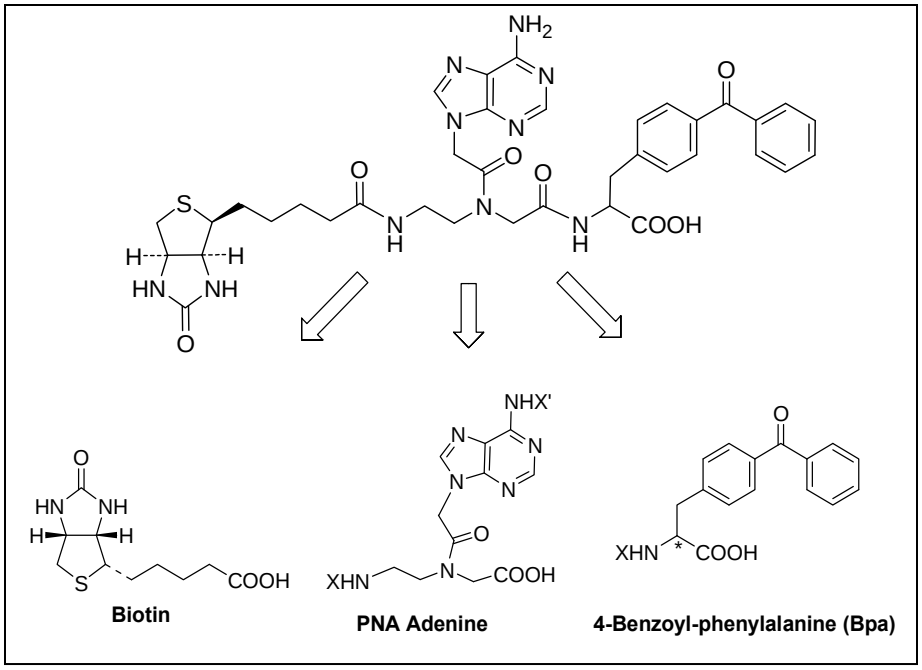

Figure 6. Retro synthesis of prototype probe.

II.3. Binding Selectivity Evaluation

Protein-binding selectivity of each probe was evaluated using the procedure outlined in Figure 7: First, protein mixtures from various cancer cell lines, as well as purified kinases were incubated with the probes with or without the presence of free adenine, benzophenone, and biotin, which served as blockers allowing additional insight into probe-protein interaction. For example, binding of proteins that recognize our probes mainly through the benzophenone moiety will be affected by the presence of free benzophenone. After incubation with the probes, proteins that bound tightly to the probes were photocrosslinked to give a labeled protein mixture, which was then separated by SDS-PAGE. Labeled proteins were then visualized by western blotting followed by chemiluminescence detection.

The number of visualized bands is used to assess protein binding selectivity of each probe. When necessary, the biotin unit was used to purify the labeled proteins for further characterization.

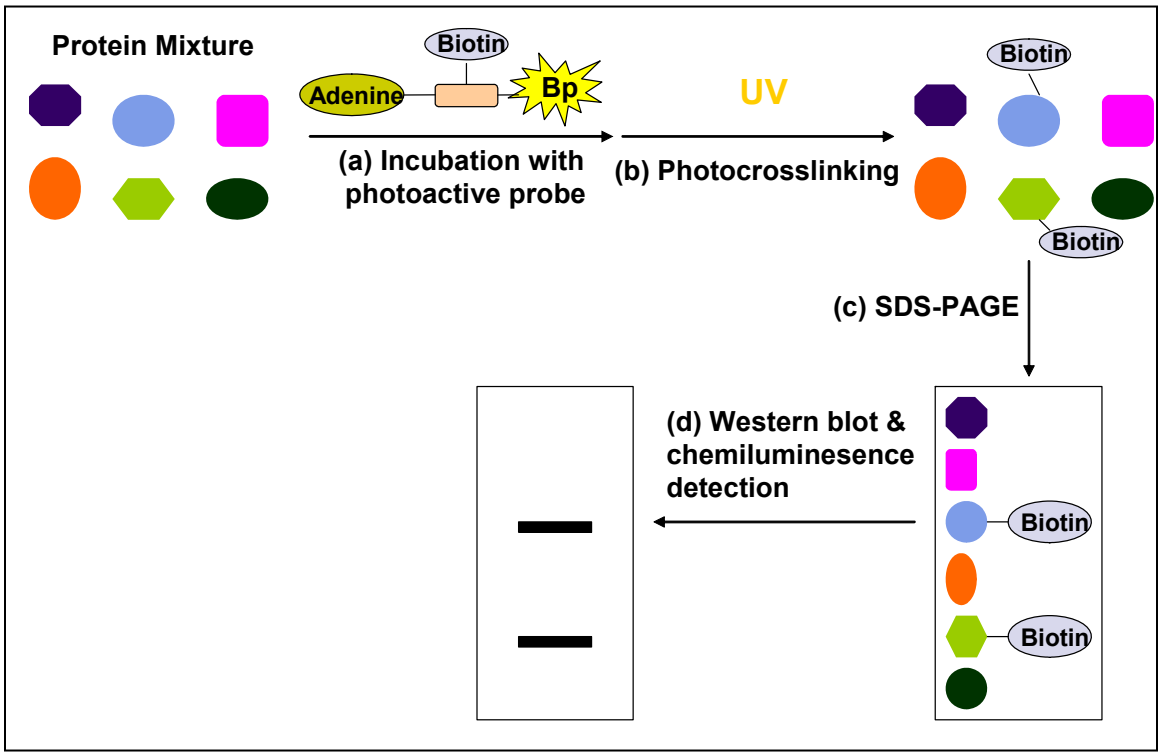

Figure 7. Experimental procedure for evaluation of protein binding selectivity. (a) Protein mixture is incubated with photoactive probes. (b) Upon UV irradiation, proteins that bind tightly to the probe are photocrosslinked. (c) Proteins are separated by SDS-PAGE. (d) Labeled proteins are visualized by Western blot followed by chemiluminescence detection.

II.4. Binding Site Identification

Isolation and purification of tagged proteins from a cell lysate mixture can be conducted using affinity chromatography based on strong non-covalent interactions between biotinylated proteins and streptavidin-agarose beads.[8] After isolation and purification, tagged proteins can be digested with trypsin and identified by peptide mass

fingerprinting analysis, which matches the tryptic peptide masses in the mass spectrum to the calculated tryptic peptide masses for proteins in a database.[52] The accurate molecular weights of tagged proteins can be determined by MALDI-TOF.[17,53] To identify the binding site of highly selective probes, the labeled protein is digested enzymatically by trypsin and its fragments submitted to mass spectrometric analysis. The binding site is examined by MS/MS fragmentation, and spectra of fragmented ions are analyzed to identify the location of photocrosslinking of the examined probe (Figure 8).

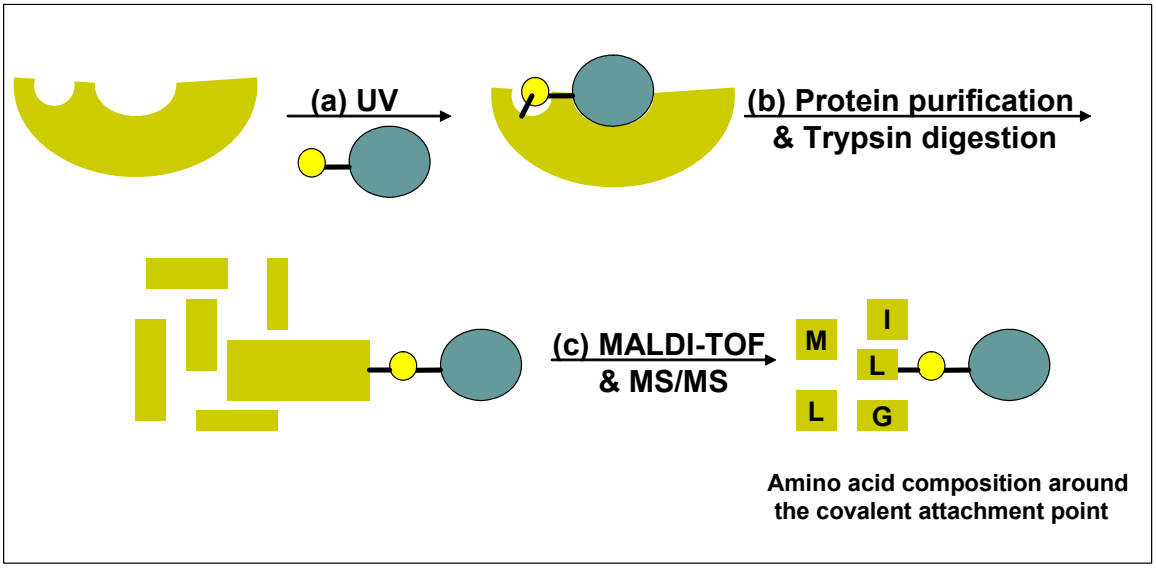

Figure 8. Experimental procedure for the determination of binding site: (a) UV irradiation of the probe in the presence of target protein results in covalent labeling of the protein. (b) The labeled protein is purified and digested enzymatically by trypsin. (c) The fragments are submitted to mass spectrometric analysis and the amino acid composition around the covalent attachment point is determined.

Chapter III

Photoactive Probes for Protein Kinases

III.1. Introduction

Protein kinases comprise the largest mammalian enzyme family in the human proteome with more than 500 members (Figure 9).[54,55] These enzymes catalyze the transfer of the γ-phosphoryl group from ATP to serine, threonine, or tyrosine residues of proteins. These phosphorylation reactions are often associated with regulation of complex cellular functions and pathways.[23,55,56] In addition, nearly every human malady has been linked to abnormal protein kinase activity.[57] The pharmacological importance of protein kinases has created considerable effort aimed at identifying and characterizing these proteins in order to develop modulators of their activities.[54] However, the study of protein kinases is often complicated by a high degree of post-translational regulation, low expression levels, and overlapping substrate selectivity.[23,54] Thus, despite intense efforts, there are still unresolved fundamental questions about the structure and function of kinases.

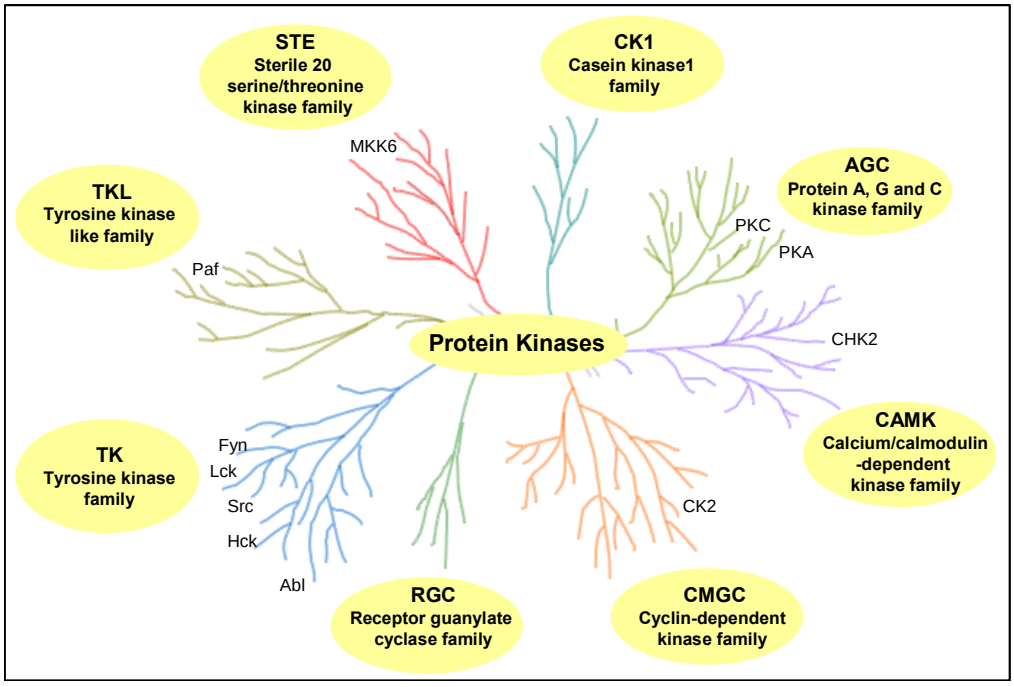

Figure 9. Protein kinase subfamilies.

Several chemical approaches for profiling the function and expression of protein kinases have been developed in recent years. For example, Patricelli and co-workers developed a probe-based technology for comprehensive screening of protein kinases in native proteomes (Figure 10a). This approach employs biotinylated-ATP to selectively label protein kinases in a complex proteome. Furthermore, it allows profiling of the selectivity of kinase inhibitors against a broad range of protein kinases in native proteomes.[54] Another biotinylated-ATP methodology for studying of protein kinases was recently described by Pflum *et al*[58] (Figure 10b). This approach utilizes γ-phosphate-modified ATP analogues for monitoring the phosphorylation activity of kinases in cellular lysates. The biotinylated γ-phosphate-ATP acts as a kinase cosubstrate to promote phosphorylation-dependent biotinylation of peptides and proteins.

These approaches, while expanding the use of chemical probes in kinases profiling, do not offer selectivity toward different families of kinases. Our molecular probes, on the other hand, can be tuned to selectively label different families of protein kinases based on topology around their binding site. For example, modifications of the linker between adenine and benzophenone can result in labeling of different kinases based on the differences in distance between their catalytic site and hydrophobic pockets that can accommodate benzophenone. Similarly, modification of the stereochemistry of the probe and incorporation of additional recognition elements can lead to labeling of different kinases.

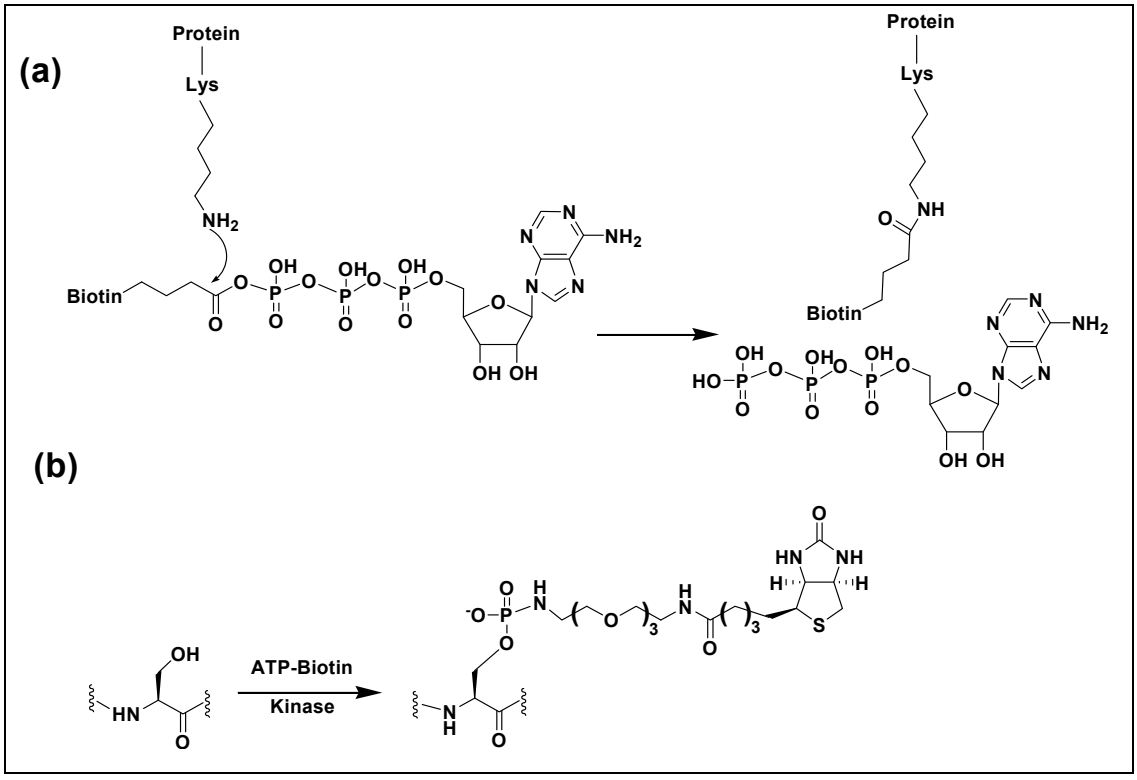

Figure 10. Chemical probes for kinase profiling: (a) Biotinylated-ATP probe for selective labeling of protein kinases in complex proteome. The ε-amino group of the lysine attacks the carbonyl carbon of the probe, releasing ATP and covalently attaching the biotin moiety to the kinase.[54] (b) ATP-biotin probe for monitoring phosphorylation activity of kinases in cellular lysates.[58] This probe acts as a kinase cosubstrate to selectively biotinylate phosphoproteins and allows the detection of phosphorylation activity of kinases.

III.2. Probe Design and synthesis

Probe Design

With the aim of developing photoactive probes for selective tagging of protein kinases, an initial set of 6 molecular probes was designed and synthesized (Figure 11). To evaluate the effect of chirality and distance between the probes' units on binding selectivity, our probes were designed as 3 pairs of diastereoisomers: (**1-S** and **1-R**), (**2-S** and **2-R**) and (**3-S** and **3-R**), in which the letters, **R** and **S,** denote the configurations of the chiral center in the Bpa unit. In comparison to probes **1-S** and **1-R**, probes **2-S** and **2-R** have a longer linker between the adenine and benzophenone units whereas probes **3-S** and **3-R** have a longer linker between the benzophenone and biotin units.

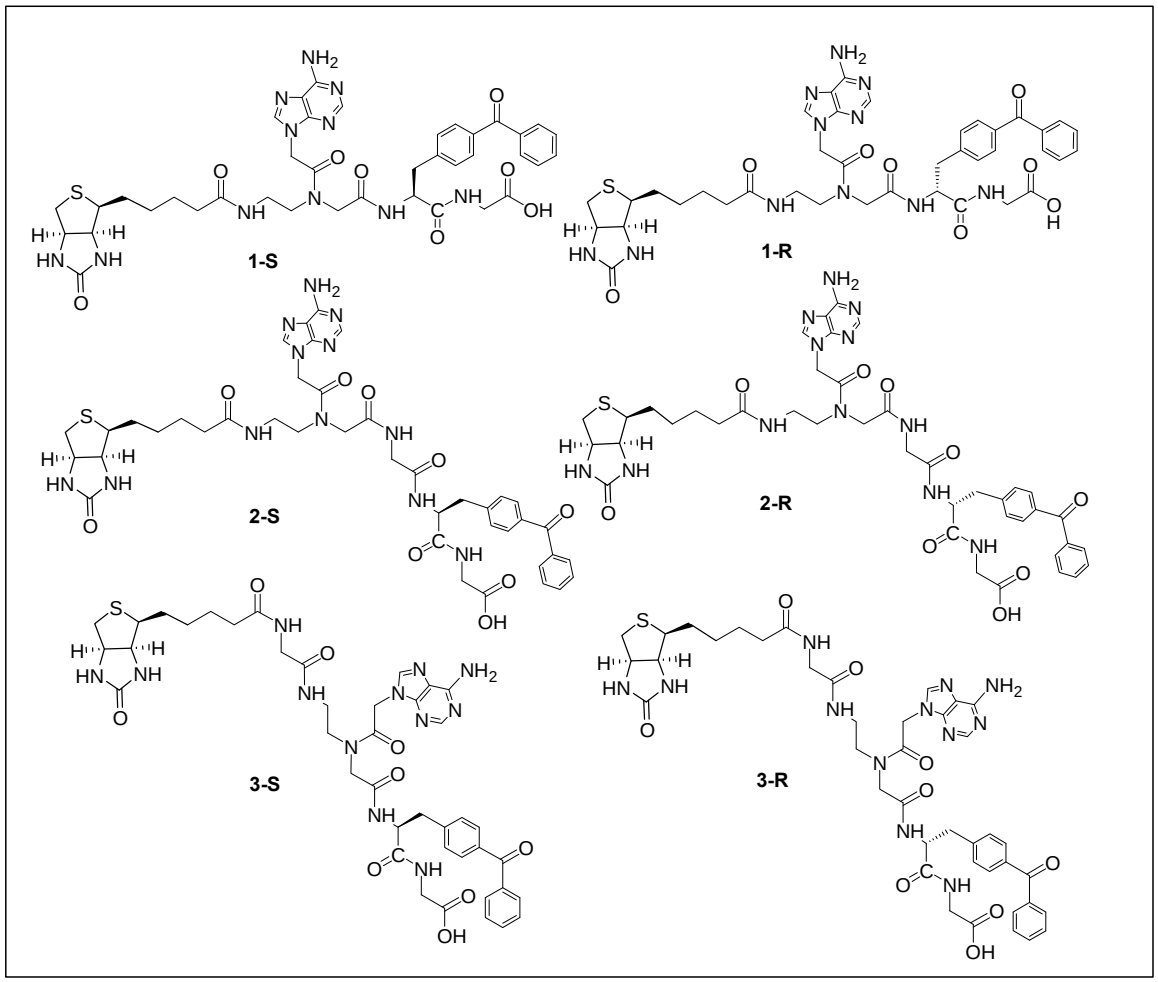

Figure 11. Structures of photoactive probes for selective labeling of protein kinases.

In order to distinguish between protein-probe interactions which are based on affinity to benzophenone and those based on affinity to adenine, a set of control probes was prepared (Figure 12). This set consists of two pairs of diastereoisomers in which the adenine group is missing and the distance between benzophenone and biotin moieties is maintained, as in original probes, by introducing glycine groups. **Controls 1-S** and **1-R**

serve as controls for **1-S** and **1-R**, respectively. **Controls 2-S** and **2-R** serve as controls for **2-S**, **2-R**, **3-S** and **3-R.**

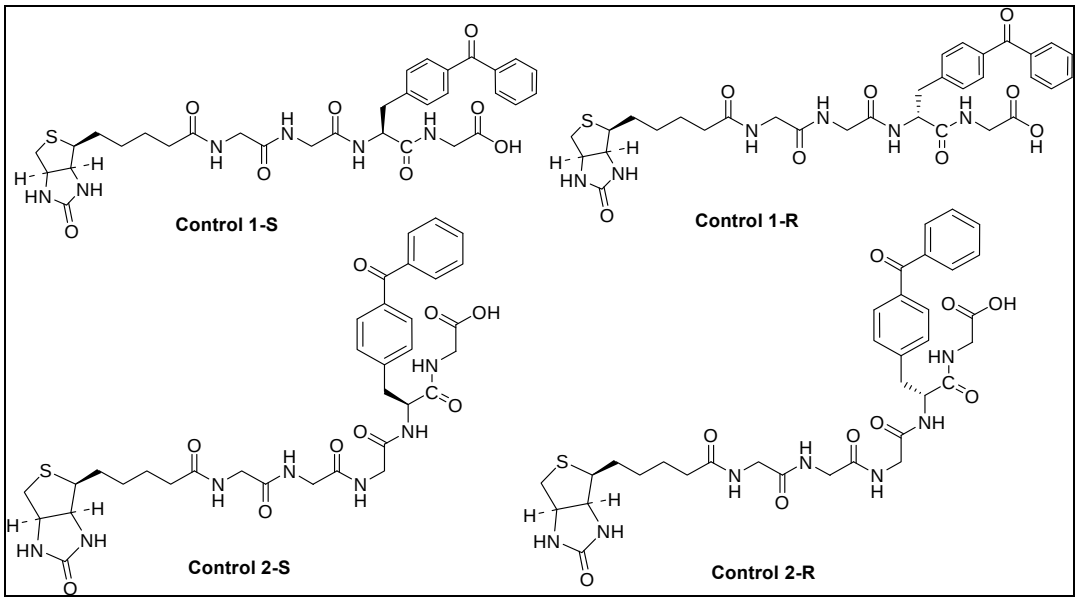

Figure 12. Structures of control probes for selective labeling of protein kinases.

Probe Synthesis

Probes were prepared manually on solid phase support using standard Fmoc/Bhoc chemistry.[59] Scheme 1 describes the synthesis of **1-S**. Starting with Fmoc-Gly-Wang resin, Fmoc was removed under basic conditions (20% piperidine in DMF). Next, Fmoc-4-benzoyl-L-phenylalanine (Fmoc-Bpa-OH) was coupled using *N*,*N*'-dicyclohexylcarbodiimide (DCC) and 1-hydroxybenzotriazole (HOBT) as coupling reagents. After deprotection of the Fmoc group, the Fmoc-protected peptide nucleic acid (PNA) adenine monomer, *N*-(N^6-Bhoc-adenine-N^9-acetyl)-*N*-(2-Fmocaminoethyl)glycine (Fmoc-PNA-adenine(Bhoc)-OH), was introduced. The new *N*-terminal was then exposed

by removal of the Fmoc group and coupled to biotin *N*-hydroxysuccinimide. The desired probe was cleaved from the resin using a solution of 95% TFA, 2.5% water, and 2.5% triisopropylsilane (TIS). Following synthesis and purification, each probe was characterized via chromatographic and spectroscopic analytical techniques. The yield for the solid phase synthesis of the probes and their controls was 28%-94%; the low yields of some probes were due to poor recovery at the precipitation of crude products in cold petroleum ether or diethyl ether.

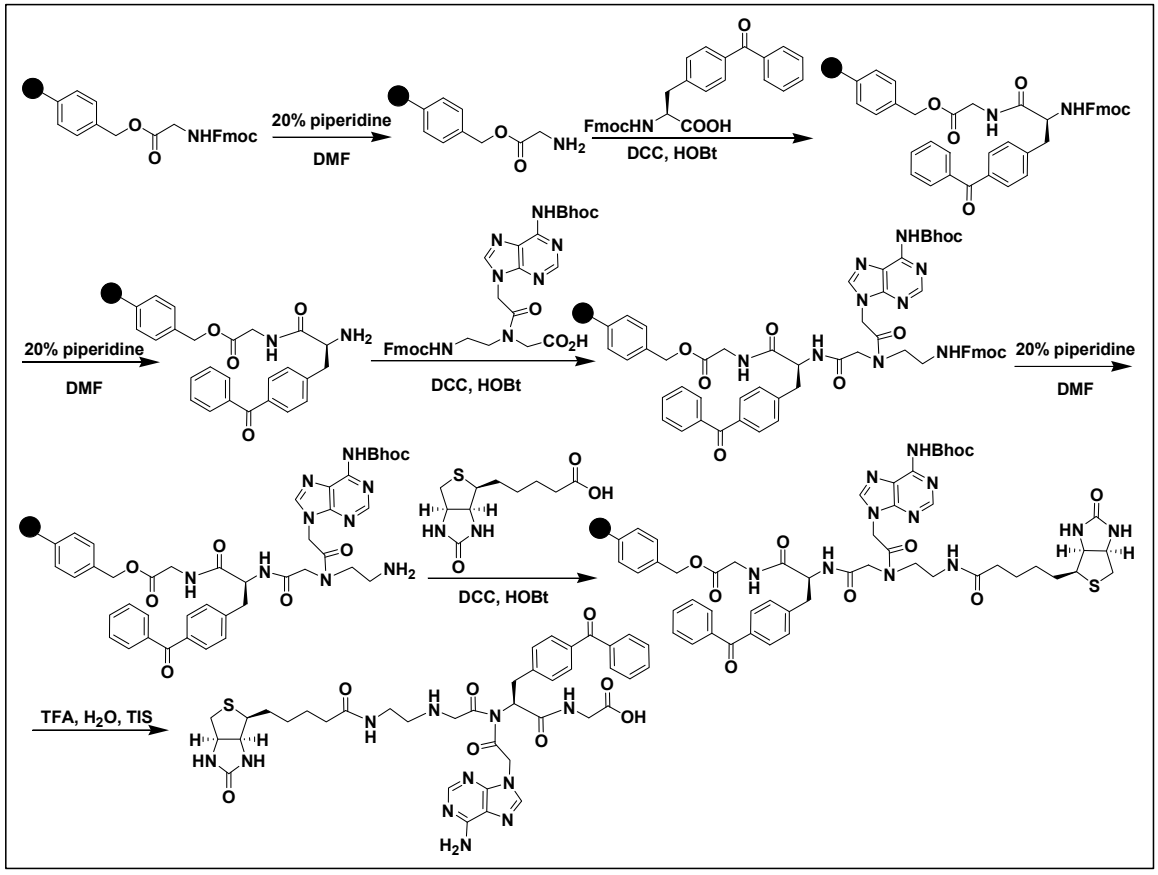

Scheme 1. Solid-phase synthesis of probe **1-S**.

III.3. Binding Selectivity Evaluation

Protein-binding selectivity of the first set of probes was evaluated, as described in Chapter II.3. (Page 18), using neuroblastoma (SK-N-SH, NB) and breast cancer (MDR-MB-231) cell lines. We chose two different cell lines to profile a variety of protein kinases and to evaluate the diagnostic potential of our probes, e.g., their ability to give different SPS-PAGE profiles with different cancer cell lines.

Binding profiles of SK-N-SH NB cell line

Labeling of SK-N-SH NB lysate with probes **1-S** and **1-R** gave one main band at 60 kDa (Figure 13a, lanes 1 and 5, respectively). No significant difference in protein-binding selectivity was observed. Blocking experiments with benzophenone resulted in a significant reduction in band intensity at 60 kDa for both **1-S** and **1-R** (Figure 13a, lane 2 and 6, respectively), whereas blocking with adenine and biotin did not show a significant effect on band intensity (Figure 13a, lanes 3, 4, 7, and 8). These results indicate that the 60 kDa protein recognizes **1-S** and **1-R** mainly through the benzophenone moiety.

The effect of the distance between recognition units on labeling selectivity was assessed by comparing the profiles of **1-S** and **1-R** (Figure 13a) to those of **2-S** and **2-R** (Figure 14a). While **1-S** and **1-R** showed only one band at 60kDa, **2-S** and **2-R** gave additional bands at 55, 45, and 27 kDa. These differences might result from increased flexibility of the longer linker allowing the labeling of additional proteins with larger distance between their adenine and benzophenone binding pockets.

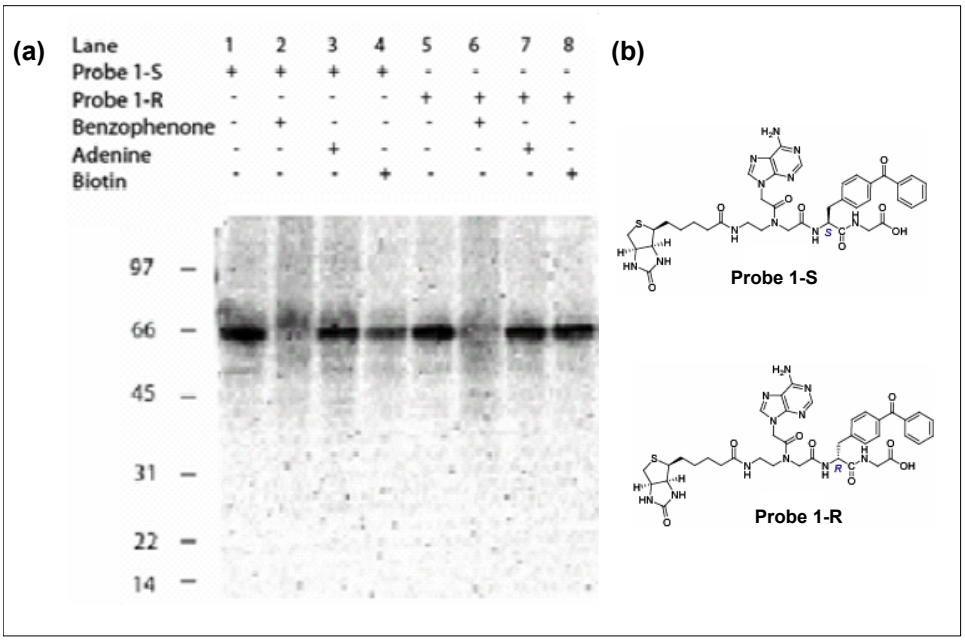

Figure 13. (a) Photolabeling study of SK-N-SH NB cell lysate tagged with probes **1-S** and **1-R**. (b) Structures of probes **1-S** and **1-R**.

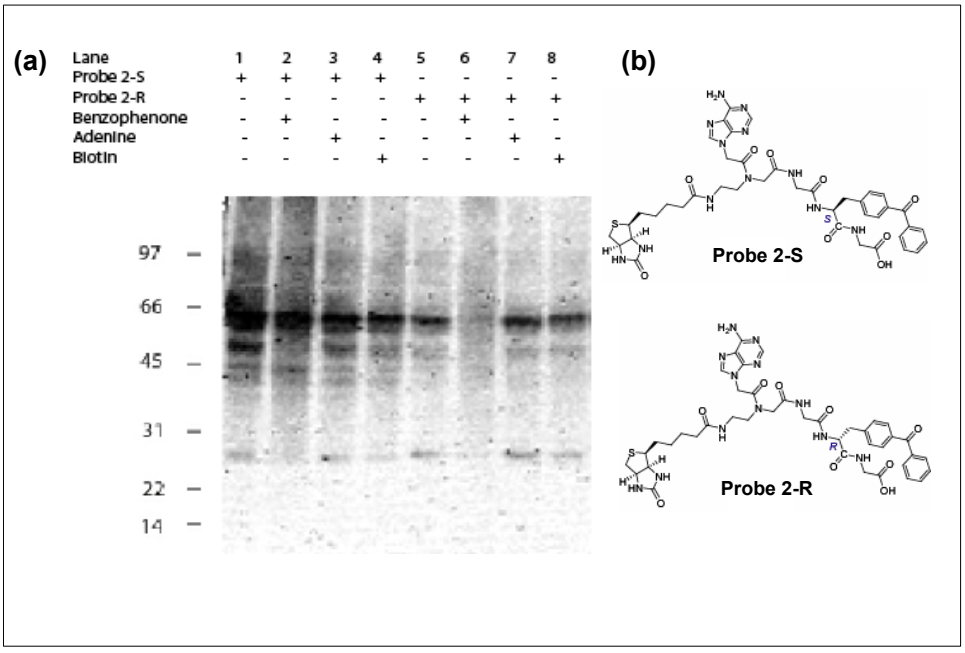

Figure 14. (a) Photolabeling study of SK-N-SH NB cell lysate tagged with probes **2-S** and **2-R**. (b) Structures of probes **2-S** and **2-R.**

A comparison of binding selectivity profiles for **2-S** and **2-R** revealed that while both probes gave a strong band at 60 kDa and weaker bands at 55 kDa and 27 kDa, the intensities of these bands are higher for **2-S** (Figure 14a, lanes 1 and 5). Furthermore, **2-S** gave additional weak bands at around 45 kDa. These results indicate that a difference in one chiral center can affect the binding selectivity of the probes.

Blocking experiments with benzophenone affected only the bands at 55 and 27 kDa in the **2-S** profile (Figure 14a, lane 2), whereas there was a significant effect on all bands in the **2-R** profile (Figure 14a, lane 5). Pretreatment with other blockers did not show a significant effect on the profiles of these probes (Figure 14a, lanes 3, 4, 7, and 8). These observations suggest that **2-R** and **2-S** interact with proteins mainly through their benzophenone unit. In addition, the labeling of proteins at 60 and 45 kDa in the presence of free benzophenone can be explained by very high affinity toward these proteins and/or high crosslinking efficiency. It is possible that labeling of the proteins at 60 and 45 kDa could be blocked by higher concentrations of benzophenone. However, poor solubility of benzophenone in the aqueous buffer used for the labeling experiments may preclude using higher concentrations of benzophenone.

Binding profile of MDR-MB-231 cell line

The significant effect of chirality on binding recognition was shown in the binding profiles of MDR-MB-231 cell lysate with **2-S** and **2-R** (Figure 15a). **2-S** gave strong bands at approximately 60 and 75 kDa and weaker bands at around 40 and 90 kDa (Figure 15a, lane 1). On the other hand, **2-R** gave a strong band at 27 kDa and weaker bands around 60, 75, and 90 kDa (Figure 15a, lane 5). These obvious differences in the

binding profiles of the stereoisomers, **2-S** and **2-R**, indicated that some proteins within the cell lysate were able to discriminate the stereochemical differences between the two probes. This chiral discrimination is achieved through unique spatial alignment of amino acid in individual asymmetric hydrophobic pockets.[31]

In the profile of **2-S**, blocking experiments revealed that the presence of free benzophenone significantly affected the band intensity at 60 kDa, whereas other bands, such as 75 and 40 kDa, were not affected (Figure 15a, lane 2). In addition, the presence of free adenine and biotin had little effect on the intensities of the bands in **2-S** profile (Figure 15a, lanes 3 and 4) implying that benzophenone has the major role in recognition of probe **2-S** by the labeled proteins.

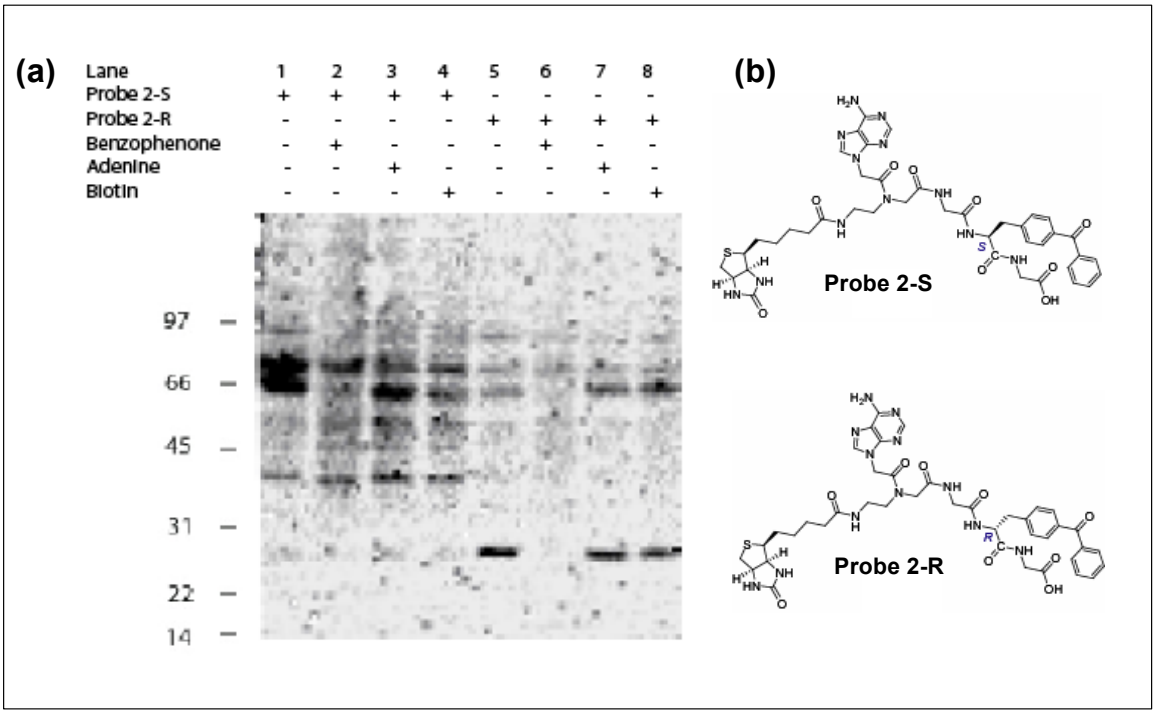

Figure 15. **(a)** Photolabeling study of breast cancer (MDR-MB-231) cell lysate tagged with probes **2-S** and **2-R. (b)** Structures of probes **2-S** and **2-R**.

In the binding profile of **2-R** (Figure 15a, lane 1), blocking with benzophenone resulted in the disappearance of all bands (Figure 15a, lane 6) revealing that **2-R** is recognized mainly through the benzophenone unit. Free adenine and biotin (Figure 15a, lanes 7 and 8) did not exhibit a significant effect on binding selectivity of **2-R**.

Comparison of the binding profile of **2-S** or **2-R** with MDR-MB-231 breast cancer (Figure 15a, lanes 1 and 5) and SK-N-SH neuroblastoma cell lines (Figure 14a, lanes l and 5) revealed interesting differences in their labeling pattern. For example, **2-S** labeled proteins of 40 kDa when incubated with MDR-MB-231 lysate but not with SK-N-SH lysate. Additionally, the binding profile **2-R** and MDR-MB-23 showed a strong band at 27 kDa, whereas, with SK-N-SH lysate this band was faint. These observations imply that our probes can monitor differences in protein expression among different cancer cell lines and, therefore, has the potential to assist in the search for cancer biomarkers.

The binding profiles of MDR-MB-231 cell lysate with **control 2-S** and **control 2-R** (Figure 16a, lanes 1 and 5) gave further evidence for the crucial role of the probes' chirality in its binding selectivity. C**ontrols 2-S** gave three strong bands at approximately 27, 60-70, and 75 kDa and weaker bands at 40 and 50 kDa. On the other hand, **control 2-R**, in addition to the three strong bands at 27, 60-60, and 75 kDa, gave a strong band at 50 kDa and did not label 40 kDa.

Blocking experiments revealed that, as expected from **1-S/R** and **2-S/R** profiles, **controls 2-S** and **2-R** also interacted with proteins mainly through their benzophenone unit (Figure 16a, lanes 2-4 and 6-8).

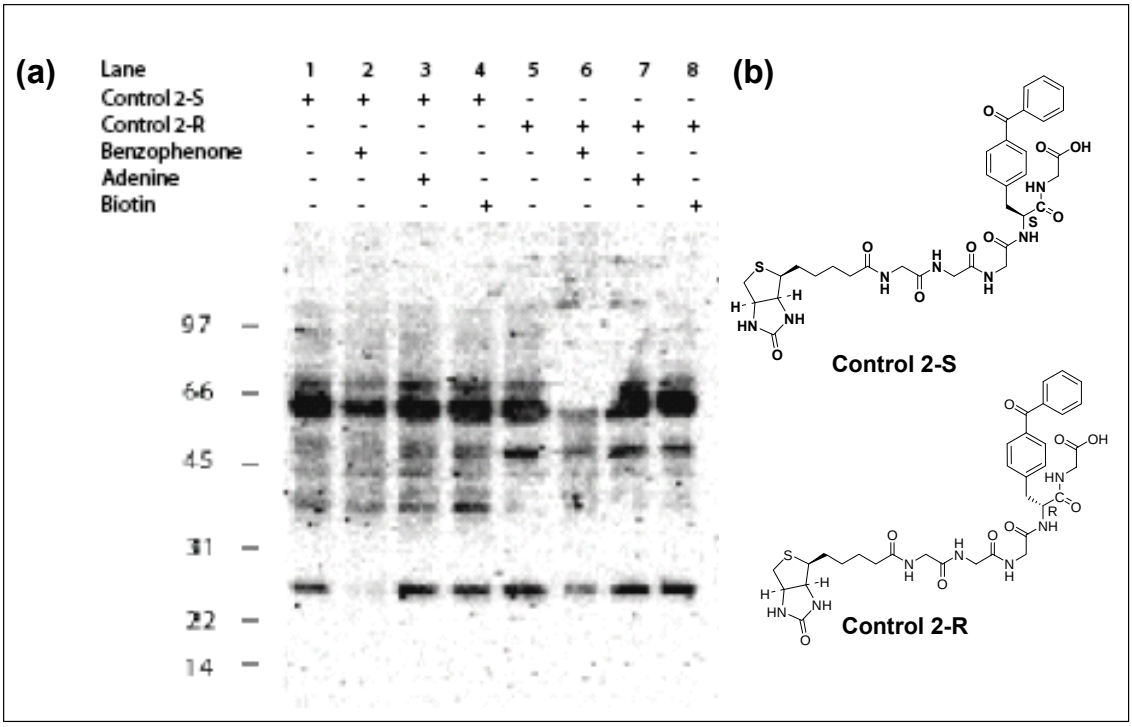

Figure 16. (a) Photolabeling study of breast cancer (MDR-MB-231) cell lysate tagged with controls **2-S** and **2-R. (b)** Structures of controls **2-S** and **2-R**.

Comparison of binding profiles of probes **2-S** and **2-R** (Figure 15a) with their control probes (Figure 16a) revealed that the adenine moiety has a significant effect on protein-binding selectivity. The 27 kDa band observed in the profile of **control 2-S** was absent in the profile of **2-S**. Likewise, the strong bands at 40 kDa and 60 kDa bands in the **control 2-R** profile mostly disappeared in the **2-R** profile. These results might suggest that binding selectivity can be improved in the presence of adenine in the vicinity of the benzophenone moiety.

However, since blocking experiments with free adenine (Figure 15a, lanes 1 and 3) showed that adenine has no significant effect on the binding profiles of probes **2-S** and **2-R,** the improved binding selectivity of these probes relative to their control resulted

from other factors than the recognition of adenine by the tagged proteins. For example, the presence of adenine in the vicinity of the benzophenone unit can create a steric hindrance that blocks the access of benzophenone to hydrophobic pockets. In addition, introducing adenine on the probe backbone reduces the flexibility of the linker between benzophenone and biotin and might result in lower probability of benzophenone to achieve the required orientation for efficient photolabeling. Taken together, the results from binding selectivity and blocking experiments implied that benzophenone is the major recognition unit in our probes.

III.4. Summary and Conclusions

In this part of our study we demonstrated that it is possible to attain high protein-binding selectivity with simple chemical probes containing adenine and benzophenone. Despite the probes' simple structure, they selectively fished out a small number of proteins from crude mixtures of cell lysates, which are expected to contain more than tens of thousands of protein species (Figures 13a-16a, lane 1 and 5).

The binding selectivity of our probes was successfully modulated by changing the chirality of the probes (e.g **2-S** and **2-R**) as well as the distance between the benzophenone and adenine units (e.g. **1-S** and **1-R** versus **2-S** and **2-R**). Blocking experiments (Figures 13a-16a, lanes 2-4 and 5-8) revealed that most of the tagged proteins recognize our probes through their benzophenone moiety and not the adenine group. The effect of adenine on binding selectivity was observed only when comparing the binding profiles of **2-S** and **2-R** with their control analogues, which lack the adenine group (Figure 15a, lane 1 and Figure 16a, lane 1). Therefore, it is possible that this effect results from altering the environment of the benzophenone unit and not from affinity interactions of the adenine group with the labeled proteins.

Differences in photolabeling results of SK-N-SH and MDR-MB-231 cancer cell lines with **2-S** or **2-R** (Figures 14 and 15) implied that our probes can contribute to the search for cancer biomarkers. Several proteomics strategies have been successfully used to investigate differential protein profiling in cancer cells and to identify proteins with potential as biomarkers in cancer classification.[6,8,60] To utilize our probes in the search for cancer biomarkers, a comprehensive screen of various cancer cell lines with our probes is

required in order to identify proteins that are correlated with different types of cancers or with different levels of invasiveness.

Our study, while proving that proteins have hydrophobic pockets that can selectively recognize benzophenone moiety and can be utilized for proteomic studies, did not demonstrate that the adenine group contributes to the recognition by tagged proteins. Since free adenine did not affect the binding selectivity of our probes and since we were not able to identify the labeled proteins, we could not confirm that our probes bind to protein kinases.

There was a possibility that the adenine was hindered between the biotin and benzophenone groups resulting in poor availability toward interactions with adenine binding proteins. Therefore, in the next stage of our study, we designed and synthesized a new set of probes in which benzophenone was placed in the middle of the probe and adenine was placed near the C-terminus. In addition, to reduce the complexity of tagged proteins' identification, we decided to focus on a specific family of protein kinases (Chapters IV and V).

In conclusion, this proof-of-principle study demonstrates that photoactive molecular probes containing benzophenone and adenine can be utilized to selectively label proteins in complex proteomes and have potential to assist in the search for cancer biomarkers. However, to increase the role of adenine in the binding interaction and to simplify the identification of labeled proteins, we had to redesign our probes and to focus on a subfamily of protein kinases. Therefore, in the next stage of this study, our simple chemical approach was used to profile the Src family of tyrosine kinases and develop selective photoligands for Lck kinase.

III.5. Materials and Methods

Materials

Fmoc-Gly-Wang resin, Fmoc-Gly, Fmoc-4-benzoyl-L-phenylalanine (Fmoc-L-Bpa), Fmoc-D-Bpa, dicyclohexylcarbodiimide (DCC), and 1-hydroxybenzotriazole (HOBT) were purchased from Fluka. Biotin-*N*-hydroxysuccinimide was obtained from Sigma-Aldrich. The Fmoc-protected peptide nucleic acid (PNA) adenine monomer, Fmoc-PNA-adenine-(Bhoc)-OH, was purchased from Applied Biosystems. Laemmli Sample Buffer and Tris-Glycine-SDS buffer were purchased from BioRad. Anti-biotin hoarse radish peroxidase (HRP)-conjugated antibody was obtained from New England Biolabs and ECL-Plus chemiluminescence reagent was obtained from Amersham Biosciences. All other chemicals and solvents were obtained through Fisher Scientific and used without further purification.

Physico-Chemical analytical methods

^{1}H NMR, ^{13}C NMR, [^{1}H, ^{1}H] COSY, and [^{1}H, ^{13}C] HSQC spectra were recorded on a Bruker Avance 500MGHz spectrometer. Chemical shifts are reported in δ units (ppm) using the solvent peak as the internal standard. ^{1}H NMR splitting patterns are designated as singlet (s), doublet (d), triplet (t), doublet of doublet (dd), and doublet of triplet (dt). Splitting patterns that could not be interpreted or easily visualized are designated as multiplet (m).

Mass spectral data were acquired on an Agilent Technologies 1100 Series LC/MSD model G1946D using electrospray (ESI) ionization. Ionization was carried out with a drying gas temperature of 175 °C, a nebulizer pressure of 40 psi and a flow rate of 13 L/min. The mass range scanned was between 140 and 1000 amu with fragmentor values of 70 volts in negative ionization mode. The capillary was set to 4000 volts. Samples were introduced into the mass spectrometer using a 1:1 mixture of water and acetonitrile containing 0.1% acetic acid and 50 μM ammonium acetate. The flow rate of the solvent was 500 μl/min. Data was processed using Agilent's Chemstation software.

RP-HPLC was performed on an Agilent HPLC system equipped with an 1100 Diode-Array detector. Analytical RP-HPLC was performed using a Zorbax, Eclipse XDB-C8 (4.6 X 150 mm) column (5 μm bead size). Semi-preparative HPLC was performed using Econosil C-18 10 u (10 X 250 mm). Separation was achieved using a linear gradient at a flow rate of 1 ml/min (Analytical HPLC) or 3ml/min (Semi-preparative HPLC) of Buffer **A** (20% MeOH), buffer **B** (100% MeOH), and 0.01% TFA. Column effluent was monitored by UV absorbance at 254, 220, and 280 nm. Elution Conditions: t = 0 min A = 100%, t = 5 min A = 100%, t = 20 min A = 50%, t = 30 min A = 0, t = 35 min A = 100%.

Chemical Synthesis

Probe synthesis was accomplished manually using a stepwise solid-phase procedure. All couplings were carried out over night in dimethylformamide (DMF) using a 2-fold excess (over resin loading) of protected monomer, activated with an equimolar of

HOBT and DCC in room temperature. Reaction was monitored using the Kaiser test for free amines.[62] *N*-Fmoc group was removed using 20% (v/v) piperidine in DMF. Probes were removed from the solid support with simultaneous sidechain deprotection using a 95% trifluoroacetic acid (TFA), 2.5% triisopropylsilane (TIS) and 2.5% water solution for 2 h at room temperature. TFA was removed under reduced pressure. Crude material was precipitated and washed with cold petroleum ether. Probes were purified using semi-preparative HPLC, and the relevant fractions were collected and lyophilized. The range of the yield was 28% - 94%. The purified probes were analyzed using Analytical HPLC, Mass Spectroscopy, and ^{1}H-NMR. For some of the probes ^{13}C-NMR, [^{1}H, ^{1}H] COSY, and [^{1}H, ^{13}C] HSQC spectra were also obtained. The ^{1}H-NMR spectra of the adenine-containing probes, **1-S**, **1-R, 2-S, 2-R, 3-S and 3-R,** exhibited conformational isomerism at room temperature, which arise from the tertiary amide conformers at the PNA adenine moiety. The ^{1}H-NMR data given below are for the major conformers of the probes.

Probe 1-S [Biotinyl-adenine-*N*^{9}-acetyl-(2-aminoethyl)glycinyl-p-benzoyl-L-phenylalanyl-glycine]

Fmoc-Gly-Wang resin (250 mg, 0.1875 mmol, loading of 0.75 mmol/gram, 1 eq) was swollen in *N*-methylpyrrolidone for 1h. The liquid was then removed and the resin was washed 3 times with DMF. In order to remove the Fmoc group, the resin was washed with 20% piperidine in DMF for 5min, and then again, with the same solution, for 20 min. Next, the resin was washed 3 times with DMF and a coupling of Fmoc-4-benzoyl-L-phenylalanine (Fmoc-L-Bpa-OH) was performed via DCC/HOBT activation: Fmoc-Bpa-OH (184 mg, 0.375 mmol, 2 eq), HOBT (0.047 ml, 0.375 mmol, 2 eq), and DCC (77 mg,

0.375 mmol, 2 eq) were dissolved in 2 ml DMF and the solution was cooled for 1h (0°C). The precipitated dicyclohexylurea (DCU) was then removed by centrifugation and the solution was added to the resin. The mixture was shaken overnight. The liquid phase was removed and the resin was washed 3 times with DMF and 3 times with DCM/Methanol (1:1). The completeness of the reaction was verified by the ninhydrin test and the Fmoc protecting group was removed as above. In the next step, Fmoc-PNA-adenine(Bhoc)-OH (272 mg, 0.375 mmol, 2eq) was coupled to the peptide-resin via DCC/HOBT activation as described above. After removal of the Fmoc group, biotin-*N*-hydroxysuccinimide (128.2 mg, 0.375 mmol, 2 eq) was coupled to the peptide-resin using the same DCC/HOBT methodology. The product was then cleaved from the resin along with side chain deprotection by adding 10 ml of a 95% TFA, 2.5% TIS and 2.5% water solution. The mixture was allowed to stand for 2h, and then the volume of TFA was reduced using N_2. The product was precipitated using cold petroleum ether and placed in the freezer overnight. Next, the product was collected and recrystallized using DCM and petroleum ether to yield 154 mg (yield = 96%) of white crystals. The crude product was purified using semipreparative HPLC, and the relevant fractions were lyophilized to give a white solid: Analytical RP-HPLC time: 14.00 min; ESIMS (expected m/z 827.3) m/z 828.2 (MH^+), 850.2 (MNa^+); ^{1}H-NMR δ ppm (500MHz, DMSO) 8.65 (1H, d, NH), 8.50 (1H, m, NH), 8.10 (1H, s, CH), 7.99 (1H, s, CH), 7.72-7.41 (9H, m, 9xCH), 7.19 (2H, s, NH_2), 6.65 (1H, s, NH), 6.50 (1H, s, NH), 5.19 (2H, m, CH_2), 4.76 (1H, m, CH), 4.30 (1H, m, CH), 4.14 (2H, m, CH_2), 4.11 (1H, m, CH), 3.60 (2H, m, CH_2), 3.26 (2H, m, CH_2), 3.18 (2H, m, CH_2), 3.05 (2H, m, CH_2), 3.02 (1H, m, CH), 2.8 (2H, dt, CH_2), 2.17 (2H, t, CH_2), 1.70-1.20 (6H, m, $CH_2CH_2CH_2$).

Probe 1-R [Biotinyl-adenine-N^9-acetyl-(2-aminoethyl)glycinyl-p-benzoyl-D-phenylalanyl-glycine]

Fmoc-Gly-Wang resin (200 mg, 0.15 mmol, loading of 0.75 mmol/gram, 1 eq) was Swollen in *N*-methylpyrrolidone for 1h. The liquid was then removed and the resin was washed 3 times with DMF. In order to remove the Fmoc group, the resin was washed with a 20% piperidine in DMF solution for 5min, and then again, with the same solution, for 20 min. Next, the resin was washed 3 times with DMF and a coupling of Fmoc-D-Bpa-OH was performed via DCC/HOBT activation: Fmoc-Bpa-OH (147.5 mg, 0.30 mmol, 2 eq), HOBT (0.041 ml, 0.30 mmol, 2 eq), and DCC (61.9 mg, 0.30 mmol, 2 eq) were dissolved in 2 ml DMF and the solution was cooled for 1h (0°C). The precipitated DCU was then removed and the solution was added to the resin. The mixture was shaken overnight. The liquid phase was removed and the resin was washed 3 times with DMF and 3 times with DCM/Methanol (1:1). The completeness of the reaction was verified by ninhydrin test and the Fmoc protecting group was removed as above. In the next step, Fmoc-PNA-adenine(Bhoc)-OH (217.7 mg, 0.30 mmol, 2eq) was coupled to the resin performed via DCC/HOBT activation as mentioned above. After removal of the Fmoc group, biotin-*N*-hydroxysuccinimide (153.6 mg, 0.30 mmol, 2 eq) was coupled to the resin via the same DCC/HOBT methodology mentioned above. The product was then cleaved from the resin along with side chain deprotection by adding 10 ml of a 95% TFA, 2.5% TIS and 2.5% water solution. The mixture was allowed to stand for 2h, and then the volume of TFA was reduced using N_2. The product was precipitated using cold petroleum ether and placed in the freezer overnight. Next, the product was collected and

recrystallized using DCM and petroleum ether to yield 56.4 mg (yield = 49%) of white crystals. The crude product was purified using semipreparative HPLC, and the relevant fractions were lyophilized to give a white solid: Analytical RP-HPLC time: 15.21 min; ESIMS (expected m/z 827.3) m/z 828.2 (MH^+), 850.3 (MNa^+), 414.7 ($M2H^+/2$); ^{1}H-NMR δppm(500MHz, DMSO) 8.31 (1H, d, NH), 8.28 (1H, m, NH), 8.06 (1H, s, CH), 7.87 (1H, s, CH), 7.72-7.41 (9H, m, 9xCH), 7.17 (2H, s, NH_2), 6.43 (1H, s, NH), 6.34 (1H, s, NH), 4.87 (1H, d, CH_2), 4.74 (1H, d, CH_2), 4.64 (1H, m, CH), 4.31 (1H, m, CH), 3.90 (1H, d, CH_2), 4.14 (1H, m , CH), 4.03 (1H, d, CH_2), 3.72 (2H, m, CH_2), 3.30 (2H, m, CH_2), 2.90 (2H, m, CH_2), 3.07 (2H, m, CH_2), 3.05 (1H, m, CH), 2.57 (2H, m, CH_2), 1.97 (2H, t, CH_2), 1.62-1.20 (6H, m, $CH_2CH_2CH_2$).

Probe 2-S [Biotinyl-adenine-*N*^{9}-acetyl-(2-aminoethyl)glycinyl-glycinyl-p-benzoyl-L-phenylalanyl-glycine]

Probe **2-S** was synthesized by the same procedure employed for probe **1-S** except for the introducing of glycine between PNA-adenine and p-benzoyl-L-phenylalanine. The crude product (79 mg, yield = 51%) was purified using semipreparative HPLC, and the relevant fractions were lyophilized to give a white solid: Analytical RP-HPLC time: 15.10 min; ESIMS (expected m/z 884.2) m/z 885.3 (MH^+), 443.2 ($M2H^+/2$); ^{1}H-NMR δ ppm (500MHz, DMSO) 8.65 (1H, d, NH), 8.48 (1H, m, NH), 8.26 (1H, m, NH), 8.10 (1H, m, CH), 7.97 (1H, s, CH), 7.75-7.25 (9H, m, 9xCH), 7.20 (2H, s, NH_2), 6.65 (1H, s, NH), 6.36 (1H, s, NH), 5.19 (2H, m, CH_2), 4.65 (1H, m, CH), 4.29 (1H, m, CH), 4.22 (2H, m, CH_2), 4.15 (1H, m, CH), 3.80 (2H, m, CH_2), 3.75 (2H, m CH_2), 3.37 (2H, m, CH_2), 3.15

(2H, m, CH_2), 3.1 (2H, m, CH_2), 3.06 (1H, m, CH), 2.75 (2H, m, CH_2), 2.17 (2H, m, CH_2), 1.60-1.20 (6H, m, $CH_2CH_2CH_2$).

Probe 2-R [Biotinyl-adenine-*N*^{9}-acetyl-(2-aminoethyl)glycinyl-glycinyl-p-benzoyl-D-phenylalanyl-glycine]

Probe **2-R** was synthesized by the same procedure employed for probe **1-R** except for the introducing of glycine between PNA-adenine and p-benzoyl-D-phenylalanine. The crude product (30 mg, yield = 28%) was purified using semipreparative HPLC, and the relevant fractions were lyophilized to give a white solid: Analytical RP-HPLC retention time: 14.90 min; ESIMS (expected m/z 884.2) m/z 885.2 (MH^+), 907.2 (MNa^+), 443.1 ($M2H^+/2$); ^{1}H-NMR δ ppm (500MHz, DMSO) 8.45 (1H, m, NH), 8.25 (1H, d, NH), 8.10 (1H, s, CH),), 7.99 (1H, s, CH), 7.72-7.35 (9H, m, 9xCH), 7.20 (2H, s, NH_2), 6.60 (1H, s, NH), 6.45 (1H, s, NH), 5.20 (2H, m, CH_2), 4.65 (1H, m, CH), 4.30 (1H, m, CH), 4.22 (2H, m, CH_2), 4.15 (1H, m, CH), 3.96 (2H, m, CH_2), 3.51 (2H, m CH_2), 3.36 (2H, m, CH_2), 3.15 (2H, m, CH_2), 3.05 (2H, m, CH_2), 3.04 (1H, m, CH) 2.75 (2H, m, CH_2), 2.19 (2H, m, CH_2), 1.60-1.20 (6H, m, $CH_2CH_2CH_2$).

Probe 3-S [Biotinyl-glycinyl- adenine-*N*^{9}-acetyl-(2-aminoethyl)glycinyl-p-benzoyl-L-phenylalanyl-glycine]

Probe **3-S** was synthesized by the same procedure employed for probe **1-S** except for the introducing of glycine between biotin and PNA-adenine. The crude product (146mg, yield = 94%) was purified using semipreparative HPLC, and the relevant fractions were lyophilized to give a white solid: Analytical RP-HPLC time: 15.20 min; ESIMS

(expected m/z 884.2) m/z 885.2 (MH^+), 907.1 (MNa^+); ^{1}H-NMR δppm(500MHz, DMSO) 8.65 (1H, d, NH), 8.50 (1H, m, NH), 8.33 (1H, m, NH), 8.12 (1H, s, CH), 8.07 (1H, s, CH), 7.72-7.41 (9H, m, 9xCH), 7.19 (2H, s, NH_2), 6.41 (1H, s, NH), 6.34 (1H, s, NH), 5.14 (2H, m, CH_2), 4.80 (1H, m, CH), 4.31 (1H, m, CH), 4.18 (1H, m, CH_2), 4.12 (1H, m, CH), 4.11(1H, m, CH_2), 3.74 (2H, m, CH_2), 3.29 (2H, m, CH_2), 3.18 (2H, m, CH_2), 3.09 (2H, m, CH_2), 3.04 (1H, m, CH), 2.81 (2H, dt, CH_2), 2.11 (2H, t, CH_2), 1.70-1.20 (6H, m, $CH_2CH_2CH_2$).

Probe 3-R [Biotinyl-glycinyl-adenine-*N*^{9}-acetyl-(2-aminoethyl)glycinyl-p-benzoyl-D-phenylalanyl-glycine]

Probe **3-R** was synthesized by the same procedure employed for probe **1-R** except for the introducing of glycine between PNA-adenine and biotin. The crude product (10 mg, yield = 56%) was purified using semipreparative HPLC, and the relevant fractions were lyophilized to give a white solid: HPLC retention time: 14.99 min; ESIMS (expected m/z 884.2) m/z 885.3 (MH^+), 907.1 (MNa^+), 443.2 ($M2H^+/2$); ^{1}H-NMR δ ppm (500MHz, DMSO) 8.75 (1H, m, NH), 8.50 (1H, m, NH), 8.25 (1H, m, NH), 8.10 (1H, s, CH), 8.06 (1H, s, CH), 7.70-7.30 (9H, m, 9xCH), 7.17 (2H, s, NH_2), 6.61 (1H, m, NH), 6.4 (1H, m, NH), 5.18 (2H, m, CH_2), 4.80 (1H, m, CH), 4.31 (1H, m, CH), 4.20 (2H, m, CH_2), 4.12 (1H, m, CH), 3.75 (2H, m, CH_2), 3.60 (2H, m, CH_2), 3.50 (2H, m, CH_2), 3.30 (2H, m, CH_2), 3.24 (2H, m, CH_2), 3.10 (2H, m, CH_2), 3.08 (1H, m, CH), 2.75 (2H, dt, CH_2), 2.17 (2H, m, CH_2), 1.70-1.20 (6H, m, $CH_2CH_2CH_2$).

Control 1-S [Biotinyl-glycinyl-glycinyl-p-benzoyl-L-phenylalanyl-glycine]

Fmoc-Gly-Wang resin (150 mg, 0.1125 mmol, loading of 0.75 mmol/gram, 1 eq) was swelled in *N*-methylpyrrolidone for 1h. The liquid was then removed and the resin was washed 3 times with DMF. In order to remove the Fmoc group, the resin was washed with a 20% piperidine in DMF solution for 5min, and then again, with the same solution, for 20 min. Next, the resin was washed 3 times with DMF and a coupling of Fmoc-L-Bpa-OH was performed via DCC/HOBT activation: Fmoc-L-Bpa-OH (110 mg, 0.225 mmol, 2 eq), HOBT (30 mg, 0.225 mmol, 2 eq), and DCC (46 mg, 0.225 mmol, 2 eq) were dissolved in 2 ml DMF and the solution was cooled for 1h (0°C). The precipitated DCU was then removed and the solution was added to the resin. The mixture was shaken overnight. The liquid phase was removed and the resin was washed 3 times with DMF and 3 times with DCM/Methanol (1:1). The completeness of the reaction was verified by the ninhydrin test and the Fmoc protecting group was removed as above. In the next step, Fmoc-glycine (67 mg, 0.225 mmol, 2eq) was coupled to the resin performed via DCC/HOBT activation as mentioned above. After removal of the Fmoc group, another Fmoc-glycine (67 mg, 0.225 mmol, 2eq) was coupled to the resin via DCC/HOBT activation. In the next step, Fmoc group was removed and D-(+)-biotin (55 mg, 0.225 mmol, 2 eq) was coupled to the resin via the same DCC/HOBT methodology mentioned above. The product was then cleaved from the resin along with side chain deprotection by adding 10 ml of a 95% TFA, 2.5% TIS and 2.5% water solution. The mixture was allowed to stand for 2h, and then the volume of TFA was reduced using N_2. The product was precipitated using cold petroleum ether and placed in the freezer overnight. Next, the product was collected and recrystallized using DCM and petroleum ether to yield 34

mg (yield = 45%) of white crystals. The crude product was purified using semipreparative HPLC, and the relevant fractions were lyophilized to give a white solid: HPLC retention time: 15.49 min; ESIMS (expected m/z 666.24) m/z 667.0 (MH^+), 689.1 (MNa^+); ^{1}H-NMR δ ppm (500MHz, DMSO) 8.28 (1H, m, NH), 8.19 (1H, m, NH), 8.10 (1H, m, NH), 8.00 (1H, m, NH), 7.73-7.44 (9H, m, 9xCH), 6.49 (1H, s, NH), 6.38 (1H, s, NH), 4.57 (1H, m, CH), 4.30 (1H, m, CH), 4.13 (1H, m, CH), 3.74-3.58 (6H, m, 3xCH_2), 3.16 (1H, m, CH_2), 3.09 (1H, m, CH), 2.88 (1H, t, CH_2), 2.81 (1H, dd, CH_2), 2.58 (1H, d, CH_2), 2.13 (2H, t, CH_2), 1.59-1.29 (6H, m, $CH_2CH_2CH_2$).

Control 1-R [Biotinyl-glycinyl-glycinyl-p-benzoyl-D-phenylalanyl-glycine]

Control 1-R was synthesized by the same procedure employed for control **1-S** except for the use of Fmoc-D-Bpa-OH instead of Fmoc-L-Bpa. After cleavage from the resin, the product was precipitated using cold petroleum ether and placed in the freezer overnight. Next, the product was collected and recrystallized using DCM and petroleum ether to yield 22 mg (yield = 29%) of white crystals. The crude product was purified using semipreparative HPLC, and the relevant fractions were lyophilized to give a white solid: HPLC retention time: 15.45 min; ESIMS (expected m/z 666.24) m/z 667.0 (MH^+), 689.1 (MNa^+); ^{1}H-NMR δ ppm (500MHz, DMSO) 8.25 (1H, m, NH), 8.20 (1H, d, NH), 8.14 (1H, m, NH), 8.05 (1H, m, NH), 7.74-7.43 (9H, m, 9xCH), 6.46 (1H, s, NH), 6.38 (1H, s, NH), 4.60 (1H, m, CH), 4.29 (1H, m, CH), 4.12 (1H, m, CH), 3.76-3.59 (6H, m, 3xCH_2), 3.12 (1H, m, CH_2), 3.09 (1H, m, CH), 2.88 (1H, t, CH_2), 2.80 (1H, dd, CH_2), 2.58 (1H, d, CH_2), 2.14 (2H, m, CH_2), 1.58-1.30 (6H, m, $CH_2CH_2CH_2$).

Control 2-S [Biotinyl-glycinyl-glycinyl-glycinyl-p-benzoyl-L-phenylalanyl-glycine]

Control 2-S was prepared as **control 1-S** except for the introduction of additional glycine group between biotin and p-benzoyl-L-phenylalanine. The crude product (18 mg, yield = 24%) was purified using semipreparative HPLC, and the relevant fractions were lyophilized to give a white solid: Analytical RP-HPLC retention time: 17.02 min; ESIMS (expected m/z 723.27) m/z 724.2 (MH^+), 746.2 (MNa^+); ^{1}H-NMR δ ppm (500MHz, DMSO) 8.47 (1H, m, NH), 8.36 (1H, d, NH), 8.24 (1H, m, NH), 7.74-7.43 (9H, m, 9xCH), 6.70 (1H, s, NH), 6.41 (1H, s, NH), 4.52 (1H, m, CH), 4.29 (1H, m, CH), 4.15 (1H, m, CH), 3.77-3.57 (8H, m, 4xCH_2), 3.19 (1H, m, CH_2), 3.09 (1H, m, CH), 2.91 (1H, t, CH_2), 2.82 (1H, dd, CH_2), 2.55 (1H, d, CH_2), 2.22 (2H, m, CH_2), 1.58-1.30 (6H, m, $CH_2CH_2CH_2$).

Control 2-R [Biotinyl-glycinyl-glycinyl-glycinyl-p-benzoyl-D-phenylalanyl-glycine]

Control 2-R was prepared as **control 1-R** except for the introduction of additional glycine group between biotin and p-benzoyl-D-phenylalanine. The crude product (24 mg, yield = 32%) was purified using semipreparative HPLC, and the relevant fractions were lyophilized to give a white solid: Analytical RP-HPLC retention time: 17.02 min;
ESIMS (expected m/z 723.27) m/z 724.2 (MH^+), 746.2 (MNa^+); ^{1}H-NMR δ ppm (500MHz, DMSO) 8.60 (1H, s, NH), 8.41 (1H, s, NH), 8.25 (1H, m, NH), 8.20 (1H, m, NH), 7.85 (1H, s, NH), 7.74-7.43 (9H, m, 9xCH), 6.70 (1H, s, NH), 6.41 (1H, s, NH), 4.52 (1H, m, CH), 4.29 (1H, m, CH), 4.15 (1H, m, CH), 3.77-3.57 (8H, m, 4xCH_2), 3.20 (1H, m, CH_2), 3.11 (1H, m, CH), 2.91 (1H, t, CH_2), 2.80 (1H, dd, CH_2), 2.60 (1H, d, CH_2), 2.22 (2H, m, CH_2), 1.58-1.30 (6H, m, $CH_2CH_2CH_2$).

Biological Assays

Cell Culture and Preparation of Cell Lysate

Neuroblastoma (SK-N-SH) and breast cancer (MDR-MB-231) cell lines were maintained in Dulbecco's Modified Eagle Media containing 10% fetal calf serum and 1% penicillin-streptomycin-fungizone in a 37 ºC, 5% CO_2 incubator. For each labeling experiment, cells were harvested at the log phase (50-70% confluency) and plated onto a 10 cm tissue culture dish. Cells were then incubated overnight in a 37 ºC 5% CO_2 incubator. Preparation of cell lysate was carried out using Promega M-Per® Mammalian Protein Extraction Reagent. During the protein preparation and labeling, samples were kept on ice or in a chromatography refrigerator (4 ºC). Briefly, the cell monolayer was rinsed once with ice-cold TBS (1×). Cells were directly lysed on the tissue culture plate with 500 µl of Promega M-Per® Mammalian Protein Extraction Reagent, which is formulated to retain the native structures of proteins. Cell lysates were scraped off from the plates and transferred into microfuge tubes. The lysates were centrifuged (10,000 rpm, 4 ºC), and the resulting supernatant was concentrated to 10 µg/µL using a Millipore Centricon 10 (6000 rpm, 90 min, 4 ºC). Protein concentration was quantified with Promega Commassie Plus™ Protein Assay Reagent and adjusted to 2 µg/µL using TBS (1×): the final ratio of TBS to the Extraction reagent was 4:1. Prepared samples were submitted immediately to the probe treatment as described below.

Evaluation of Protein-binding Selectivity

20 μL aliquots of the lysate (2 μg/μL) were mixed with 2 μL of 1 mM probe solution in DMSO. For blocking experiments, 20 μL aliquots of the lysate were mixed first with 2 μL of a blocking solution in DMSO (10 mM adenine, 10 mM benzophenone, 10 mM biotin, or DMSO control) and then with 2 μL of 1 mM probe solution in DMSO. The mixtures were incubated at 4 ºC for 1 h. Photocrosslinking was carried out under six Sylvania 350 Blacklight lamps (15 W, λ_{max} 350 nm) for 2 h, in which samples were kept on ice and placed approximately 5 cm below the lamps. Following the photocrosslinking, samples were mixed with Laemmli Sample Buffer with 5%(v/v) 2-mercaptoethanol, denatured at 80 ºC for 5 min and separated on SDS-PAGE (5-20% Tris-HCl gel, 200 V, 1 h) in 1× Tris-Glycine-SDS buffer. Gels were blotted onto a PVDF membrane (200 mA, 1h) in a cold transfer buffer (20% methanol in 1×Tris-Glycine buffer). The blotted membrane was blocked with 5% non-fat milk in Tris-buffered saline containing 1% Tween 20 (TBS-T) for 1 h. Blocked membrane was rinsed with TBS-T (10 min×3), treated with an anti-biotin hoarse radish peroxidase (HRP)-conjugated antibody (1:100 dilution in 2% non-fat milk in TBS-T) for 3 h, and washed with TBS-T (10 min×3). The washed membrane was treated with the ECL-Plus chemiluminescence reagent for 5 min. Bands were observed with the BioRad ChemiDoc gel documentation system.

Chapter IV

Photoactive Probes for the Src Family of Kinases:

Selective Photoligands for Lck

IV.1. Introduction

Our proof of concept study, as described in Chapter III, demonstrated that chemical probes containing adenine and benzophenone can be employed for selective tagging of different proteins.[31] In this chapter, our simple chemical approach was utilized to develop a focused library of photoactive probes for selective tagging of the Src family of tyrosine kinases (SFKs). During this process we discovered a selective photoactive ligand for one of the Src family members, lymphocyte specific kinase (Lck).[39]

The SFKs are non-transmembrane tyrosine kinases involved in signal transduction pathways that regulate cell growth, differentiation, activation, and transformation.[63-65] Abnormal SFK signaling has been linked to several disease states, including osteoporosis[66,67] and metastatic cancer (Table 1).[63,65,68-70] Therefore, SFKs have emerged as a molecular target for the discovery of ATP-competitive inhibitors.[63,65,71] Selectivity toward different members of SFK has great significance for the development of therapeutic agents. However, due to the large homology in their ATP binding site, developing inhibitors with selectivity within the SFKs is a challenging task.[72,73]

The SFK contains nine family members: Src, Blk, Yes, Yrk, Fgr, Hck, Fyn, Lyn and Lck, which share a high degree of homology within their ATP-binding regions.[68] The primary structure of the Src kinases is comprised of an N-terminal unique domain followed by regulatory SH3 and SH2 domains and the tyrosine kinase domain containing the active site (Figure 17).[74]

Table 1. Src family kinases expression and oncogenic forms.[63,65,68-70]

Src Family Member	*Pattern of Expression*	*Oncogenic forms*
Blk	B cells	
Fgr	Myeloid cells, B cells	Overexpressed in leukemias and lymphomas
Fyn	Ubiquitous	
Hck	Myeloid cells	
Lck	T cells	Overexpressed in T-cell acute lymphocytic leukemias
Lyn	Brain, B cells, myeloid cells	
Src	Ubiquitous	Mutated in Colon cancer, overexpressed in mammary, pancreatic and other cancers
Yes	Ubiquitous	Overexpressed in colon, malignant melanoma and other cancers
Yrk	Ubiquitous	

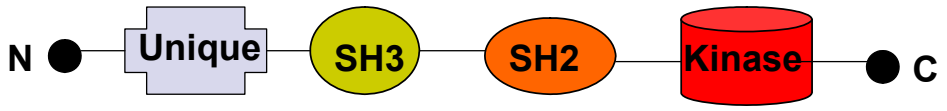

Figure 17. The domain structure of the Src protein tyrosine kinase family.[74]

As a member of SFKs, Lck shows their common domain architecture. However, the unique domain of Lck possesses the greatest sequence diversity within this group of enzymes. This domain is thought to be involved in the interaction of Lck with specific cellular proteins including Lck substrate. In T-cells, it is known to mediate association with the cytoplasmic tail of T-cell co-receptors CD4 and CD8 and it plays a key role in T-cell antigen receptor (TCR)-linked signal transduction pathways.[54,75,76] The SH3 domain is involved mainly in the regulation of protein-protein interactions by recognizing proline-rich regions found in guanine nucleotide exchange factors and GTPase activating proteins. The SH2 domain of Lck recognizes phosphorylated tyrosine residues on other proteins, thereby facilitating formation of tyrosine phosphorylation-induced multimeric complexes.

The tyrosine kinase domain is the catalytic domain of Lck, catalyzing the transfer of the γ-phosphate from ATP to tyrosine residues. The catalytic domain contains an autophosphorylation site (Tyr-394), which plays an important role in regulating protein kinase activity.

Lck's critical role in T-cell activation and differentiation, rendered it as a target for treatment of T-cell mediated autoimmune and inflammatory disorders and prevention of transplant rejection.[76,77] Several potent and bioavailable Lck inhibitors have been shown to have inhibitory activities *in vivo* in models of T-cell-dependent immune responses.[73,76-79] For example, A-770041[79] is a selective Lck inhibitor that was proven to prevent rejection of heart transplants in rats.

In addition to its role in T-cell activation, Lck is necessary for the early steps in the mitochondrial apoptosis signaling cascade and is essential for apoptosis induction by cytotoxic drugs.[80] Furthermore, abnormalities in Lck structure have been linked to several genetic diseases. One example is the severe combined immunodeficiency (SCID) phenotype, which includes defects in cellular and humoral immunity.[81] Another example is the autosomal recessive disease Hereditary Haemochromatosis (HH), which is associated with decrease in Lck activity in CD8 T cells.[70] Lck function is also impaired in people infected with the human immunodeficiency virus (HIV) and contributes to the pathogenesis of HIV, which is characterized by a depletion of CD4+ T cells.[82]

Molecules that selectively bind Lck can, therefore, be developed as useful tools for both clinical and basic biomedical research. They can aid in the search for Lck inhibitors as well as biomarkers for clinical research of human diseases.[76,77]

IV.2. Probe Design and Synthesis

Probe Design

SFKs were chosen as a target in this part of our study because, in addition to their crucial role in cell proliferation and differentiation,[65] they possess a conserved substrate binding site containing an adenine binding site and hydrophobic pockets, which can be targeted by benzophenone (Figure 18a).

To rationally design our probes, we computationally estimated the location of hydrophobic pockets that can accommodate benzophenone using a modeling protocol called multiple copy simultaneous search (MCSS) analysis.[83] MCSS is based on a combination of Monte Carlo and energy minimization-quenched dynamic techniques.[84] This method allows the efficient determination of energetically favorable positions and orientations of functional groups in a protein binding site whose three-dimensional structure is known.[83,85] The crystal structures of Lck, Src, and Fyn with a bound ATP-analogue were obtained from of the Protein Data Base (PDB) and used for MCSS analysis, which allowed the prediction of potential benzophenone-binding sites near the adenine binding area.

Figure 18 illustrates a MCSS analysis in which multiple p-methyl benzophenone molecules were randomly generated on top of the hydrophobic region near the substrate-binding site and subjected to simultaneous energy minimization. Figure 18c shows the preferred orientation of p-methyl benzophenone in a hydrophobic pocket near the adenine binding site. This analysis revealed that the spatial distance between N^9-methyl group of the bound adenine and the p-methyl group of energy-minimized benzophenone is

approximately 13 Å (Figure 19). This distance was used to design a linker of appropriate length between the adenine and benzophenone moieties in our probes.

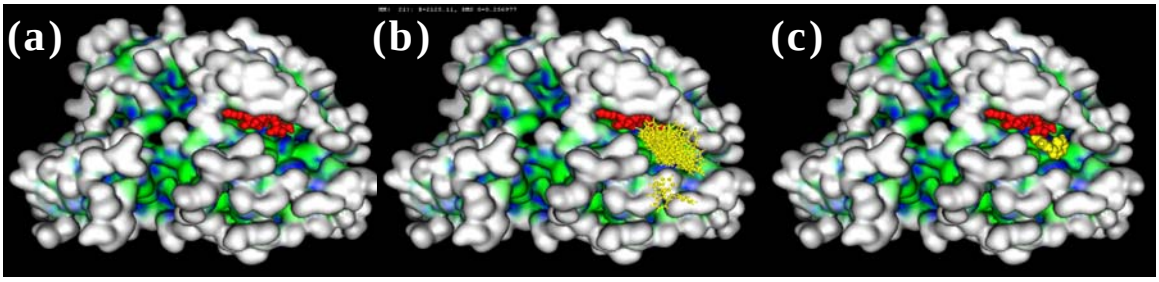

Figure 18. MCSS analysis of benzophenone-binding pockets on Src-family tyrosine kinases. (a) Src catalytic domain with ATP (red); hydrophobic pockets (green); hydrophilic pockets (dark blue); and solvent exposed area (white). (b) Multiple p-methylbenzophenone molecules (yellow) randomly generated on the hydrophobic substrate-binding region (green). (c) Minimized energy orientation of p-methyl-benzophenone (yellow). Method: See *Materials and Methods.*

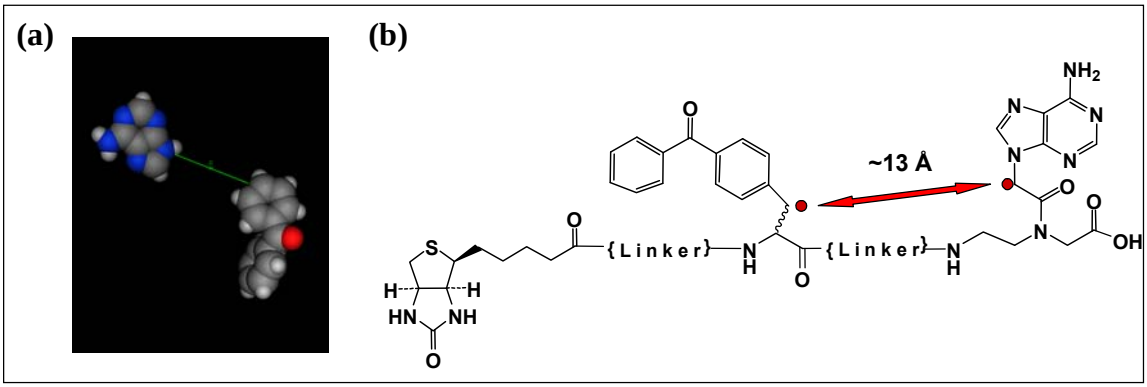

Figure 19. (a) Estimated distance between energy minimized adenine and p-methylbenzophenone as calculated from MCSS. (b) The minimum distance, required for the binding of adenine and benzophenone, was calculated from the N^9-methyl group of the bound adenine to the p-methyl group of the energy minimized benzophenone.

Figure 20 presents the set of photoactive ligands that were designed and synthesized to target SFKs. In the probes described in Chapter III (Figure 11), benzophenone was positioned near the C-terminus of the probe and was shown to be the major recognition unit. We suspected that the poor role of adenine in protein recognition of these probes resulted from steric hindrance by the benzophenone and biotin moieties. Therefore, when designing the photoactive probes for SFKs, we decided to switch the positions of adenine and benzophenone and place the adenine near the C-terminus of the probe (Figure 20). This switch was expected to increase the exposure of adenine to target proteins and enhance its role in the recognition by kinases.

To evaluate the effect of probes' chirality on binding selectivity two pairs of diastereoisomers were prepared (Figure 20). Since the calculated distance between adenine and benzophenone units was a linear (through-space) distance, the ideal through-bond distance was expected to be longer. Therefore, we treated the calculated through-space distance as the minimum distance, which was required to attain efficient interactions of the adenine and benzophenone with the adenine binding site and nearby hydrophobic area, respectively. Probes **4-S** and **4-R** have a through-bond distance of approximately 13 Å between the N^9-methyl group of the adenine and the p-methyl group of the benzophenone, whereas, in probes **5-S** and **5-R**, this distance is longer, e.g. approximately 16.5 Å.

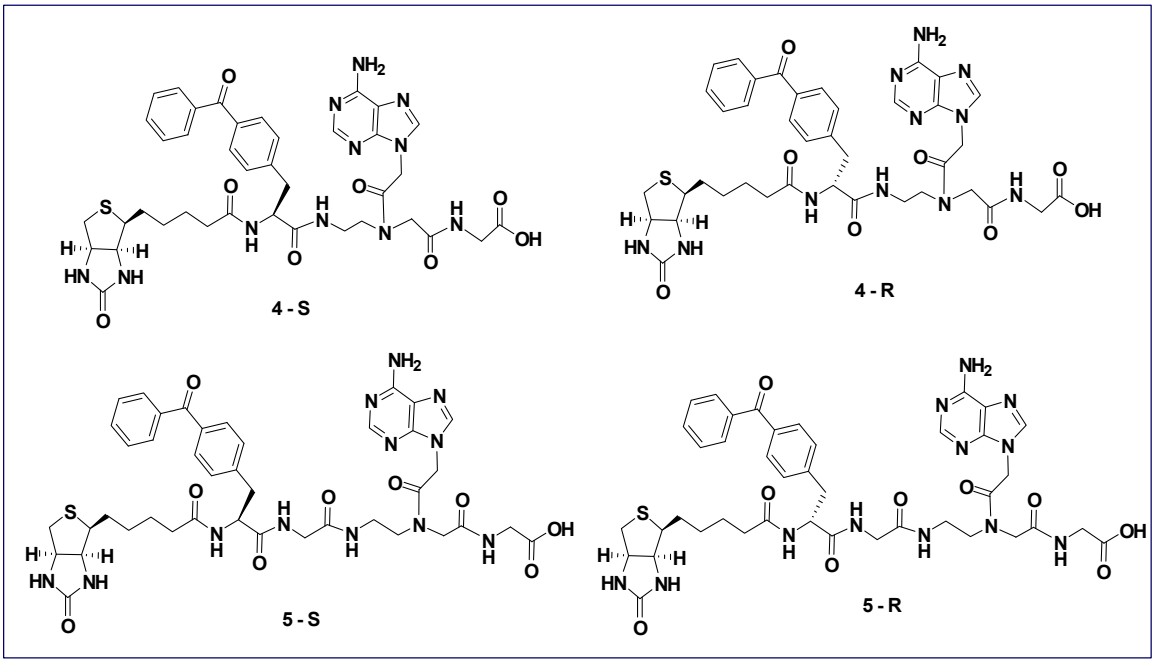

Figure 20. Structures of photoactive probes for selective labeling of the Src family of tyrosine kinases.

Probe Synthesis

Probe synthesis was performed on solid phase support using standard Fmoc/Bhoc chemistry (Scheme 2).[59] Starting with Fmoc-Gly-Wang resin, the Fmoc was removed under basic conditions (20% piperidine in DMF). Next, *N*-(N^6-Bhoc-adenine-N^9-acetyl)-*N*-(2-Fmoc-aminoethyl)glycine (Fmoc-PNA-adenine(Bhoc)-OH) was coupled using *N*,*N*'-dicyclohexylcarbodiimide (DCC) and HOBT as coupling reagents. After deprotection of the Fmoc group, the subsequent monomer, Fmoc-glycine, was introduced. The new N-terminal was then exposed by removal of the Fmoc group, and

coupled to Fmoc-4-benzoyl-L-phenylalanine (Fmoc-Bpa-OH). After removing of the Fmoc group, biotin *N*-hydroxysuccinimide was coupled to the Bpa monomer.

The desired probe is cleaved from the resin using a solution of 95% TFA, 2.5% water, 2.5% triisopropylsilane (TIS). Following synthesis and purification, each probe was characterized via chromatographic and spectroscopic analytical techniques. The crude yields for the solid phase synthesis of probes **4-S/R** and **5-S/R** were 70-80%.

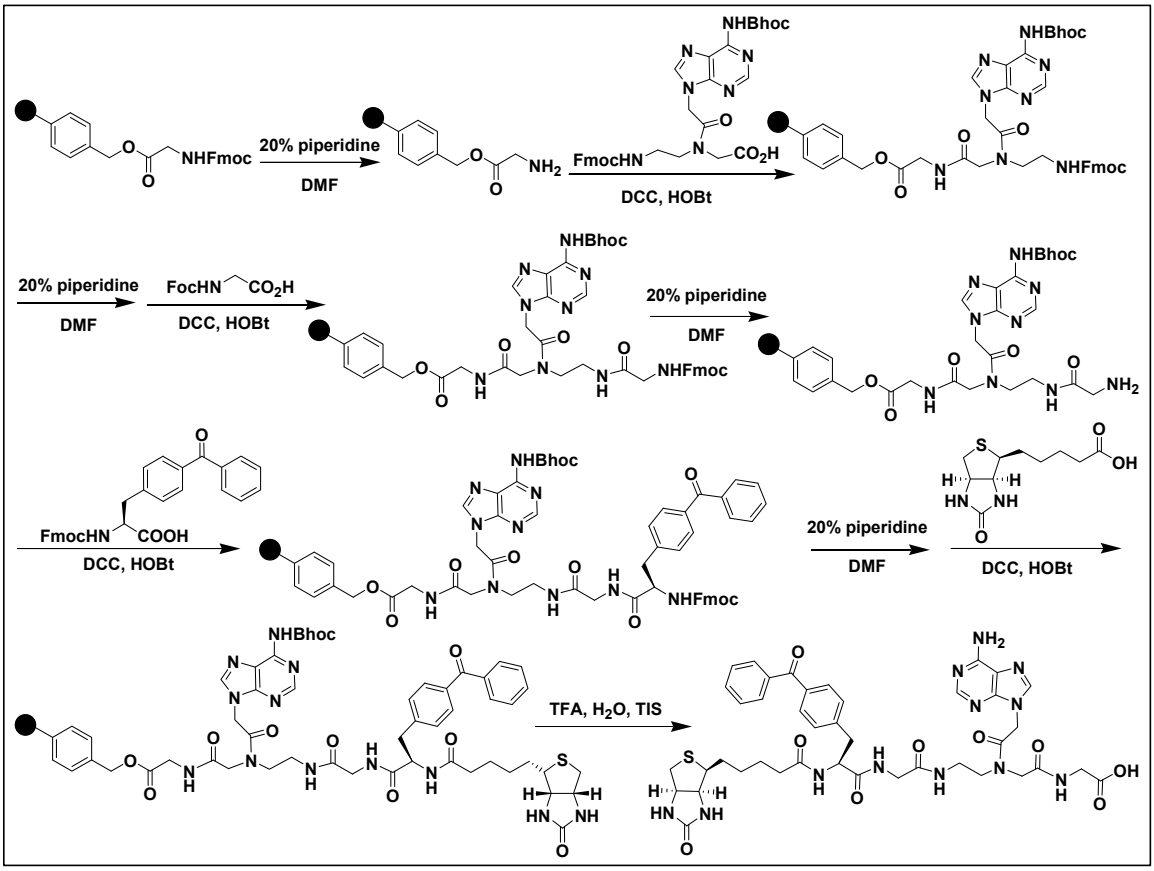

Scheme 2. Solid-phase synthesis of probe **5-S**.

IV.3. Binding Selectivity Evaluation

Binding Selectivity with Purified Kinases

To evaluate the binding selectivity of probes **4-S**, **4-R**, **5-S**, and **5-R**, we initially screened a panel of six commercially available kinases, including PKA, GSK3, CK1, Src, Fyn, and Lck. Kinases were incubated with probes and irradiated under an UV-A lamp (λ_{max}=350nm). Samples were then subjected to denaturing SDS-PAGE and blotted onto PVDF membrane. Blotted membrane was treated with an anti-biotin horseradish peroxidase-conjugated antibody, and biotinylated proteins were visualized by chemiluminescence.

Our original expectation was that probes would show some selectivity toward all Src-family kinases (Src, Fyn, Lck) over other kinases (Ser/Thr kinases), since Src-family kinases share substrate specificity. However, probe **5-S** showed great selectivity within SFKs by labeling only Lck (Figure 21a). Interestingly, its stereoisomer, probe **5-R**, did not label any of the kinases, underscoring the importance of stereochemistry in probe-Lck interaction (Figure 21b). Probes **4-S** and **4-R** showed no bands when assessed with purified kinases (data not shown). Next, we examined the selectivity of probe **5-S** toward additional kinases, e.g. VEGFR2, EGFR, MAPK, CK2, and PKC. As shown in Figure 22, only Lck was labeled when probe **5-S** was incubated with ten different kinases. This selectivity might result from sequence differences within the hydrophobic pocket of the structurally related SFKs.[77] This point will be further discussed in Chapter V.

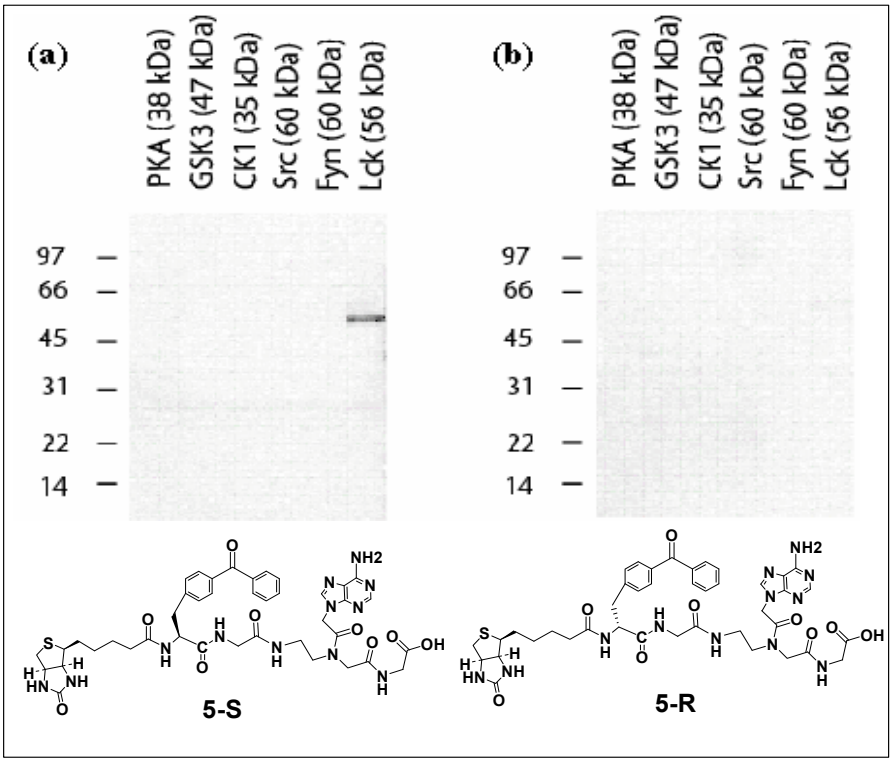

Figure 21. Photolabeling studies of a panel of six purified kinases (a) Selective labeling of Lck with probe **5-S** (b) None of the six kinases was labeled with probe **5-R**.

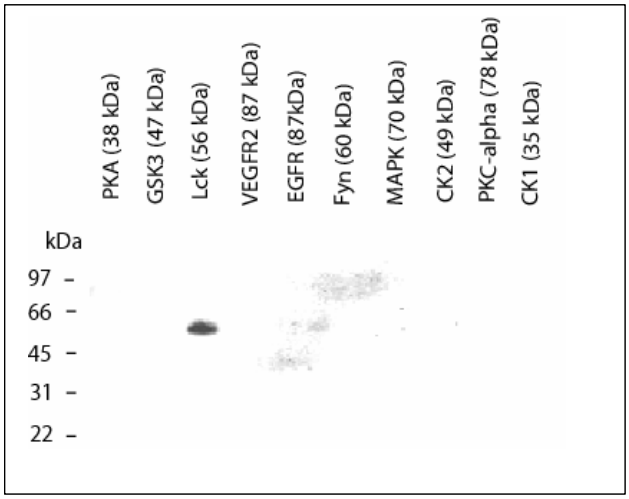

Figure 22. Photolabeling study of a panel of ten purified kinases tagged with probe **5-S**. Only Lck was labeled with **5-S**.

The binding profile of each of the ten kinases was subsequently evaluated using all probes: **1-S**, **1-R**, **2-S**, **2-R**, **3-S**, **3-R**, **4-S**, **4-R**, **5-S**, and **5-R**. However, only Lck and probe **5-S** showed a binding interaction resulting in an intense band around 57 kDa (Figure 23).

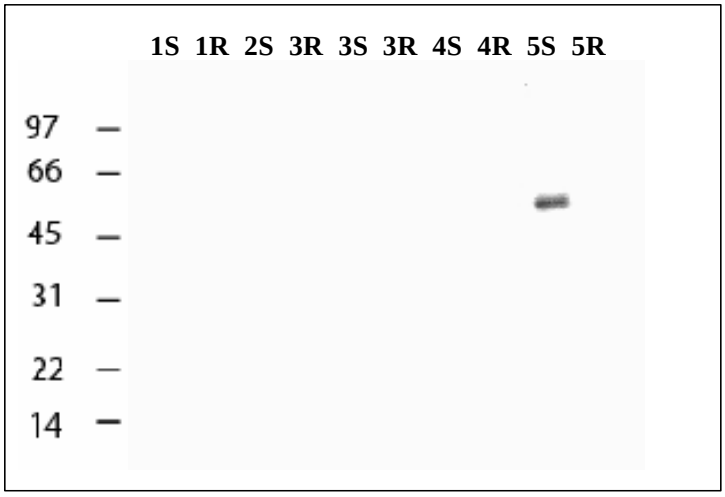

Figure 23. Photolabeling study of Lck with probes **1-S**, **1-R**, **2-S**, **2-R**, **3-S**, **3-R**, **4-S**, **4-R**, **5-S**, and **5-R**. Only **5-S** labeled Lck.

Considering the labeling results of Lck with **1-S/R-5-S/R** and the structural differences among these probes, we identified several structural motifs crucial for Lck-probe interaction. First, the location of the adenine unit within the probe is important for Lck recognition. **5-S**, in which adenine is near the C-terminus of the probe, labeled Lck. However, **2-S**, in which the adenine moiety is in the middle of the probe, did not label Lck. This observation may result from steric hinderance of the adenine group by the neighboring benzophenone and biotin units preventing its interactions with the ATP-binding site on Lck.

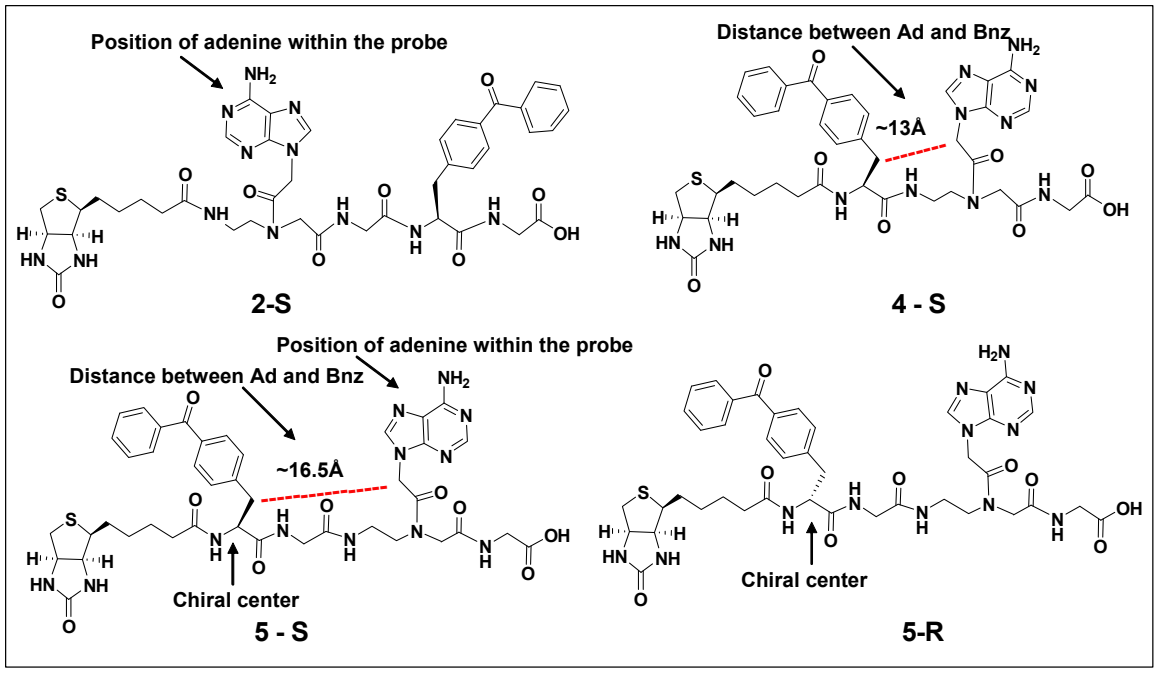

Figure 24. Structural motifs important for Lck-probe **5-S** interaction: probe's chirality, distance between adenine and benzophenone, and position of adenine within the probe.

Another important structural motif is the distance between the benzophenone and adenine, as shown by comparing **4-S** and **5-S**. **4-S**, in which the through-bond distance between the N^9-methyl group of the adenine and the p-methyl group of the benzophenone was approximately 13 Å, did not label Lck, whereas **5-S**, in which this distance was 16.5 Å, labeled Lck. This result may indicate that in order to attain the ideal 13 Å through-space distance between adenine and benzophenone a longer through-bond distance is required, probably due to bond angels and three-dimensional structure of our probe.

Finally, the chirality of the probe was found to be crucial for Lck recognition, as accentuated by labeling of Lck with **5-S** and not its diastereoisomer, **5-R**. This chiral

recognition can be explained by interactions of **5-S** with asymmetric hydrophobic pockets containing distinctive spatial alignment of amino acid.

To gain additional insight into the interaction between Lck and probe **5-S**, a series of blocking experiments was carried out. Lck was pre-incubated with an excess (10×) of adenine, benzophenone, or biotin prior to photolabeling with probe **5-S**. As shown in Figure 25, free benzophenone significantly reduced band intensity (lane 2), whereas free adenine resulted in the disappearance of the band (lane 3). As expected, biotin showed no effect on probe-Lck interaction (lane 4). These results are consistent with the rational design of our probe, as they indicate that both adenine and benzophenone play a role in **5-S** recognition by Lck.

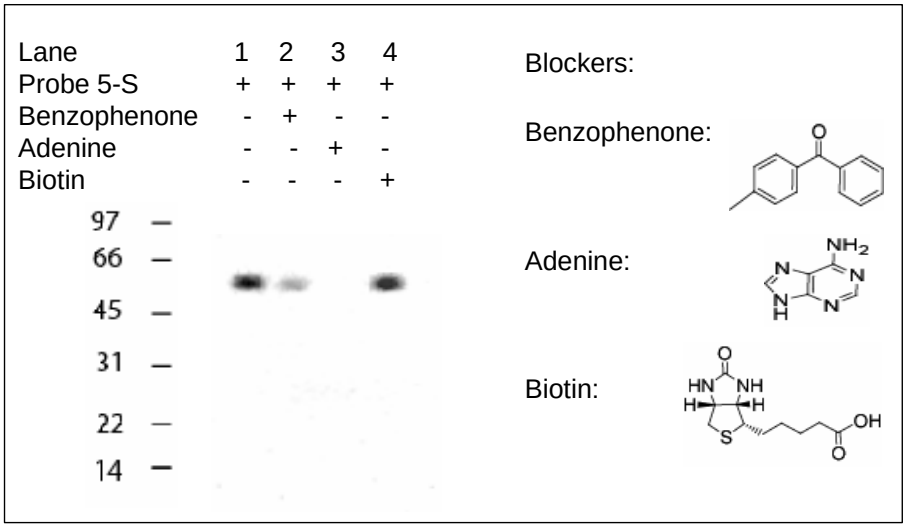

Figure 25. Blocking experiments. (a) photolabeling study of Lck with probe **5-S** in the presence or absence of free benzophenone, adenine, and biotin as blocker. (b) Structures of benzophenone, adenine, and biotin blockers.

Binding Selectivity in Protein Mixture

After demonstrating the selectivity of **5-S** toward Lck using purified kinases, we aimed to establish its selectivity in a complex mixture of proteins. Selectivity of probe **5-S** toward Lck in a complex proteome was examined using cytosolic proteins from Jurkat, a lymphocyte cell line known to express Lck. Protein were extracted by suspension of Jurkat cell pellets in a hypotonic lysing buffer and concentrated to a final concentration of 0.7 μg/μl (see *Materials and Methods*).

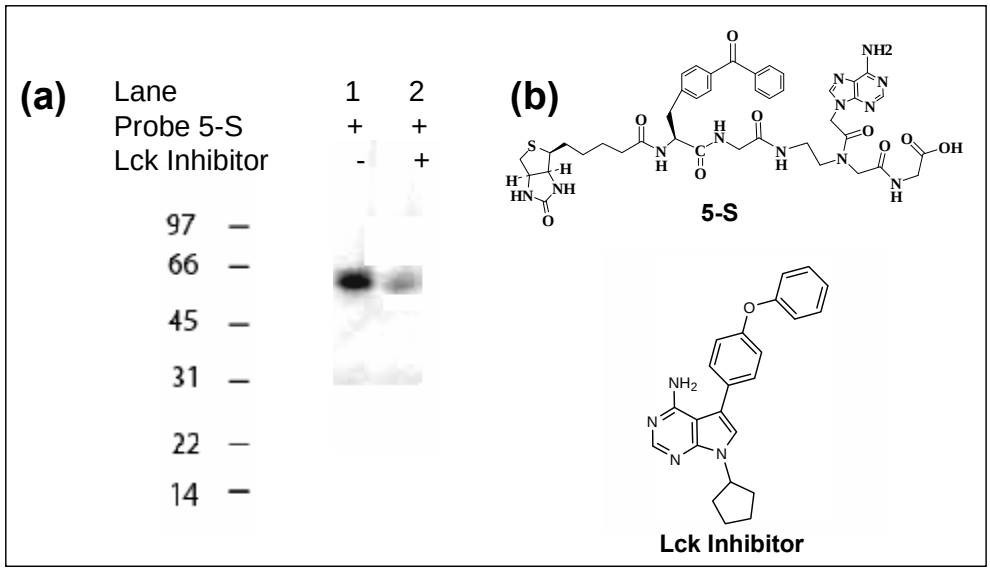

Figure 26. Photolabeling study of cytosolic extract of Jurkat Cells with probe **5-S** and Lck inhibitor. (a) Selective labeling of Lck in cytosolic extract of Jurkat cells. (b) Structure of probe **5-S** and Lck inhibitor.

Photolabeling of cytosolic proteins with probe **5-S** gave an intense band at approximately 60 kDa, which corresponds to the molecular weight of Lck (Figure 26a, lane 1). To verify that the observed band was due to labeling of Lck by **5-S**, we

performed blocking experiments using ATP-competitive inhibitor of Lck.[78] When Jurkat lysate was pre-incubated with an ATP-competitive inhibitor of Lck[78] (Figure 26b), the intensity of the band at 60 kDa significantly decreased (Figure 26a, lane 2).

These results confirmed that probe **5-S** selectively tagged Lck, even in a complex mixture of proteins.[39] Furthermore, the effect of ATP-competitive inhibitor on the labeling of Lck by probe **5-S** implied that our probe binds at the catalytic binding site of Lck as originally expected.

IV.5. Summary and Conclusions

In this part of my thesis, our proteomic chemical methodology was successfully employed for development of a prototype photoactive probe (**5-S**) for selective labeling of Lck.[39] This probe was one of several compounds originally designed to target the active site of SFKs based on the unique topology of their substrate-binding site. All probes consist of biotin, benzophenone, and adenine moieties tethered through a peptide backbone with different length or stereochemistry. However, only probe **5-S** selectively labeled Lck kinase when screened with a panel of purified kinases. Furthermore, probe **5-S** showed high selectivity toward Lck in a lysate of Jurkat cells.

Blocking experiments revealed that both adenine and benzophenone were involved in the recognition of **5-S** by Lck. Furthermore, blocking experiment using ATP-competitive inhibitor of Lck, confirmed that labeling of Lck by **5-S** depended on the probe's binding affinity toward the active site of the enzyme.

The structural motifs crucial for **5-S**-Lck interactions were identified as the adenine and benzophenone units, the distance between them and their position within the probe. In addition, the stereochemistry of the peptide backbone in the base of the benzophenone unit was shown to have crucial role in recognition of **5-S** by Lck.

Based on these findings, we aimed to continue our study toward developing new probes of higher affinity and selectivity toward Lck as well as other SFKs. To accomplish this task, we first had to study the **5-S**-Lck complex and understand the molecular basis for the selectivity toward Lck.

In conclusion, we identified a photoactive Lck ligand, **5-S**, which can selectivity tag Lck in complex proteome. We determined the key structural motifs crucial for **5-S**-Lck interactions and confirmed that the labeling by **5-S** depends on the probe's binding affinity toward the active site of the enzyme.

The **5-S**-Lck complex is an interesting system of molecular recognition for further study to improve our probes' design strategy. Therefore, our next steps, as described in Chapter V, were to determine **5-S** binding site, obtain a structural model of **5-S**-Lck complex and perform structure affinity relationship studies.

IV.6. Materials and Methods

Multiple copy simultaneous search analysis (MCSS)

All calculations were carried out using the Molecular Operating Environment (MOE) package (Chemical Computing Group Inc., Quebec, Canada). Crystal structures of Lck, Src, and Fyn combined with ATP-analogue were obtained from Protein Data Bank. After addition of hydrogens, the energy of these complexes was minimized using Assisted Model Building and Energy Refinement (AMBER). The sugar and phosphate parts of the ATP analogue were then cut off, and on top of each of the hydrophobic pockets one hundred benzophenone molecules were randomly generated. The resulting complex was energy minimized using Merck Molecular Force Field 94 (MMFF94).[86] To reduce computational time, this study was carried out without considering solvent effects. (Parameters: Copies of benzophenone generated: 100, Copies RMSD: 0.2, RMS gradient: 0.01, Belly distance: 0).

Materials & Physico-chemical analytical methods

See page 39-40.

Chemical Synthesis

Probe synthesis was accomplished manually using a stepwise solid-phase procedure. All couplings were carried out for 10 hours in dimethylformamide (DMF) using a 2-fold excess (over resin loading) of protected monomer, activated with an equimolar of HOBt and DCC. Reaction was monitored using the Kaiser test for free amines.[62] *N*-Fmoc group was removed using 20% (v/v) piperidine in DMF. Probes were removed from the solid support with simultaneous sidechain deprotection using a 95%

trifluoroacetic acid (TFA), 2.5% triisopropylsilane (TIS) and 2.5% water solution for 2 h at room temperature. TFA was removed under reduced pressure. Crude material was precipitated and washed with cold petroleum ether. Probes were purified using semi-preparative HPLC. Crude yield's range was 28% - 94%. The purified probes were analyzed using Analytical HPLC, Mass Spectroscopy, and ^{1}H-NMR.

Probe 4-S [Biotinyl-p-benzoyl-L-phenylalanyl-adenine-*N*^{9}-acetyl-(2-aminoethyl) glycinyl-glycine]

^{1}H-NMR δ ppm (500MHz, DMSO) 8.55 (1H, t, NH), 8.32 (1H, m, NH), 8.30 (1H, m, CH), 8.15 (1H, s, CH), 7.60-7.25 (9H, m, 9xCH), 7.15 (2H, s, NH_2), 6.00 (2H, m, 2xNH), 5.20 (2H, m, CH_2), 4.35 (1H, m, CH), 4.19 (1H, m, CH), 4.15 (2H, m, CH_2), 4.10 (1H, m, CH), 3.78 (2H, m, CH_2), 3.55 (2H, m CH_2), 3.30 (2H, m, CH_2), 3.20 (2H, m, CH_2), 2.85 (1H, m, CH), 2.70 (2H, m, CH_2), 2.08 (2H, m, CH_2), 1.52-1.05 (6H, m, $CH_2CH_2CH_2$). ESIMS (expected m/z 827.3) m/z 828.5 (MH^+), 414.75 ($M2H^+/2$). Analytical RP-HPLC retention time: 17.00 min.

Probe 4-R [Biotinyl-p-benzoyl-D-phenylalanyl-adenine-*N*^{9}-acetyl-(2-aminoethyl) glycinyl-glycine]

^{1}H-NMR δ ppm (500MHz, DMSO) 8.60 (1H, t, NH), 8.42 (1H, m, NH), 8.35 (1H, m, CH), 8.05 (1H, s, CH), 7.64-7.25 (9H, m, 9xCH), 7.19 (2H, s, NH_2), 6.05 (2H, m, 2xNH), 5.25 (2H, m, CH_2), 4.25 (1H, m, CH), 4.18 (1H, m, CH), 4.15 (2H, m, CH_2), 4.10 (1H, m, CH), 3.70 (2H, m, CH_2), 3.50 (2H, m CH_2), 3.35 (2H, m, CH_2), 3.24 (2H, m, CH_2), 2.85 (1H, m, CH), 2.70 (2H, m, CH_2), 2.10 (2H, m, CH_2), 1.60-1.10 (6H, m, $CH_2CH_2CH_2$).

ESIMS (expected m/z 827.3) m/z 828.7 (MH^+), 414.70 ($M2H^+/2$). Analytical RP-HPLC retention time: 17.15 min.

Probe 5-S [Biotinyl-p-benzoyl-L-phenylalanyl-glycinyl-adenine-*N*^{9}-acetyl-(2-aminoethyl)glycinyl-glycine]

^{1}H-NMR δ ppm (500MHz, DMSO) 8.65 (1H, t, NH), 8.48 (1H, m, NH), 8.40 (1H, m, NH), 8.30 (1H, m, CH), 8.15 (1H, s, CH), 7.75-7.30 (9H, m, 9xCH), 7.25 (2H, s, NH_2), 6.36 (2H, m, 2xNH), 5.19 (2H, m, CH_2), 4.65 (1H, m, CH), 4.29 (1H, m, CH), 4.22 (2H, m, CH_2), 4.10 (1H, m, CH), 3.80 (2H, m, CH_2), 3.65 (2H, m CH_2), 3.40 (2H, m, CH_2), 3.20 (2H, m, CH_2), 3.1 (2H, m, CH_2), 2.95 (1H, m, CH), 2.75 (2H, m, CH_2), 2.17 (2H, m, CH_2), 1.60-1.15 (6H, m, $CH_2CH_2CH_2$). ESIMS (expected m/z 884.2) m/z 885.3 (MH^+), 443.2 ($M2H^+/2$). Analytical RP-HPLC retention time: 18.30 min.

Probe 5-R [Biotinyl-p-benzoyl-D-phenylalanyl-glycinyl-adenine-*N*^{9}-acetyl-(2-aminoethyl)glycinyl-glycine]

^{1}H-NMR δ ppm (500MHz, DMSO) 8.55 (1H, t, NH), 8.48 (1H, m, NH), 8.30 (1H, s, CH), 8.25 (1H, s, CH), 7.80-7.35 (9H, m, 9xCH), 7.30 (2H, s, NH_2), 6.30 (2H, m, 2xNH), 5.20 (2H, m, CH_2), 4.65 (1H, m, CH), 4.30 (1H, m, CH), 4.22 (2H, m, CH_2), 4.05 (1H, m, CH), 3.75 (2H, m, CH_2), 3.60 (2H, m CH_2), 3.46 (2H, m, CH_2), 3.25 (2H, m, CH_2), 3.10 (2H, m, CH_2), 2.9 (1H, m, CH) 2.75 (2H, m, CH_2), 2.19 (2H, m, CH_2), 1.10-1.55 (6H, m, $CH_2CH_2CH_2$). ESIMS (expected m/z 884.2) m/z 885.2 (MH^+), 907.2 (MNa^+), 443.1 ($M2H^+/2$). Analytical RP-HPLC retention time: 18.25 min.

Biological Assays

Photolabeling of kinases

20 µl aliquots of purified kinases (1 µg/µL) were mixed with 2 µl of 1 mM probe solution in DMSO. For blocking experiments, 20 µl aliquots of the lysate were mixed first with 2 µl of a blocking solution in DMSO (10 mM adenine, 10 mM benzophenone, 10 mM biotin, or DMSO control) and then with 2 µl of 1 mM probe solution in DMSO. The mixtures were incubated at 4 ºC for 1 h. Photocrosslinking was carried out under six Sylvania 350 Blacklight lamps (15 W, λ_{max} 350 nm) for 2 h, in which samples were kept on ice and placed approximately 5 cm below the lamps. Following the photocrosslinking, samples were mixed with Laemmli Sample Buffer with 5%(v/v) 2-mercaptoethanol, denatured at 80 ºC for 5 min and separated on SDS-PAGE (5-20% Tris-HCl gel, 200 V, 1 h) in 1× Tris-Glycine-SDS buffer. Gel was blotted onto PVDF membrane (200 mA, 1h) in a cold transfer buffer (20% methanol in 1× Tris-Glycine buffer). Blotted membrane was blocked with 5% non-fat milk in Tris-buffered saline containing 1% Tween 20 (TBS-T) for 1 h. Blocked membrane was rinsed with TBS-T (10 min × 3), treated with an anti-biotin hoarse radish peroxidase (HRP)-conjugated antibody (1:100 dilution in 2% non-fat milk in TBS-T) for 3 h, and washed with TBS-T (10 min × 3). The washed membrane was treated with the ECL-Plus chemiluminescence reagent for 5 min. Bands were observed with the BioRad ChemiDoc gel documentation system.

Photolabeling of Jurkat cytosolic proteins

Jurkat cells were maintained in Dulbecco's Modified Eagle Media containing 10% fetal calf serum and 1% penicillin-streptomycin-fungizone in a 37 ºC, 5% CO_2

incubator. For each labeling experiment, cells were harvested at the log phase (50-70% confluency) and plated onto a 10 cm tissue culture dish. Cells were then incubated overnight in a 37 ºC 5% CO_2 incubator. Cell pellets were then suspended in a hypotonic lysing buffer (pH 8, 10mM HEPES, 1.5mM $MgCl_2$, 10mM KCl, 0.1mM EDTA, and 1mM PMSF) and incubated at room temperature for 10 min. The swelled cells were then lysed by gentle pipetting. The lysates were centrifuged (10,000 rpm, 4 ºC). In the subsequent steps, protein solutions were always kept on ice or in a chromatography refrigerator (4 ºC). Protein concentration was quantified with Promega Commassie Plus™ Protein Assay Reagent. The final protein concentration used for the experiment shown in Figure 9 was 0.7 μg/μl. Photolabeling was carried out as described above, in the ***Photolabeling of Kinases*** section, using 2 μl of 1 mM probe solution and 2 μl of 1 μM of ATP-competitive inhibitor of Lck.

Chapter V

Characterization of Probe-Lck Complex

V.1. Binding Site Determination

To further investigate the unique selectivity of **5-S** toward Lck, we identified its binding site using MALDI-TOF mass spectrometry and LC/MS/MS. Samples were prepared by incubation of Lck with probe **5-S** in DMSO, or with a DMSO control, followed by photocrosslinking. Samples were then separated by SDS-PAGE and coomassie-stained protein bands were excised from the gel and submitted to mass spectrometric analysis. Proteins in excised bands were reduced with dithiothreitol (DTT) and digested with trypsin. Using a MALDI-TOF mass spectrometer, we identified a peptide fragment (m/z 1746.8) corresponding to Ile379-Arg386 (mw=861.9) (IADFGLAR) tagged with probe **5-S** (mw=884.9) (Figure 27). Peptides observed in this mapping covered 82% of the protein sequence. The unmodified peptide, IADFGLAR, was observed in both samples, but its intensity was lower in the sample treated with probe **5-S**.

To identify the exact covalent attachment point, LC-MS-ESI was employed. The triply charged ion (m/z 582.9) of labeled fragment IADFGLAR was eluted from the LC column at 29.24 minutes and analyzed by MS/MS (Figure 28). This analysis revealed that probe **5-S** is covalently attached to either Gly384 or Leu385 (Table 2), both of which are located near the adenine binding site of Lck.

Fragment ions resulting from cleavage between these two residues were not observed, despite numerous attempts. However, literature search revealed that, in biological systems, the most effective H-donors that can react with benzophenone carbonyl radical include electron-rich tertiary centers such as Cγ-H of leucine and C_β-H of valine, and those CH_2 groups adjacent to heteroatoms in lysine, arginine, and

methionine.[36] Additionally, since Leu385 is located in the outer edge of the hydrophobic pocket it is more accessible than Gly384 for interactions with probe **5-S**. Therefore, it is likely that the benzophenone moiety of probe **5-S** is photocrosslinked to the Leu384 residue of Lck.

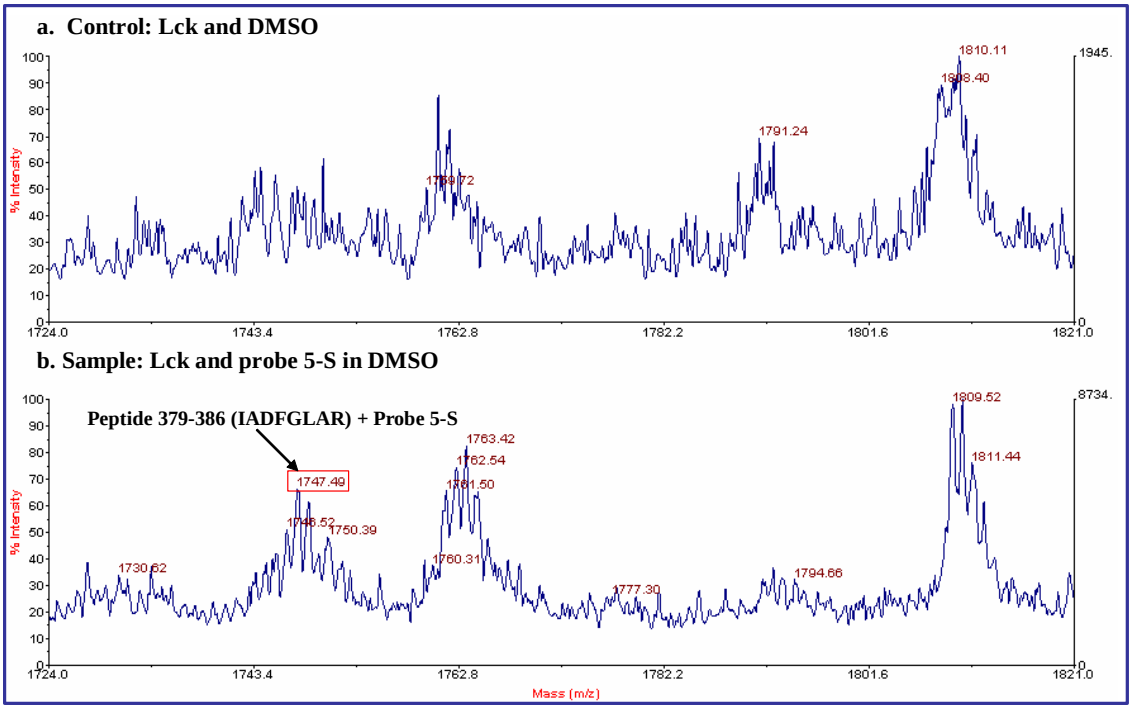

Figure 27. MALDI-TOF analysis of **a.** Control: Lck and DMSO and **b.** Sample: Lck tagged with probe **5-S**.

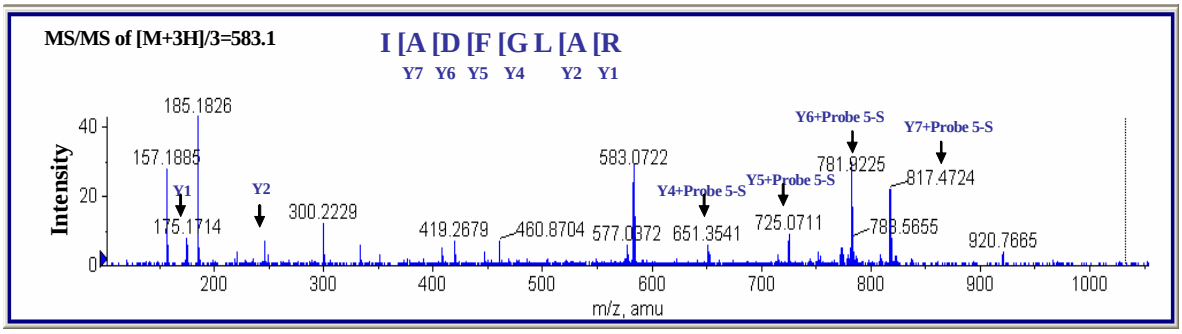

Figure 28. MS/MS analysis of the triply charged ion at m/z 582.9.

Table 2. MS/MS analysis of peptide IADFGLAR tagged with probe **5-S.**

Fragment	AA sequence	Calculated mw (g/mol)	Observed m/z
Y_1	R	174.2	MH^+ 175.17
Y_2	AR	245.3	MH^+ 246
Y_4	GLAR + probe **5-S**	1300.4	[M+2]/2 651.35
Y_5	FGLAR + probe **5-S**	1447.6	[M+2]/2 725.1
Y_6	DFGLAR + probe **5-S**	1562.6	[M+2]/2 781.9
Y_7	ADFGLAR + probe **5-S**	1633.7	[M+2]/2 817.47
	IADFGLAR + probe **5-S**	1747.49	[M+3]/3 583.1

V.2. Structural Model for 5-S-Lck Complex

MS/MS analysis confirmed that benzophenone binds to a hydrophobic region near the adenine binding site of Lck (Figure 29a). Based on this analysis and published data regarding the binding of adenine to its binding site on kinases,[72,76,77] we performed a conformational search of probe **5-S** within the binding site of Lck.

We used a stochastic search,[87,88] in which 10,000 conformers of probe **5-S** were randomly generated in the substrate binding site region of Lck with restrictions of 1-3 Å distance between the carbonylic radical of benzophenone and Cγ-H of the Leu384 residue of Lck. The energy of the generated molecules was then minimized using MMFF94. The conformational search resulted in a global minimum conformation which was more than

7 Kcal/mol lower than any other conformers. This global minimum conformation was used to obtain a structural model showing that the benzophenone moiety is surrounded by Phe255, Met279, Val258, Ala286 Glu287, Gly383, and Leu384 (Figure 29b). This model provides a structural basis for designing new Lck ligands with higher binding affinity and selectivity, as described in **V.4**.

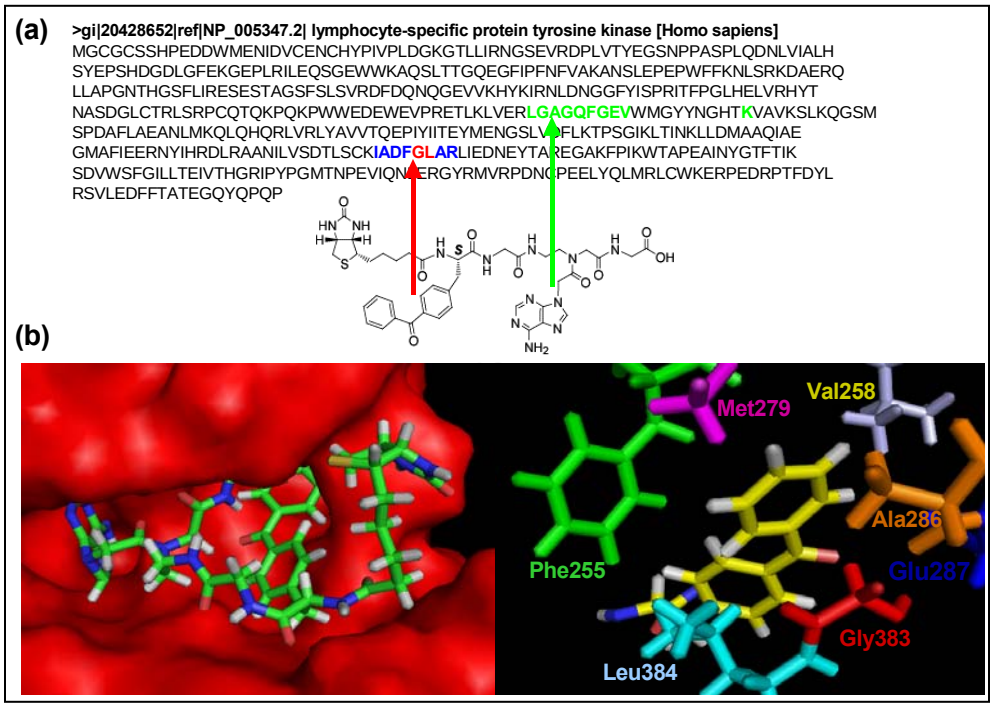

Figure 29. The current model of **5-S**-Lck complex. (a) Amino acid sequence of Lck's binding pockets (shown in blue and red). The amino acid sequence of the adenine binding site is shown in green. (b) Surface presentation of probe **5-S** in its binding pockets (shown on the left) and amino acid residues surrounding the benzophenone moiety (shown on the right).

V.3. On the Selectivity toward Lck

To understand the unique selectivity of probe **5-S** toward Lck, we focused our attention on the structural model of the **5-S**-Lck complex and the amino acid sequence of SFKs. Our current model of the **5-S**-Lck complex, and MS/MS analysis, showed that the probe binding site is located within the well conserved region of SFKs.[39] As illustrated in Figure 30, the photocrosslinking site (shown in red) as well as other amino acids around it (shown in blue) are conserved in Lck, Src and Fyn. Another binding site of **5-S** is the ATP-binding pocket (shown in green), which is also highly conserved among all kinases. Furthermore, all hydrogen bonding and hydrophobic interactions between **5-S** and Lck are mediated through amino acid residues (marked with blue asterisks) that are well conserved in SFKs. Therefore, it was surprising to find that **5-S** did not label other kinases with seemingly identical binding pockets.

```
                                                          *    *   ***          *
sp|P06239|LCK_HUMAN           TRLSRPCQTQKP----QKPWWEDEWEVPRETLKLVERLGAGQFGEVWMGYYNGHTKVAVK
sp|P06241|FYN_HUMAN           CRLVVPCHKGMPRLTDLSVKTKDVWEIPRESLQLIKRLGNGQFGEVWMGTWNGNTKVAIK
sp|P12931|SRC_HUMAN           HRLTTVCPTSKP---QTQGLAKDAWEIPRESLRLEVKLGQGCFGEVWMGTWNGTTRVAIK

                                    *    *  *            *               *
sp|P06239|LCK_HUMAN           SLKQGSMSPDAFLAEANLMKQLQHQRLVRLYAVVTQEPIYIITEYMENGSLVDFLKTPSG
sp|P06241|FYN_HUMAN           TLKPGTMSPESFLEEAQIMKKLKHDKLVQLYAVVSEEPIYIVTEYMNKGSLLDFLKDGEG
sp|P12931|SRC_HUMAN           TLKPGTMSPEAFLQEAQVMKKLRHEKLVQLYAVVSEEPIYIVTEYMSKGSLLDFLKGETG

                                                  * * **         ** **
sp|P06239|LCK_HUMAN           IKLTINKLLDMAAQIAEGMAFIEERNYIHRDLRAANILVSDTLSCKIADFGLARLIEDNE
sp|P06241|FYN_HUMAN           RALKLPNLVDMAAQVAAGMAYIERMNYIHRDLRSANILVGNGLICKIADFGLARLIEDNE
sp|P12931|SRC_HUMAN           KYLRLPQLVDMAAQIASGMAYVERMNYVHRDLRAANILVGENLVCKVADFGLARLIEDNE
```

Figure 30. Sequence alignment of Lck, Fyn, and Src. The probe-binding region of Lck was aligned with Fyn and Src using CLUSTAL W (1.82) on Expasy. The ATP-binding site is shown in green. The photocrosslinking site on Lck, Gly383/Leu384, is highlighted in red and the amino acids around it are highlighted in blue.

Since amino acid sequence alignment of Src, Fyn and Lck did not account for **5-S** selectivity, differences in their three-dimensional structures were examined. Crystal structures of Src, Fyn, and Lck were superimposed on MOE (Figure 31) revealing some differences in their three-dimensional structures. The crystal structure of Src did not resolve a loop around the benzophenone binding site, implying that the loop region has high mobility. This region, might therefore reduce benzophenone accessibility into the hydrophobic area and prevent **5-S** from labeling Src. Additionally, there are differences in protein folding in the upper part of the pocket that might account for differences in binding selectivity.

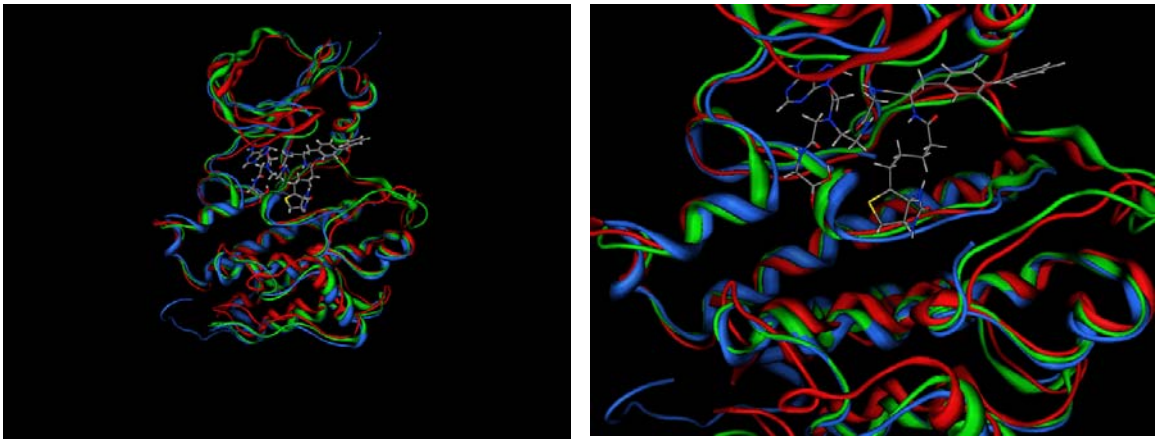

Figure 31. Spatial alignment of Lck (red), Src (blue), and Fyn (green).

It is important to note that in order to obtain efficient labeling of a target protein with our probe (Figure 32), an initial binding affinity interaction needs to coexist with specific orientation of the benzophenone photophore in order to satisfy the geometrical requirements of the photocrosslinking reaction.[36,49] Therefore, it is possible that probe **5-**

S has affinity interactions with other kinases in addition to Lck, but benzophenone orientation allows efficient labeling only in **5-S**-Lck complex. To test this possibility, we have to examine the affinity and selectivity of **5-S** toward SFKs regardless of the photocrosslinking step. This can be done by affinity studies using avidin-coated resin, as discussed in Chapter VI.

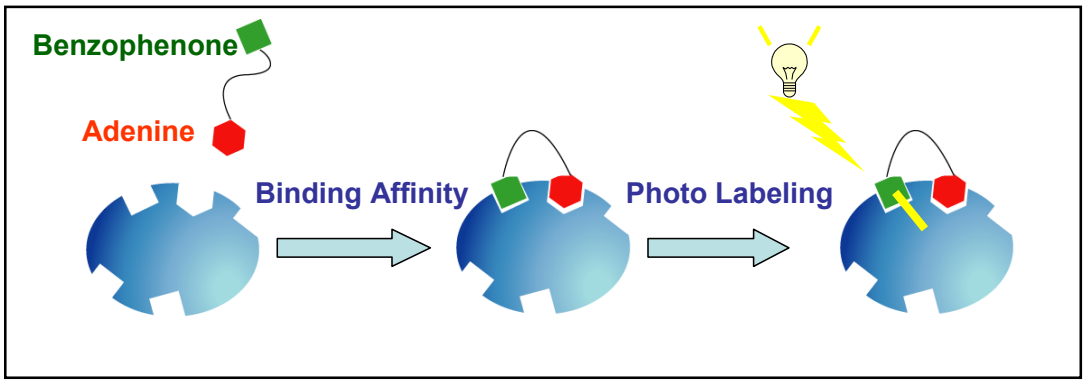

Figure 32. Photoaffinity labeling with our adenine-benzophenone conjugate probe. To attain an efficient labeling, the binding affinity interaction needs to be followed by an efficient photolabeling reaction.

V.4. Structure Affinity Relationship Study on Probe 5-S

To confirm our structural model for the **5-S**-Lck complex, and to identify structural motifs for increased affinity and selectivity, we carried out structure affinity relationship studies on probe **5-S**. A new set of probes was designed and synthesized on a solid phase support as described before (See Materials & Methods). Structures of new probes were derived from the structure of **5-S,** with modifications to the peptide backbone connecting the adenine, benzophenone, and biotin moieties (Figure 33).

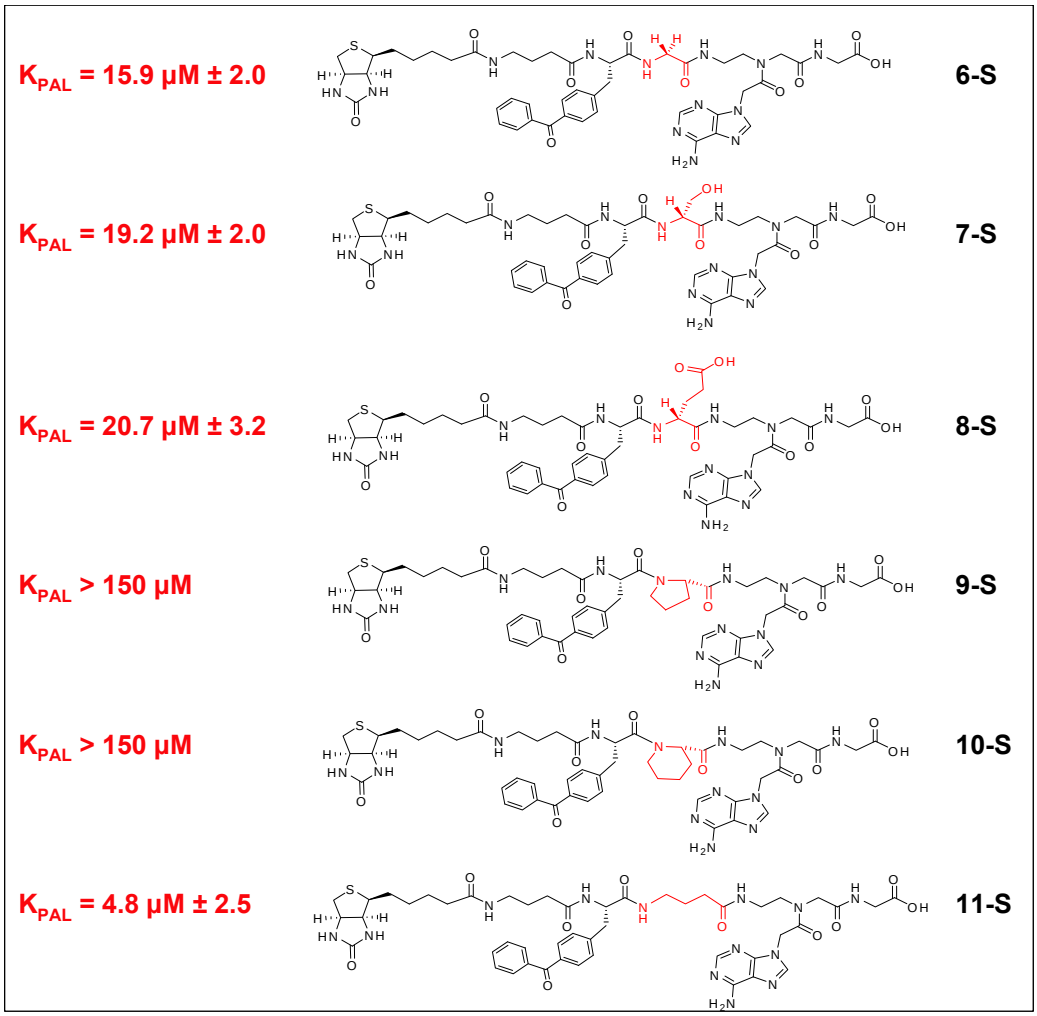

Figure 33. Structures of the modified probes and their photoaffinity labeling constants (K_{PAL}).

Binding selectivity of these probes was evaluated as described in chapter II, using Lck, Src, Fyn, BCR-Abl, PKA, GSK3, CK1, VEGFR, EGFR, CK2, MAP42 and PKC. All probes showed selectivity toward Lck and did not label other kinases. Since labeling of Lck requires both affinity toward the substrate-binding site of Lck and efficient photolabeling, we quantified the efficiency of our probes by calculating their relative photoaffinity labeling constant (K_{PAL}). This constant was obtained by photolabeling of Lck with different concentrations of each probe. Intensities of the observed bands were plotted against probe concentration and the concentration that resulted in 50% of the maximum intensity was taken as K_{PAL} (Figure 34). Triplicate experiments were carried out for each probe.

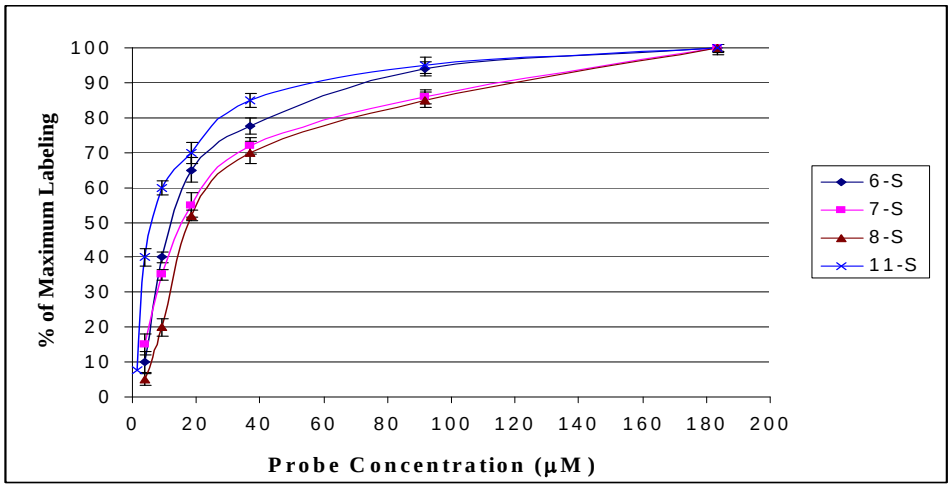

Figure 34. Photoaffinity labeling curves of Lck with probes **6-S**, **7-S**, **8-S**, and **11-S**. Data is taken from triplicate labeling experiments of Lck with different concentrations (3, 9, 18, 36, 90, 180, and 360 mM) of probes **6-S, 7-S, 8-S**, and **11-S**.

As shown in Figure 35a, **5-S** was first modified by introducing γ-amino butyric acid between biotin and benzophenone to obtain **6-S**. One reason for this modification

was to confirm our structural model. Since biotin is sticking out of the binding pocket (Figure 35b) and does not participate in recognition by Lck, changing its distance from the benzophenone unit was not expected to affect binding selectivity or photoaffinity. As expected, **6-S** labeled only Lck with the same photoaffinity binding as **5-S**.

Another reason for this modification was to increase the distance between the biotin and benzophenone units. The longer linker allowed the use of avidin horseradish peroxidase (HRP), instead of anti-biotin HRP conjugated antibody, for more sensitive detection of tagged kinases. Since **6-S** maintained the same selectivity and photoaffinity as **5-S** while offering a technical advantage over **5-S**, we used the structure of **6-S** as a model for further modifications.

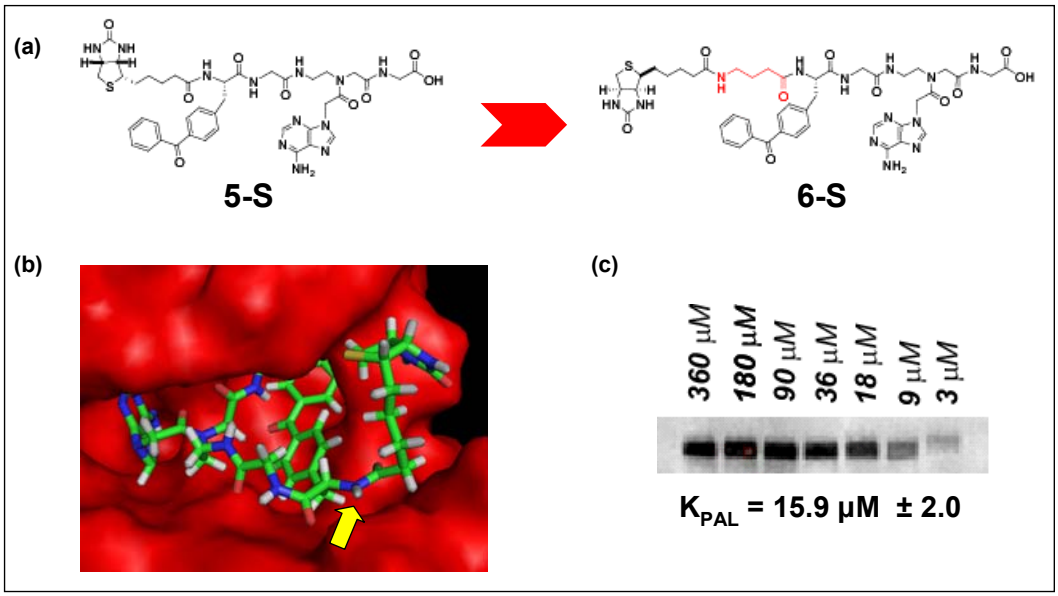

Figure 35. (a) Structures of probes **5-S** and **6-S**. (b) Model of probe **5-S** in its binding pocket. The modified site is indicated by an arrow. (c) Photolabeling of Lck with different concentrations of probe **6-S** and the calculated K_{PAL} value.

To improve the photoaffinity labeling of **6-S** (K_{PAL} = 15.9 μM ± 2.0), its pro-*R* hydrogen in the glycine between adenine and benzophenone was modified (Figure 36b). This hydrogen does not participate in the binding interactions with Lck, therefore it was replaced with serine (probe **7-S**) and glutamic acid (probe **8-S**) residues (Figure 36a). This modification was expected to allow additional interactions between the probe and polar amino acids in the substrate binding site, without impairing existing interactions. For example, the hydroxyl group of serine residue or carbonylic group of glutamic residue could form hydrogen bonding with the peptidic backbone.[77]

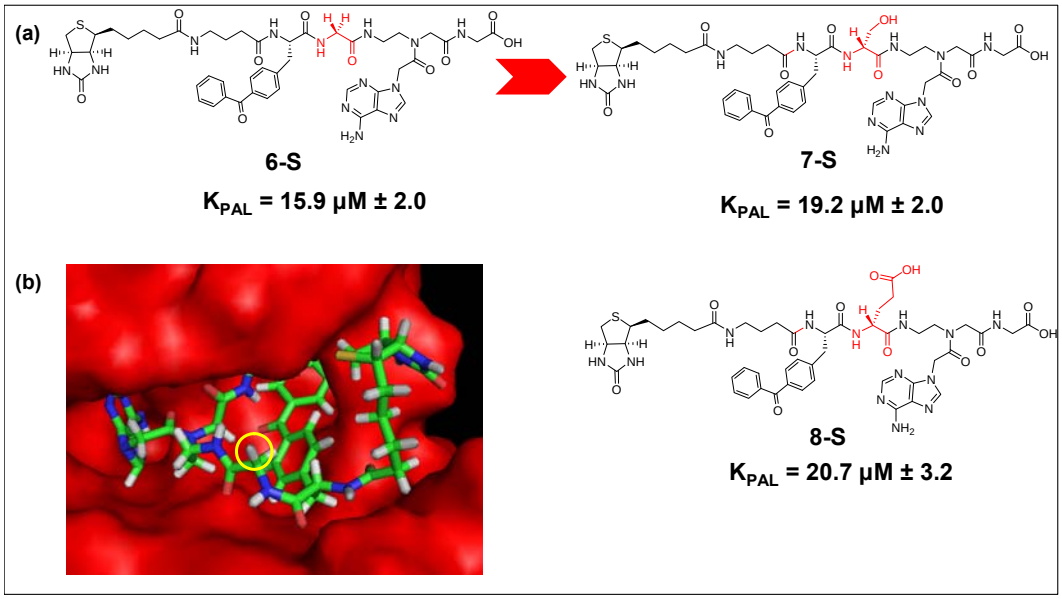

Figure 36. (a) Structures of probes **6-S**, **7-S**, and **8-S** and their photoaffinity labeling constant (K_{PAL}). (b) Model of probe **5-S** in its binding pocket. The modified hydrogen is indicated by a circle.

However, probes **7-S** and **8-S** (K_{PAL} = 19.2 μM ± 2.0 and 20.7 μM ± 3.2, respectively) did not show significant differences in their photoaffinity labeling when

compared to **6-S**. One reason might be that the distance between the probe and Lck at the modified point is too big to be bridged by these residues. Additionally, it is possible that these residues do form additional interactions with Lck, however, these interactions may not affect the overall photoaffinity labeling efficiency.

In an effort to further improve photoaffinity labeling of our probes, we increased the rigidity of the linker between benzophenone and adenine by replacing the glycine linker in proline (probe **9-S**) and piperidine (probe **10-S**) (Figure 37a).

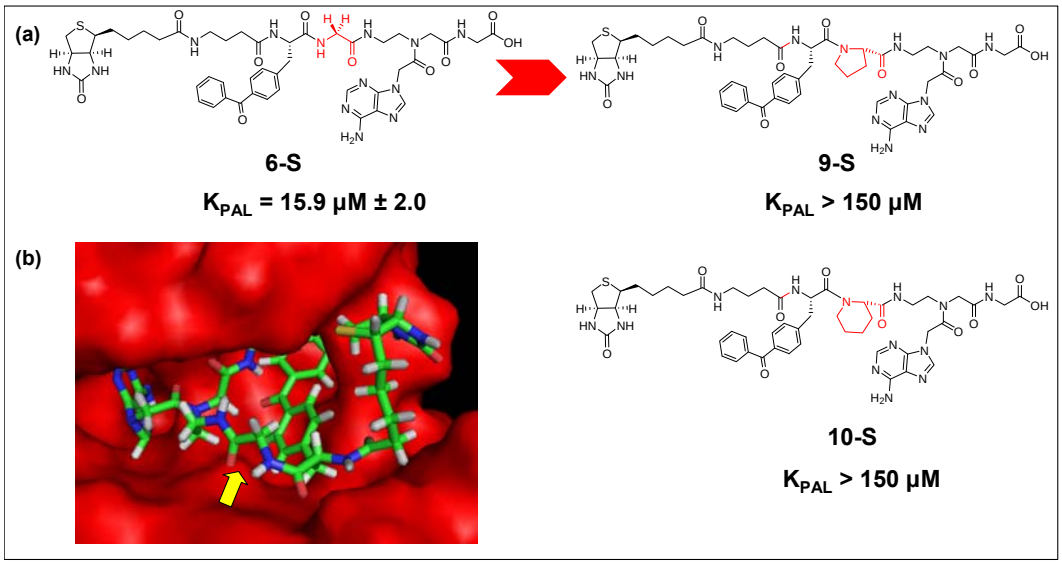

Figure 37. (a) Structures of probes **6-S**, **9-S**, and **10-S** and their photoaffinity labeling constant (K_{PAL}) (b) Model of probe **5-S** in its binding pocket. The modified site is indicated by an arrow.

This modification restricted the conformational freedom of benzophenone and adenine and was expected to improve binding affinity by reducing the entropic penalty that has to be paid in the formation of Lck-**5-S** complex.[36,72] However, this modification

resulted in dramatic reduction of the photoaffinity labeling of the probes (K_{PAL} > 150 μM ± 2.0). The reasons for the reduced activity can be the loss of binding interactions between the probe and Lck or loss of ability of the benzophenone to achieve the geometric requirements for the labeling reaction.[36]

Poor photoaffinity labeling of **9-S** and **10-S** implied that flexibility of the linker between recognition units of the probe is essential for recognition by Lck. Therefore, we decided to increase the length and flexibility of the linker between the adenine and benzophenone units by replacing the glycine with γ-amino butyric (Figure 38). This modification resulted in a three-fold increase in photoaffinity labeling of Lck by probe **11-S** (K_{PAL} = 4.8 μM ± 2.5) relative to **6-S** (K_{PAL} = 15.9 μM ± 2.0).

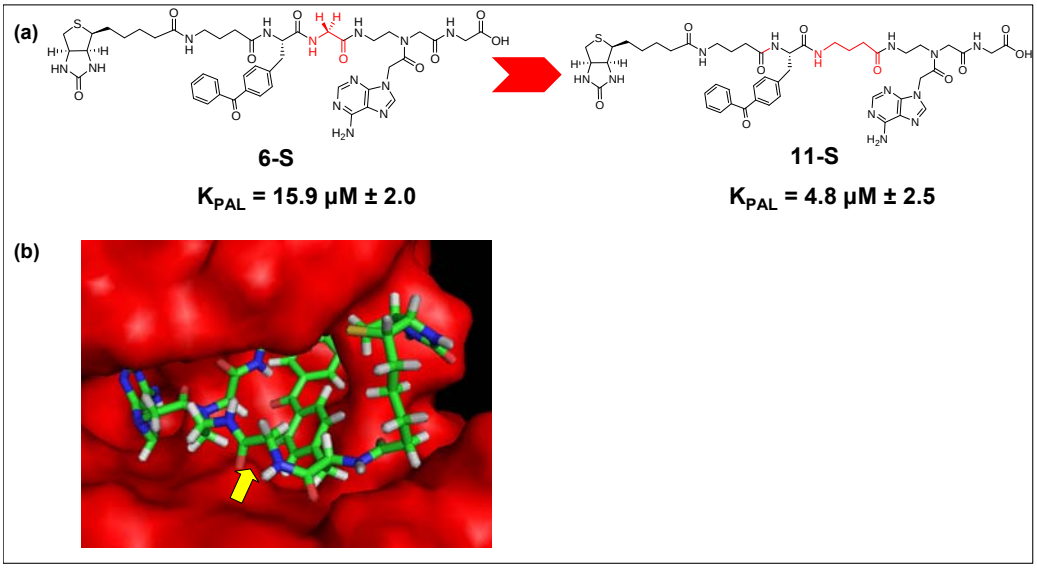

Figure 38. (a) Structures of probes **5-S** and **11-S** and their photoaffinity labeling constant (K_{PAL}). (b) Model of probe **5-S** in its binding pocket. The modified site is indicated by an arrow.

One reason for the increased photolabeling by **11-S** can be that the probability of achieving an optimal geometry for covalent attachment of benzophenone radical to Lck is improved by using a flexible linker. By increasing the linker flexibility further we might increase the efficiency of the labeling even more. However, such modification might impair the selectivity of our probes. Thus, to maintain the highest regioselectivity, the flexibility of the linker has to be limited to only that which is necessary to achieve efficient H-abstraction and C-C recombination.[36]

V.5. Summary and Conclusions

To characterize **5-S**-Lck interactions, the binding site was determined and a structural model of **5-S**-Lck complex was obtained. MS/MS analysis confirmed that the benzophenone moiety in probe **5-S** binds to either the Gly384 or Leu385 residue in the substrate-binding site of Lck, near the adenine binding site. Since Cγ-H of leucine is an electron rich center that is likely to react with the benzophenone radical we can suggest that our probe covalently label Lck in its Leu385 residue.

Selectivity among different SFKs can arise from variations among amino acid residues within the adenine or benzophenone binding areas.[72] However, since these binding sites are well conserved among SFKs, it was surprising to find that **5-S** did not label other SFKs. Furthermore, this unique selectivity toward Lck could not be fully explained by amino acid sequence and spatial alignment of Src, Fyn, and Lck. These results suggest that subtle differences in structure and/or dynamics between Lck and other SFKs culminated in the distinct differences in the photoaffinity labeling by **5-S**. Since photoaffinity labeling depends on both affinity interactions and efficiency of photocrosslinking reaction, further studies are required in order to distinguish which factor has the major role in the selectivity of **5-S** toward Lck.

To improve the efficiency of the photoaffinity labeling by **5-S**, we carried out structure affinity relationship studies in which the peptide backbone of **5-S** was modified in several ways. First, to confirm our structural model and allow using avidin conjugated antibody for the detection and purification of tagged proteins, the glycine linker between the benzophenone and biotin moieties was replaced γ-amino butyric acid (probe **6-S**).

Then, **6-S** was further modified by replacing the glycine group between benzophenone and adenine with serine (probe **7-S**), glutamic acid (probe **8-S**), proline (probe **9-S**), piperidine (probe **10-S**), and γ-amino butyric acid (probe **11-S**). All probes maintained their selectivity toward Lck, however, with different photoaffinity labeling constants. Relative to probe **6-S**, probes **9-S** and **10-S,** in which the flexibility of the linker between benzophenone and adenine was constrained**,** exhibited more than 10 fold reduction in their photoaffinity labeling. On the other hand, probe **11-S,** in which the length and flexibility of the linker was increased, showed a 3-fold increase in its photoaffinity labeling potency relative to **6-S**. Therefore, we conclude that a certain degree of the flexibility in the linker between adenine and benzophenone is fundamental for the labeling of Lck by our probe. Furthermore, this conclusion is supported by previous studies that show that the efficiency of the labeling by benzophenone containing ligands is governed significantly by the amount of conformational space that can be explored by the side-chain CH_2-benzophenone moiety.[37]

In conclusion, we identified the binding site of probe **5-S** and obtained molecular model of its complex with Lck. The selectivity toward Lck could not be fully explained by amino acid sequence analysis and spatial alignment of different SFKs. Thus, further studies are required to find the origin of this selectivity. Structure affinity relationship studies revealed that the flexibility of the linker between the benzophenone and adenine group is crucial for the labeling by our probes.

V.6. Materials and Methods

Materials & Physico-chemical analytical methods

See pages 39-40.

Stochastic Search of probe 5-S on Lck

10,000 molecules of probe **5-S** were randomly generated in the substrate binding site region of Lck with the following distance restrictions: the distance between the benzophenone carbonylic radical and Cγ-H of Leu385 residue as well as the distance between the primary amine of adenine and the carbonyl oxygen of the Glu317 residue were restricted to 1-3 Å. The protein and the probe's chiral center were fixed and the energy of the generated molecules was minimized using MMFF94 calculations. (Parameters: Mode for bond rotation: bias 30, Delta for Cartesian perturbation: 0.001, RMS gradient for Cartesian minimization: 0.01, Energy cutoff: 7 Kcal/mol, Failure limit: 20, RMS tolerance: 0.1, Conformational limit: 10000, Iteration limit: 10000, MM Iteration limit: 200).

Chemical Synthesis

Probe synthesis was accomplished manually using a stepwise solid-phase procedure. All couplings were carried out for 10 hours in dimethylformamide (DMF) using a 2-fold excess (over resin loading) of protected monomer, activated with an equimolar of HOBt and DCC. Reaction was monitored using the Kaiser test for free amines.[62] *N*-Fmoc group was removed using 20% (v/v) piperidine in DMF. Probes were removed from the solid support with simultaneous sidechain deprotection using a 95%

trifluoroacetic acid (TFA), 2.5% triisopropylsilane (TIS) and 2.5% water solution for 2 h at room temperature. TFA was removed under reduced pressure. Crude material was precipitated and washed with cold petroleum ether. Probes were purified using semi-preparative HPLC. Yield's range was 28% - 94%. The purified probes were analyzed using Analytical HPLC, Mass Spectroscopy, and ^{1}H-NMR.

Probe 6-S [Biotinyl-γ–aminobutyryl-p-benzoyl-L-phenylalanyl-glycinyl-adenine-*N*^{9}-acetyl-(2-aminoethyl)glycinyl-glycine]

^{1}H-NMR δ ppm (500MHz, DMSO) 8.50 (1H, t, NH), 8.42 (1H, m, NH), 8.29 (1H, s, CH), 8.25 (1H, s, CH), 8.04 (1H, m, NH), 7.70-7.22 (9H, m, 9xCH), 7.30 (2H, s, NH_2), 6.35 (2H, m, 2xNH), 5.25 (2H, m, CH_2), 4.65 (1H, m, CH), 4.32 (1H, m, CH), 4.20 (2H, m, CH_2), 4.15 (1H, m, CH), 3.70 (2H, m, CH_2), 3.60 (2H, m CH_2), 3.40 (2H, m, CH_2), 3.29 (2H, m, CH_2), 3.20 (2H, t, CH_2), 3.10 (2H, m, CH_2), 2.90 (1H, m, CH) 2.75 (2H, m, CH_2), 2.19-2.17 (4H, m, 2xCH_2), 1.82 (2H, m, CH_2), 1.10-1.55 (6H, m, $CH_2CH_2CH_2$). ESIMS (expected m/z 970.06) m/z 971.07 (MH^+), 993.06 (MNa^+), 486.03 ($M2H^+/2$). Analytical RP-HPLC retention time: 19.01 min.

Probe 7-S [Biotinyl-γ-aminobutyryl-p-benzoyl-L-phenylalanyl-D-serinyl-adenine-*N*^{9}-acetyl-(2-aminoethyl)glycinyl-glycine]

Probe **7-S** was syntesized by Doina Mihai.

^{1}H-NMR δ ppm (500MHz, DMSO) 8.64 (1H, t, NH), 8.48 (1H, m, NH), 8.25 (1H, s, CH), 8.20 (1H, s, CH), 8.04 (1H, m, NH), 7.75-7.20 (9H, m, 9xCH), 7.30 (2H, s, NH_2), 6.37 (2H, m, 2xNH), 5.20 (2H, m, CH_2), 4.55 (1H, m, CH), 4.40 (1H, m, CH), 4.32 (1H, m, CH), 4.18 (2H, m, CH_2), 4.15 (1H, m, CH), 3.75 (2H, m, CH_2), 3.62 (2H, m CH_2),

3.44 (2H, m, CH_2), 3.26 (2H, m, CH_2), 3.20 (2H, t, CH_2), 3.08 (2H, m, CH_2), 2.90 (1H, m, CH) 2.75 (2H, m, CH_2), 2.30-2.20 (4H, m, 2xCH_2), 2.04 (1H, t, OH), 1.80 (2H, m, CH_2), 1.15-1.60 (6H, m, $CH_2CH_2CH_2$). ESIMS (expected m/z 1000.09) m/z 1002.00 (MH^+), 501.03 ($M2H^+/2$). Analytical RP-HPLC retention time: 16.05 min.

Probe 8-S [Biotinyl-γ-aminobutyryl-p-benzoyl-L-phenylalanyl-D-glutamyl-adenine-*N*^{9}-acetyl-(2-aminoethyl)glycinyl-glycine]

Probe **8-S** was syntesized by Doina Mihai.

^{1}H-NMR δ ppm (500MHz, DMSO) 8.45 (1H, t, NH), 8.42 (1H, m, NH), 8.30 (1H, s, CH), 8.23 (1H, s, CH), 8.10 (1H, m, NH), 7.70-7.20 (9H, m, 9xCH), 7.27 (2H, s, NH_2), 6.30 (2H, m, 2xNH), 5.25 (2H, m, CH_2), 4.75 (1H, m, CH), 4.60 (1H, m, CH), 4.42 (1H, m, CH), 4.25 (1H, m, CH), 3.75 (2H, m, CH_2), 3.60 (2H, m CH_2), 3.54 (2H, m, CH_2), 3.36 (2H, m, CH_2), 3.22 (2H, t, CH_2), 3.10 (2H, m, CH_2), 2.80 (1H, m, CH) 2.65 (2H, m, CH_2), 2.47-2.35 (4H, m, 2xCH_2), 2.30-2.17 (4H, m, 2xCH_2), 1.82 (2H, m, CH_2), 1.20-1.60 (6H, m, $CH_2CH_2CH_2$). ESIMS (expected m/z 1042.12) m/z 1043.23 (MH^+), 522.06 ($M2H^+/2$). Analytical RP-HPLC retention time: 16.10 min.

Probe 9-S [Biotinyl-γ-aminobutyryl-p-benzoyl-L-phenylalanyl-D-prolinyl-adenine-*N*^{9}-acetyl-(2-aminoethyl)glycinyl-glycine]

^{1}H-NMR δ ppm (500MHz, DMSO) 8.60 (1H, t, NH), 8.45 (1H, m, NH), 8.40 (1H, s, CH), 8.35 (1H, s, CH), 8.15 (1H, m, NH), 7.65-7.20 (9H, m, 9xCH), 7.20 (2H, s, NH_2), 6.35 (2H, m, 2xNH), 5.48 (2H, m, CH_2), 4.52 (1H, m, CH), 4.32 (1H, m, CH), 4.24 (1H, t, CH), 4.10 (1H, m, CH), 3.70 (2H, m, CH_2), 3.65 (2H, m CH_2), 3.38-3.47 (4H, m,

2xCH_2), 3.20 (2H, m, CH_2), 3.16 (2H, m, CH_2), 3.10 (2H, m, CH_2), 2.80 (1H, m, CH) 2.75 (2H, m, CH_2), 2.15-2.05 (4H, m, 2xCH_2), 1.18 (2H, m, CH2), 1.75(2H, m, CH_2), 1.45-1.55 (4H, m, 2xCH_2), 1.10-1.34 (6H, m, $CH_2CH_2CH_2$). ESIMS (expected m/z 1024.15) m/z 1025.16 (MH^+), 513.58 ($M2H^+/2$). Analytical RP-HPLC retention time: 20.15 min.

Probe 10-S [Biotinyl-γ-aminobutyryl-p-benzoyl-L-phenylalanyl-D-piperidyl-adenine-*N*^{9}-acetyl-(2-aminoethyl)glycinyl-glycine]

^{1}H-NMR δ ppm (500MHz, DMSO) 8.65 (1H, t, NH), 8.50 (1H, m, NH), 8.39 (1H, s, CH), 8.30 (1H, s, CH), 8.10 (1H, m, NH), 7.70-7.20 (9H, m, 9xCH), 7.25 (2H, s, NH_2), 6.30 (2H, m, 2xNH), 5.40 (2H, m, CH_2), 4.60 (1H, m, CH), 4.30 (1H, m, CH), 4.24 (1H, t, CH), 4.15 (1H, m, CH), 3.75 (2H, m, CH_2), 3.60 (2H, m CH_2), 3.35-3.45 (4H, m, 2xCH_2), 3.29 (2H, m, CH_2), 3.24 (2H, t, CH_2), 3.15 (2H, m, CH_2), 2.90 (1H, m, CH) 2.80 (2H, m, CH_2), 2.19-2.17 (6H, m, 3xCH_2), 1.19 (2H, m, CH2), 1.80 (2H, m, CH_2), 1.15-1.50 (6H, m, $CH_2CH_2CH_2$). ESIMS (expected m/z 1010.12) m/z 1011.11 (MH^+), 506.55 ($M2H^+/2$). Analytical RP-HPLC retention time: 20.05 min.

Probe 11-S [Biotinyl-γ-aminobutyryl-p-benzoyl-L-phenylalanyl-γ-aminobutyryl-adenine-*N*^{9}-acetyl-(2-aminoethyl)glycinyl-glycine]

^{1}H-NMR δ ppm (500MHz, DMSO) 8.55 (1H, t, NH), 8.45 (1H, m, NH), 8.30 (1H, s, CH), 8.20 (1H, s, CH), 8.14 (1H, m, NH), 7.70-7.20 (9H, m, 9xCH), 7.20 (2H, s, NH_2), 6.25 (2H, m, 2xNH), 5.20 (2H, m, CH_2), 4.62 (1H, m, CH), 4.31 (1H, m, CH), 4.15 (2H, m, CH_2), 4.10 (1H, m, CH), 3.74 (2H, m, CH_2), 3.60 (2H, m CH_2), 3.45 (2H, m, CH_2),

3.30 (2H, m, CH_2), 3.25-3.18 (4H, m, 2xCH_2), 3.15 (2H, m, CH_2), 2.95 (1H, m, CH) 2.70 (2H, m, CH_2), 2.20-2.10 (8H, m, 4xCH_2), 1.80 (2H, m, CH_2), 1.15-1.55 (6H, m, $CH_2CH_2CH_2$). ESIMS (expected m/z 998.10) m/z 999.12 (MH^+), 1021.10 (MNa^+), 500.04 ($M2H^+/2$). Analytical RP-HPLC retention time: 19.25 min.

Biological Assays

Preparation of tagged Lck for mass spectrometry analysis

400 µl aliquots LCK (182 µg) were mixed with 40 µl of probe 5-S (5 mM in DMSO) solution and 350 µl aliquots LCK were mixed with 35 µl of DMSO as control. The mixtures were incubated at 4 ºC for 1 h. Photocrosslinking was carried out under six Sylvania 350 Blacklight lamps (15 W, λ_{max} 350 nm) for 2 h, in which samples were kept on ice and placed approximately 5 cm below the lamps.

Following the photocrosslinking, samples were mixed with Laemmli Sample Buffer (BioRad) and separated on SDS-PAGE (5-20% Tris-HCl gel, 200 V, 1 h) in 1× Tris-Glycine-SDS buffer (BioRad). Gel was stained for 5 minutes with 0.5% Coomassie blue G-250 in a solution of 50% methanol / 10% acetic acid. Stain was discarded and the gel was rinsed briefly with high purity water. The gel was then destained with repeating washes with a solution of 40% methanol / 10% acetic acid for 10-20 minutes until faint bands are observed. Gel was further destained using high purity water after which bands were excised and submitted for analysis.

Binding Site Determination

Binding site determination using MALDI-TOF and LC-MS/MS analysis was done by Dr. Haiteng Deng at the Proteomics Resource Center of Rockefeller University.

The gel bands corresponding to untreated and photo-crosslinked Lck were excised from the gel, reduced with 10mM of DTT and alkylated with 55 mM iodoacetamide, and then digested with Sequence Grade Modified Trypsin (Promega) in ammonium bicarbonate buffer at 37 ºC overnight. The digestion products were analyzed by MALDI-TOF to identify peptides that have photo-crosslinkers with a PerSeptive MALDI-TOP DE-STR mass spectrometer. Half of the digestion products for each sample were also analyzed by LC-MS/MS. For LC-MS/MS analysis, each digestion product was separated by gradient elution with the Dionex capillary/nano-HPLC system and analyzed by Applied Biosystems QSTAR XL mass spectrometer using information-dependent, automated acquisition.

Photolabeling of kinases

20 µl aliquots of purified kinases (1 µg/µL) were mixed with 2 µl of 1 mM probe solution in DMSO. For blocking experiments, 20 µl aliquots of the lysate were mixed first with 2 µl of a blocking solution in DMSO (10 mM adenine, 10 mM benzophenone, 10 mM biotin, or DMSO control) and then with 2 µl of 1 mM probe solution in DMSO. The mixtures were incubated at 4 ºC for 1 h. Photocrosslinking was carried out under six Sylvania 350 Blacklight lamps (15 W, λ_{max} 350 nm) for 2 h, in which samples were kept on ice and placed approximately 5 cm below the lamps. Following the photocrosslinking, samples were mixed with Laemmli Sample Buffer with 5%(v/v) 2-mercaptoethanol,

denatured at 80 ºC for 5 min and separated on SDS-PAGE (5-20% Tris-HCl gel, 200 V, 1 h) in 1× Tris-Glycine-SDS buffer. Gel was blotted onto PVDF membrane (200 mA, 1h) in a cold transfer buffer (20% methanol in 1× Tris-Glycine buffer). Blotted membrane was blocked with 5% non-fat milk in Tris-buffered saline containing 1% Tween 20 (TBS-T) for 1 h. Blocked membrane was rinsed with TBS-T (10 min × 3), treated with an anti-biotin hoarse radish peroxidase (HRP)-conjugated antibody (1:100 dilution in 2% non-fat milk in TBS-T) for 3 h or avidin-HRP for 30 min, and washed with TBS-T (10 min × 3). The washed membrane was treated with the ECL-Plus chemiluminescence reagent for 5 min. Bands were observed with the BioRad ChemiDoc gel documentation system.

Chapter VI

Research Outlook and Prospective

VI.1. Summary

The study described in this thesis aimed to develop a simple chemical approach for profiling protein kinases. Considerable efforts have been directed toward the study of these proteins due to their importance in regulation of various cellular activities.[23,54-57] However, the majority of existing methodologies for analysis of kinases do not offer selectivity toward different members of this family. Our study, on the other hand, offers such selectivity based on differences in the topology around the ATP-binding site of kinases.

In the first part of this study, we demonstrated that our probes, despite their simple structure, have reasonable selectivity toward different proteins in complex mixture. Additionally, we revealed that chiral recognition has an important role in photoaffinity labeling of target proteins by our probes.[31]

In the second part of this work, we refined our chemical methodology to develop selective photoaffinity probes for SFKs. During this effort we discovered a photoactive probe, **5-S** (Figure 39), that selectively labeled Lck in complex proteomes.[39] We showed that Lck recognized both adenine and benzophenone moieties of probe **5-S** and that the chirality of the probe is crucial for this recognition.

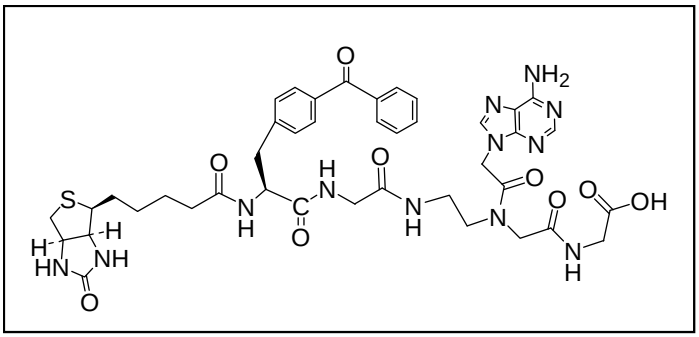

Figure 39. Structure of prototype probe (**5-S**) for selective photolabeling of Lck.

Structure affinity relationship studies revealed that the length of the linker between the adenine and benzophenone units has a significant effect on photoaffinity labeling potential of our probes. Although the calculated spatial distance between the N^9-methyl group of the adenine and p-methyl group of the benzophenone was approximately 13 Å, a longer through-bond distance (16-19 Å) was required to obtain efficient photoaffinity labeling. The longer linker allows additional conformational freedom that increases the probability of the benzophenone radical to achieve the geometric requirements for an efficient photocrosslinking reaction.[10,36,37]

The binding site of probe **5-S** was identified within the well-conserved region of SFKs as expected at the onset of this study. What was surprising, however, is the fact that probe **5-S** did not label other kinases with seemingly identical binding pocket.[39] We are presently unable to offer a full structural explanation for the observed selectivity. However, it is important to note that in order to obtain labeling of target kinases two distinct processes, e.g. binding interaction and photocrosslinking reaction, are required. First, the adenine and benzophenone moieties are expected to form binding interactions

with ATP-binding site and nearby hydrophobic pockets, respectively. Then, to obtain covalent labeling of target kinase upon UV irradiation, the benzophenone diradical and an electron rich C-H bond of the kinase have to attain spatial orientation that satisfies the geometrical requirements of the photocrosslinking reaction (see Chapter II).[36,37] Therefore, it is possible that probe **5-S** has affinity interactions with kinases other than Lck, but the orientation of benzophenone in the hydrophobic pocket allows efficient labeling only in the **5-S**-Lck complex.

VI.2. Prospective and Applications

To determine whether the observed selectivity toward Lck results from differences in binding affinity interactions or photolabeling efficiency, we need to evaluate the selectivity of our probes regardless of the photocrosslinking step. For this purpose, a new set of probe (Figure 40), in which the biotin and benzophenone are tethered through a polyethyleneglycol (PEG) linker, was prepared. These probes can be immobilized using sterptavidin-agarose beads and used for affinity purification (Figure 41).[89] The PEG linker should provide enough space between biotin and the recognition units, allowing adenine and benzophenone to interact with their target binding sites without steric hindrance by the biotin-avidin system.

Using streptavidin-agarose beads, kinases involved in affinity interactions with the immobilized probes can be isolated and visualized without the need for covalent labeling. The affinity constant of our probes can be quantified by titration of Lck with different concentrations of immobilized PEG-probes. The results of such studies are

expected to improve our understanding of the structural basis for the observed photolabeling selectivity toward Lck.

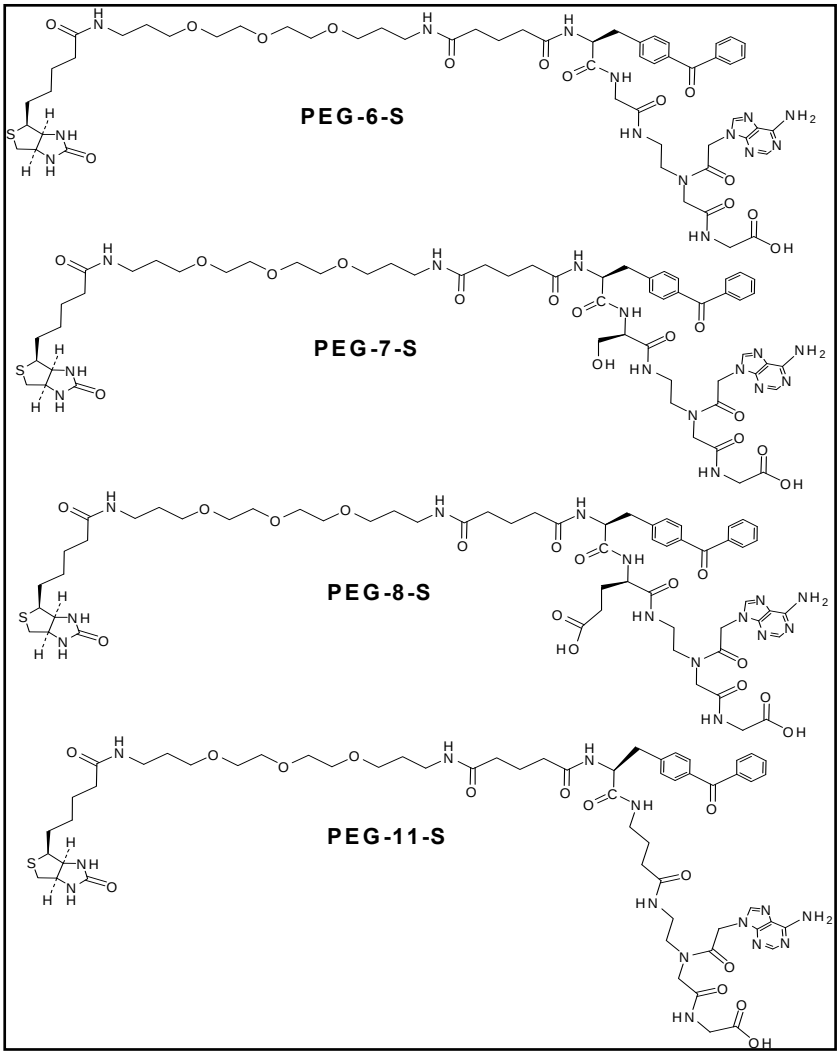

Figure 40. Structures of newly synthesized probes for affinity studies. These probes contain polyethyleneglycol (PEG) linker between their benzophenone and biotin units and can be immobilized using avidin beads.

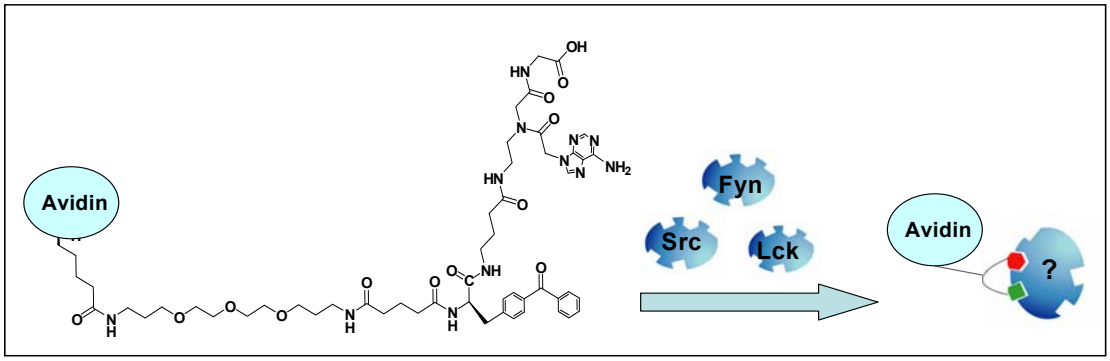

Figure 41. Affinity and selectivity of PEG-probes toward SFKs can be examined by immobilizing our probes on avidin beads and study their affinity interactions with different SFKs.

Once we obtain better understanding of the molecular basis for the selectivity toward Lck we can develop additional probes with increased affinity and selectivity toward Lck as well as other SFKs. The significance of such probes derives from their potential applications not only in the field of proteomics studies but also in pharmaceutical and clinical research.

Lck is a very attractive target for treatment of T-cell mediated disorders[20,65,73,77-79,81] as it plays a critical role in T-cell activation and proliferation.[65,69,70,79,81] Compounds that selectively label Lck can, therefore, be developed as modulators of Lck activity or aid in the search for Lck inhibitors.

Considerable effort in the pharmaceutical industry is currently directed at the generation of novel protein kinase inhibitors.[54,90,76,78] For example, A-770041, a selective Lck inhibitor is currently in development for preventing heart allograft rejection.[79] In addition, other kinase inhibitors have been recently approved for clinical indications,

including the anticancer drugs Gleevec,[91] a protein-tyrosine kinase inhibitor that inhibits the *bcr-abl* tyrosine kinase, and Iressa,[92] a protein kinase inhibitor that blocks the epidermal growth factor. These drugs, as well as the majority of other kinase inhibitors in development, are designed to bind to the kinase ATP-binding site, thereby preventing substrate phosphorylation. Since the ATP-binding sites are well conserved, the identification of inhibitors that are both potent and selective is challenging.[23,54]

In order to develop our probes as Lck inhibitors, their inhibition potency needs to be fully characterized. The inhibitory activity of our probes can initially be evaluated using Kinase-Glo luminescent kinase assay (Figure 42a).[93] In this assay, luciferin is oxidized in the presence of luciferase to produce oxyluciferin and energy in the form of light. Since this reaction requires ATP, the luminescence obtained is directly related to the concentration of ATP in the reaction mixture and, therefore, inversely related to kinase activity.

Preliminary inhibition study (Figure 42b) revealed that probe **5-S** has the largest inhibitiory effect on Lck activity when compared to probes **4-S**, **4-R**, and **5-R**. Interestingly, probes **4-R** and **5-R**, which did not label Lck, showed inhibition effect on Lck activity implying that these probes binds at the ATP-binding site of Lck. These observation support our assumption that **5-S**-Lck is not the only probe-kinase complex formed in our photoaffinity experiments. However, only in the **5-S**-Lck complex the conditions for efficient photolabeling reaction are fulfilled. To quantify the inhibition potency of all our probes and calculate their IC_{50} further comprehensive inhibition studies are required.

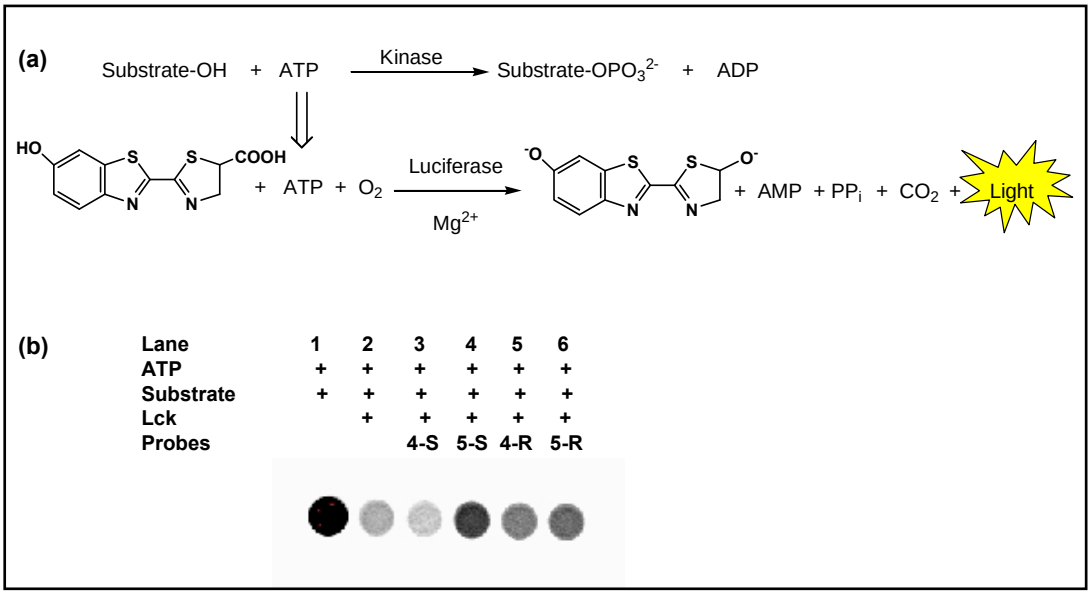

Figure 42. Kinase-Glo luminescent kinase assay. (a) Evaluation of kinase activity using kinase-Glo luminescent kinase assay. (b) Inhibitory effect of probes **4-S/R-5-S/R (**0.4 μM) on phosphorylation activity of Lck (0.2 units) using 25 μM ATP, 25 μM substrate, and 50 μl Kinase-Glo solution.

In addition to the potential application of our probes as Lck activity modulators, they can be used to profile the selectivity of novel kinase inhibitors toward Lck. Several affinity-based labeling approaches were used in the past to develop robust screens for small molecules inhibitors of a specific enzyme target.[1,21,54,60] One example is the use of the papain probe DCG-04 to screen inhibitor libraries designed to target cystein proteases in the human malaria parasite *Plasmodium falciparum*.[94] In our study, when Lck was labeled with probe **5-S** in the presence of an ATP-competitive inhibitor of Lck[78] the intensity of the band correspond to labeled Lck was dramatically reduced (Figure 26, page 66). Similarly, the selectivity of other potential ATP-competitive Lck inhibitors can

be screened using our selective Lck photo labelers. Furthermore, once we fully characterize the inhibitory activity of our probes, they can be used to evaluate not only the selectivity of potential Lck inhibitors but also their inhibitory potency.

Another possible application of our probes is to serve as diagnostic tools in maladies linked to abnormalities in Lck structure or function.[70,81] Many biomarkers development studies have been focused on cancer, where proteomics tools were proven to have the potential to allow earlier diagnosis.[6,95,96] For example, a proteomics study has identified serum protein patterns that distinguish patients with ovarian cancer from unaffected women with a positive predictive value of 94%.[95] Another example is the use of serine hydrolase activity-based probes to profile enzyme activities in a diverse range of cancer cell lines.[9,97] At the onset of our study (Chapter III), we demonstrated that our chemical probes give different photolabeling patterns with different cancer cell lines, e.g. breast cancer (MDR-MB-231) and neuroblastoma (SK-N-SH). These preliminary results indicate that our affinity-based methodology has the potential to aid in the search for biomarkers for cancer classification. For example, by screening different cancer cell lines with our probes, we can identify proteins that are highly expressed in metastatic versus non-metastatic breast cancer cell lines.

In addition to the use of chemical probes in the search for cancer biomarkers, there are other kinase-related diseases that can be diagnosed with proteomics tools. For example, abnormalities in Lck structure have been linked to several genetic diseases, including the severe combined immunodeficiency (SCID) phenotype[81] and the autosomal recessive disease Hereditary Haemochromatosis (HH).[70] Therefore, our selective Lck ligands can be

used to screen for differences in Lck expression in pathological processes related to abnormalities in Lck structure of function.

VI.3. Conclusions

The simplicity and versatility of our approach increases the value of this study. Considering the difficulty in developing selective ligands for different kinases, our probes are remarkable simple and their selectivity and affinity can be easily modified by variations in the linker between the two recognition units, e.g. adenine and benzophenone. Based on our findings we can develop a new set of higher affinity and selectivity for labeling of Lck as well as other SFKs. Furthermore, our methodology can be generalized to other families of proteins by swapping the adenine moiety with other biological recognition units. For example, we can target carbohydrate-binding proteins[98,99] using sugars as recognition units.

In conclusion, this study provides a foundation for the development of simple and general approach for chemical proteomics. The simplicity of this methodology, in terms of probe synthesis and profiling analysis, makes it suitable for a variety of applications, especially the development of molecular tools for biomarker discovery and inhibitors screening. Since selectivity of our probes is based on structural recognition instead of chemical reactivity, our strategy can greatly expand the scope of existing activity-based proteomics tools. Therefore, it is our expectation that our simple and highly selective chemical approach will make significant contributions to various applied sciences as well as fundamental protein research.

References

1. Chan, E. W.; Chattopadhaya, S.; Panicker, R. C.; Huang, X.; Yao, S. Q., Developing photoactive affinity probes for proteomic profiling: hydroxamate-based probes for metalloproteases. *J Am Chem Soc* **2004,** 126, (44), 14435-14446.

2. Miklos, G. L. G.; Maleszka, R., Integrating molecular medicine with functional proteomics: realities and expectations. *Proteomics* **2001,** 1, (1), 30-41.

3. Chen, G. Y. J.; Uttamchandani, M.; Lue, R. Y. P.; Lesaicherre, M.-L.; Yao, S. Q., Array-based technologies and their applications in proteomics. *Curr Top Med Chem* **2003,** 3, 705-724.

4. Gregory C. Adam, E. J. S., Benjamine F. Cravatt, Chemical strategies for functional proteomics. *Mol Cell Proteomics* **2002,** 1, 781-790.

5. Cravatt, B. F.; Sorensen, E. J., Chemical strategies for the global analysis of protein function. *Curr Opin Chem Biol* **2000,** 4, 663-668.

6. Qoronfleh, M. W., Role and challenges of proteomics in pharma and biotech: technical, scientific and commercial perspective. *Expert Review of Proteomics* **2006,** 3, (2), 179-195.

7. Marko-Varga, G., Proteomics principles and challenges. *Pure Appl Chem* **2004,** 76, (4), 829-837.

8. Jeffery, D. A.; Bogyo, M., Chemical proteomics and its application to drug discovery. *Curr Opin Chem Biotechnol* **2003,** 14, 87-95.

9. Adam, G. C.; Sorensen, E.; Cravatt, B. F., Proteomic profiling of mechanistically distinct enzyme classes using a common chemotype. *Nat Biotechnol* **2002,** 20, 805-809.

10. Salisbury, C. M.; Cravatt, B. F., Activity-based probes for proteomic profiling of histone deacetylase complexes. *Proc Natl Acad Sci U. S. A.* **2007,** 104, (4), 1171-1176.

11. Marley, K.; Mooney, D. T.; Clark-Scannell, G.; Tong, T. T.; Watson, J.; Hagen, T. M.; Stevens, J. F.; Maier, C. S., Mass tagging approach for mitochondrial thiol proteins. *J Proteome Res* **2005,** 4, (4), 1403-12.

12. Oda, Y.; Owa, T.; Sato, T.; Boucher, B.; Daniels, S.; Yamanaka, H.; Shinohara, Y.; Yokoi, A.; Kuromitsu, J.; Nagasu, T., Quantitative chemical proteomics for identifying candidate drug targets. *Anal Chem* **2003,** 75, 2159-2165.

13. Mann, M.; Hendrickson, R. C.; Pandey, A., Analysis of proteins and proteomes by mass spectrometry. *Annu Rev Biochem* **2001,** 70, 437-473.

14. Aebersold, R.; Goodlett, D., Mass Spectrometry in Proteomics. *Chem Rev* **2001,** 101, 269-295.

15. Eriksson, J.; Fenyö, D., Protein identification in complex mixtures. *J Proteome Res* **2005,** 4, (2), 387-393.

16. Ong, S. E.; Mann, M., Mass spectrometry-based proteomics turns quantitative. *Nature Chem Biol* **2005,** 1, (5), 252-262.

17. Mann, R. A. a. M., Mass spectrometry-based proteomics. *Nature* **2003,** 422, 198-207.

18. Kidd, D.; Liu, Y.; Cravatt, B. F., Profiling Serine Hydrolase Activities in Complex Proteomes. *Biochemistry* **2001,** 40, (13), 4005-4015.

19. Gygi, S. P.; Rist, B.; Gerber, A.; Turecek, F.; Gelb, M. H.; Aebersold, R., Quantitative analysis of complex protein mixtures using isotope-coded affinity tags. *Nat. Biotechnol* **1999,** 11, 994-999.

20. Snow, R. J.; Cardozo, M. G.; Morwick, T. M.; Busacca, C. A.; Dong, Y.; Eckner, R. J.; Jacober, S.; Jakes, S.; Kapadia, S.; Lukas, S.; Panzenbeck, M.; Peet, G. W.; Peterson, J. D.; Prokopowicz, A. S.; Sellati, R.; Tolbert, R. M.; Tschantz, M. A.; Moss, N., Discovery of 2-phenylamino-imidazo[4,5-h]isoquinolin-9-ones: A new class of inhibitors of Lck kinase. *J Med Chem* **2002,** 45, (16), 3394-3405.

21. Jessani, N.; Cravatt, B. F., The development and application of methods for activity-based protein profiling. *Curr Opin chem biol* **2004,** 8, 54-59.

22. J. Hemelaar, P. J. G., A. Borodovsky, B. M. Kessler, H. L. Ploegh, and H. Ovaa, Chemistry-based functional proteomics: mechanism-based activity-profiling tools for ubiquitin and ubiquitin-like specific proteases. *J. Proteome Res.* **2004,** 3, 268-276.

23. Cole, P. A.; Sondhi, D.; Kim, K., Chemical approaches to the study of protein tyrosine kinases and their implications for mechanism and inhibitor design. *Pharmacol Ther* **1999,** 82, (2), 219-229.

24. Adam, G. C.; Burbaum, J.; Kozarich, J. W.; Patricelli, M. P.; Cravatt, B. F., Mapping enzyme active sites in complex proteomes. *J Am Chem Soc* **2004,** 126, (5), 1363-1368.

25. Saghatelian, A.; Jessani, N.; Joseph, A.; Joseph, M.; Humphrey, M.; Cravatt, B. F., Activity-based probes for proteomics profiling of metalloproteases. *PNAS* **2004,** 101, (27), 10000-10005.

26. Greenbaum, D.; Medzihradszky, K. F.; Burlingame, A.; Bogyo, M., Epoxide electrophiles as activity-dependent cystein protease profiling and discovery tools. *Chem Biol* **2005** 7, 569-581.

27. Liu, Y.; Patricelli, M. P.; Cravatt, B. F., Activity-based protein profiling: the serine hydrolases. *Proc Natl Acad Sci U. S. A* **1999,** 96, (26), 14694-14699.

28. Brehmer, D.; Godl, K.; Zech, B.; Wissing, J.; Daub, H., Proteome-wide identification of cellular targets affected by bisindolylmaleimide-type protein kinase C inhibitors. *Mol Cell Proteomics* **2004,** 3, (5), 490-500.

29. Ovaa, H., Activity-based ubiquitin-specific protease profiling of virus-infected and malignant human cells. *Proc Natl Acad Sci USA* **2004,** 101, 2253-2258.

30. Kumar, S.; Zhou, B.; Liang, F.; Wang, W.-Q.; Huang, Z.; Zhang, Z.-Y., Activity-based probes for protein tyrosine phosphatases. *PNAS* **2004,** 101, 7943-7948.

31. Kawamura, A.; Hindi, S., Protein fishing with chiral molecular baits. *Chirality* **2005,** 17, 332-337.

32. Son, C. D.; Sargsyan, H.; Naider, F.; Becker, J. M., Identification of ligand binding regions of the saccharomyces cerevisiae α-factor pheromone receptor by photoaffinity cross-linking. *Biochemistry* **2004,** 43, 13193-13203.

33. Henry, L. K.; Khare, S.; Son, C.; Babu, V. V. S.; Naider, F.; Becker, J. M., Identification of a contact region between the tridecapeptide α-factor mating pheromone of saccharomyces cerevisiae and its G protein-coupled receptor by photoaffinity labeling. . *Biochemistry* **2002,** 41, 6128-6139.

34. Barbeau, D.; Guay, S.; Neugebauer, W.; Escher, E., Preparation and biological activities of potential vasopressin photoaffinity labels. *J Med Chem* **1992,** 35, (1), 151-157.

35. Robinette, D.; Neamati, N.; Tomer, K. B.; Borchers, C. H., Photoaffinity labeling combined with mass spectrometric approaches as a tool for structural proteomics. *Expert Review of Proteomics* **2006,** 3, (4), 399-408.

36. Dorman, G.; Prestwich, G. D., Benzophenone photophores in biochemistry. *Biochemistry* **1994,** 33, (19), 5661-5673.

37. Saviano, M.; Improta, R.; Benedetti, E.; Carrozzini, B.; Casarano, G. L.; Didierjean, C.; Toniolo, C.; Crisma, M., Benzophenone photophore flexibility and proximity: molecular and crystal-state structure of a Bpa-containing trichogin dodecapeptide analogue. *ChemBioChem* **2004,** 5, 541-544.

38. Lee, B.-K.; Lee, Y.-H.; Hauser, M.; Son, C. D.; Khare, S.; Naider, F.; Becker, J. M., Tyr266 in the sixth transmembrane domain of the yeast a-factor receptor plays key roles in receptor activation and ligand specificity. *Biochemistry* **2002,** 41, 13681-13689.

39. Hindi, S.; Deng, H.; James, L.; Kawamura, A., Selective photolabeling of Lck kinase in complex proteome. *Bioorganic & Medicinal Chemistry Letters* **2006,** 16, 5625-5628.

40. Dill, K. A., Additivity principles in biochemistry. *J Bio Chem* **1997,** 272, (2), 701-704.

41. Maly, D. J.; Choong, I. C.; Ellman, J. A., Combinatorial target-guided ligand assembly: identification of potent subtype-selective c-Src inhibitors. *PNAS* **2000,** 97, (6), 2419-2424.

42. Olejniczak, E. T.; Marcotte, P. A.; Nettesheim, D. G.; Meadows, R. P.; Edalji, R.; Holzman, T. F.; Fesik, S. W., Stromelysin inhibitors designed from weakly bound fragments: effects of linking and cooperativity. *J Am Chem Soc* **1997,** 119, (25), 5828 -2832.

43. Jencks, W. P., On the attribution and additivity of binding energies. *Proc Natl Acad Sci U S A* **1981,** 78, (7), 4046-4050.

44. Sadaghiani, A. M.; Verhelst, S. H.; Bogyo, M., Tagging and detection strategies for activity-based proteomics. *Curr Opin chem biol* **2007,** 11, 20-28.

45. Lue, R. Y. P.; Chen, G. Y. J.; Hu, Y.; Zhu, Q.; Yao, S. Q., Versatile protein biotinylation strategies for potential high-throughput proteomics. *J Am Chem Soc* **2004,** 126, 1055-1062.

46. Bentley, R., Diastereoisomerism, contact points, and chiral selectivity: a four-site saga. *Arch Biochem Biophys* **2003,** 414, (1), 1-12.

47. Amos, L.; Lowe, J., How Taxol stabilises microtubule structure. *Chem Biol* **1999,** 6, (3), R65-R69.

48. Pérodin, J.; Deraët, M.; Auger-Messier, M.; Boucard, A. A.; Rihakova, L.; Beaulieu, M.-È.; Lavigne, P.; Parent, J.-L.; Guillemette, G.; Leduc, R.; Escher, E., Residues 293 and 294 are ligand contact points of the human angiotensin type 1 receptor. *Biochemistry* **2002,** 41, (48), 14348 -14356.

49. Kauer, J. C.; Erickson, S.; Wolfe, H. R.; Degrado, W. F., p-Benzoyl-L-phenylalanine, a new photoreactive amino acid. *J Bio Chem* **1986,** 261, (23), 10695-10700.

50. Severance, D.; Pandey, B.; Morrison, H., Reaction path analysis of hydrogen abstraction by the formaldehyde triplet state. *J Am Chem Soc* **1987,** 109, 3231-3233.

51. O'Neil, K. T.; DeGrado, W. F., The interaction of calmodulin with fluorescent and photoreactive model peptides: Evidence for a short interdomain separation. *Proteins* **1989,** 6, (3), 284-293.

52. Steen, H.; Mann, M., The ABC's (and XYZ's) of peptide sequencing. *Mol Cell Biol* **2004,** 5, 699-711.

53. Griffey, R. H.; Sannes-Lowery, K. A.; Drader, J. J.; Mohan, V.; Swayze, E. E.; Hofstadler, S. A., Characterization of low-affinity complexes between RNA and small molecules using electrospray ionization mass spectrometry. *J Am Chem Soc* **2000**, (122), 9933-9938.

54. Patricelli, M. P.; Szardenings, A. K.; Liyanage, M.; Nomanbhoy, T. K.; Wu, M.; Weissig, H.; Aban, A.; Chun, D.; Tanner, S.; Kozarich, J. W., Functional interrogation of the kinome using nucleotide acyl phosphates. *Biochemistry* **2007,** 46, (2), 350-358.

55. Manning, G.; Whyte, D. B.; Martinez, R.; Hunter, T.; Sudarssanam, S., The protein kinase complement of the human genome. *Science* **2002,** 298, (5600), 1912-1934.

56. Hunter, T., Protein Kinases and phosphatases: the yin and yang of protein phosphorylation and signaling. *Cell* **1995,** 80, 225-236.

57. Veldhuyzen, W. F.; Nguyen, Q.; McMaster, G.; Lawrence, D. S., A light-activated probe of intracellular protein kinase activity. *J Am Chem Soc* **2003,** 125, 13358-13359.

58. Green, K. D.; Pflum, M. K., Kinase-catalyzed biotinylation for phosphoprotein detection. *J Am Chem Soc* **2007,** 129, 10-11.

59. Fields, G. B.; Noble, R. L., Solid phase peptide synthesis utilizing 9-fluorenylmethoxycarbonyl amino acids. *Int J Pept Protein Res* **1990,** 35, (3), 161-214.

60. Vershelst, S. H.; Bogyo, M., Chemical Proteomics Applied in Target Identification and Drug Discovery. *Biotechniques* **2005,** 38, (2), 175-177.

61. Zhang, R.; Tremblay, T. L.; McDermid, A., Identification of differentially expressed proteins in human glioblastoma cell lines and tumors. *Glia* **2003,** 42, 194-208.

62. Kaiser, E.; Colescott, R. L.; Bossinger, C. D.; Cook, P. I., Color test for detection of free terminal amino groups in the solid-phase synthesis of peptides. *Anal Biochem* **1970,** 34, (2), 595-598.

63. Parsons, S. J.; Parsons, J. T., Src family kinases, key regulators of signal transduction *Oncogene* **2004,** 23, 7906-7909.

64. Dalgarno, D.; Stehle, T.; Narula, S.; Schelling, P.; Schravendijk, M. R. v.; Adams, S.; Andrade, L.; Keats, J.; Ram, M.; Jin, L.; Grossman, T.; MacNeil, I.; Metcalf, C.; Shakespeare, W.; Wang, Y.; Keenan, T.; Sundaramoorthi, R.; Weigele, R. B. M.; Sawyer, T., Structural basis of Src Tyrosine kinase Inhibition with a new class of potent and selective trisubstituted purine-based compounds. *Chem Biol Drug Des* **2006,** 67, (1), 46-57.

65. Palacios, E. H.; Weiss, A., Function of the Src-family kinases, Lck and Fyn, in T-cell development and activation. *Oncogene* **2004,** 23, 7990-8000.

66. Lewis, D. B.; Liggitt, H. D.; Effmann, E. L.; Motley, S. T.; Teitelbaum, S. L.; Jepsen, K. J.; Goldstein, S. A.; Bonadio, J.; Carpenter, J.; Perlmutter, R. M., Osteoporosis induced in mice by overproduction of interleukin 4. *PNAS* **1993,** 90, 11618-11622.

67. Bucay, N.; Sarosi, I.; Dunstan, C. R.; Morony, S.; Tarpley, J.; Capparelli, C.; Scully, S.; Tan, H. L.; Xu, W.; Lacey, D. L.; Boyle, W. J.; Simonet, W. S., Osteoprotegerin-deficient mice develop early onset osteoporosis and arterialcalcification. *Genes Dev* **1998,** 12, (9), 1260-1268.

68. Chow, L. M.; Veillette, A., The Src and Csk families of tyrosin protein kinases in hemopoietic cells. *Semin Immunol* **1995,** 7, 207-226.

69. Heyninck, K.; Beyaert, R., A novel link between Lck, Bak expression and chemosensitivity. *Oncogene* **2006,** 25, (12), 1693-1695.

70. Arosa, F. A.; Silva, A. J.; Godinho, I. M.; Streege, J. C.; Sousa, M., Decreased CD8-p56lck activity in peripheral blood T-lymphocyes from patients with hereditary haemochromatosis. *Scandinavian Journal of Immunology* **1994,** 39, (5), 212-217.

71. Yutong Sun; Yong-Chao Ma; Jianyun Huang; Krystina Y. Chen; Deirdre K. McGarrigle; Huang, X.-Y., Requirement of Src-Family Tyrosine Kinases in Fat Accumulation. *Biochemistry* **2005,** 44, (44), 14455 -14462.

72. Breitenlechner, C. B.; Bossemeyer, D.; Engh, R. A., Crystallography for protein kinase drug design: PKA and SRC case studies. *Biochimica et Biophysica* **2005,** 1754, (1-2), 38-49.

73. Martin, M. W.; Newcomb, J.; Nunes, J. J.; McGowan, D. C.; Armistead, D. M.; Boucher, C.; Buchanan, J. L.; Buckner, W.; Chai, L.; Elbaum, D.; Epstein, L. F.; Faust, T.; Gallant, S. F. P.; Gore, A.; Gu, Y.; Hsieh, F.; Huang, X.; Lee, J. H.; Metz, D.; Middleton, S.; Mohn, D.; Morgenstern, K.; Morrison, M. J.; Novak, P. M.; Oliveira-dos-Santos, A.; Powers, D.; Rose, P.; Schneider, S.; Sell, S.; Tudor, Y.; Turci, S. M.; Welcher, A. A.; White, R. D.; Zack, D.; Zhao, H.; Zhu, L.; Zhu, X.; Ghiron, C.; Amouzegh, P.; Ermann, M.; Jenkins, J.; Johnston, D.; Napier, S.; Power, E., Novel 2-aminopyrimidine carbamates as potent and orally active inhibitors of Lck: synthesis, SAR, and in vivo antiinflamatory activity. *J Med Chem* **2006,** 49, (16), 4981-4991.

74. Kung, C.; Thomas, M. L., Recent advances in lymphocyte signaling and regulation. *Frontiers in Bioscience* **1997,** 2, d207-221.

75. Tran, T.; Hoffmann, S.; Wiesehan, K.; Jonas, E.; Luge, C.; Aladag, A.; Willbold, D., Insights into human lck SH3 domain binding specificity: different binding modes of artificial and native ligands. *Biochemistry* **2005,** 44, (45), 15042-52.

76. Chen, P.; Doweyko, A. M.; Norris, D.; Gu, H. H.; Spergel, S. H.; Das, J.; Moquin, R. V.; Lin, J.; Wityak, J.; Iwanowicz, E. J.; McIntyre, K. W.; Shuster, D. J.; Behnia, K.; Chong, S.; Fex, H. d.; Pang, S.; Pitt, S.; Shen, D. R.; Thrall, S.; Stanley, P.; Kocy, O. R.; Witmer, M. R.; Kanner, S. B.; Schieven, G. L.; Barrish, J. C., Imidazoquinoxaline Src-Family Kinase p56Lck inhibitors: SAR, QSAR, and the discovery of (S)-N-(2-Chloro-6-methylphenyl)-2-(3-methyl-1-piperazinyl)imidazo- [1,5-a]pyrido[3,2-e]pyrazin-6-amine (BMS-279700) as a potent and orally active inhibitor with excellent in vivo antiinflammatory activity. *J Med Chem* **2004,** 47, 4517-4529.

77. DiMauro, E. F.; Newcomb, J.; Nunes, J. J.; Bemis, J. E.; Boucher, C.; Buchanan, J. L.; Buckner, W. H.; Cee, V. J.; Chai, L.; Deak, H. L.; Epstein, L. F.; Faust, T.; Gallant, P.; Geuns-Meyer, S. D.; Gore, A.; Gu, Y.; Henkle, B.; Hodous, B. L.; Hsieh, F.; Huang, X.; Joseph L. Kim, J. H. L., Matthew W. Martin, Craig E. Masse, David C. McGowan, Daniela Metz, Deanna Mohn, Kurt A. Morgenstern, Antonio Oliveira-dos-Santos, Vinod F. Patel, David Powers, Paul E. Rose,

Stephen Schneider, Susan A. Tomlinson, Yan-Yan Tudor, Susan M. Turci, Andrew A. Welcher, Ryan D. White, Huilin Zhao, Li Zhu, and Xiaotian Zhu Discovery of Aminoquinazolines as Potent, Orally Bioavailable Inhibitors of Lck: Synthesis, SAR, and in Vivo Anti-Inflammatory Activity. *J Med Chem* **2006,** 49, (19), 5671-5686.

78. Burchata, A. F.; Calderwooda, D. J.; Hirst, G. C.; Holmanb, N. J.; Johnstonb, D. N.; Munschauera, R.; Raffertyb, P.; Tometzkib, G. B., Pyrrolo[2,3-d]pyrimidines Containing an Extended 5-Substituent as Potent and Selective Inhibitors of lck II. *Bioorganic & Medicinal Chemistry Letters* **2000,** 10, (19), 2171-2174.

79. Stachlewitz, R. F.; Hart, M. A.; Bettencourt, B.; Kebed, T.; Schwartz, A.; Ratnofsky, S. E.; Calderwood, D. J.; Waegell, W. O.; Hirst, G. C., A-770041, a novel and selective small-molecule inhibitor of Lck, prevents heart allograft rejection. *The journal of Pharmacology and Experimental Therapeutics* **2005,** 315, (1), 36-41.

80. Tewari, K.; Walent, J.; Svaren, J.; Zamoyska, R.; Suresh, M., Differential requirement for Lck during primary and memory CD8+ T cell responses. *Proc Natl Acad Sci U. S. A* **2006,** 103, (44), 16388-16393.

81. Goldman, F. D.; Ballas, Z. K.; Schutte, B. C.; Kemp, J.; Hollenback, C.; Noraz, N.; Taylor, N., Defective expression of p56lck in an infant with severe combined immunodeficiency. *The Journal of Clinical Investigation* **1998,** 102, (2), 10-15.

82. Collette, Y.; Dutartre, H.; Benziane, A.; F, R.-M.; Benarous, R.; Harris, M.; Olive, D., Physical and functional interaction of Nef and Lck. HIV-1 Nef-induced T-cell signaling defects. *The Journal of Biological Chemistry* **1996,** 271, (11), 6333-6341.

83. Caflisch, A.; Miranker, A.; Karplus, M., Multiple copy simultaneous search and construction of ligands in binding sites: application to inhibitors of HIV-1 aspartic proteinase. *J Med Chem* **1993,** 36, (15), 2142-2167.

84. Ozkan, S. B.; Meirovitch, H., Efficient Conformational Search Method for Peptides and Proteins: Monte Carlo Minimization with an Adaptive Bias *J. Phys. Chem.* **2003,** 107 (34), 9128 -9131.

85. Miranker, A.; Karplus, M., Functionality maps of binding sites: a multiple copy simultaneous search method. *Proteins: Struct, Funct, and Genet* **1991,** 11, (1), 29-34.

86. Halgren, T. A., Merck molecular force field. III. Molecular geometries and vibrational frequencies for MMFF94. *J Comput Chem* **1996,** 17, 553-586.

87. Saunders, M., Stochastic search for isomers on a quantum mechanical surface. *J Comput Chem* **2004,** 25, 621-626.

88. Saunders, M., Stochastic exploration of molecular mechanics energy surface: Hunting for the global minimum. *J Am Chem Soc* **1987,** 109, 3150-3152.

89. Wilchek, M., My life with affinity. *Protein Science* **2004,** 13, 3066-3070.

90. Vieth, M.; Sutherland, J. J.; Robertson, D. H.; Campbell, R. M., Kinomics: characterizing the therapeutically validated kinase space. *Drug Discovery Today* **2005,** 10, (12), 839-846.

91. Cohen, M. H.; Dagher, R.; Griebel, D. J.; Ibrahim, A.; Martin, A.; Scher, N. S.; Sokol, G. H.; Williams, G. A.; Pazdur, R., U.S. Food and Drug Administration Drug Approval Summaries: Imatinib Mesylate, Mesna Tablets, and Zoledronic Acid *Oncologist* **2002,** 7, 390-392.

92. Penne, K.; Bohlin; Schneider, C.; Daniels, S., Gefitinib (IressaTM, ZD1839) and Tyrosine Kinase Inhibitors: The Wave of the Future in Cancer Therapy. . *Cancer Nurs* **2005,** 28, (6), 481-486.

93. Baki, A.; Bielik, A.; Molnár, L.; Szendrei, G.; Keserü, G. M., A high throughput luminescent assay for glycogen synthase kinase-3β inhibitors. *ASSAY and Drug Development Technologies* **2007,** 5, (1), 75-84.

94. Greenbaum, D. C.; Baruch, A.; Grainger, M.; Bozdech, Z.; Medzihradszky, K. F.; J, J. E.; DeRisi, J.; Holder, A. A.; Bogyo, M., A role for the protease falcipain 1 in host cell invasion by the human malaria parasite. *Science* **2002,** 298, (5600), 2002-2006.

95. Petricoin, E. F.; Ardekani, A. M.; hITT, b. a., Use of proteomic patterns in serum to identify ovarian cancer. *Lancet* **2002,** 359, 572-577.

96. Nishizuka, S.; Chen, S. T.; Gwadry, F. G., Diagnostic markers that distinguish colon and ovarian adenocarcinomas: identification by genomic, proteomic, and tissue array profiling. *Cancer Res* **2003,** 2003, (63), 5243-5250.

97. Adam, G. C.; Cravatt, B. F.; Sorensen, E. J., Profiling the specific reactivity of the proteome with non-directed activity-based probes. *Chem Biol* **2001,** 8, 81-95.

98. Ballell, L.; Alink, K. J.; Slijper, M.; Versluis, C.; Liskamp, R. M. J.; Pieters, R. J., A new chemical probe for proteomics of carbohydrate-binding proteins. *ChemBioChem* **2004,** 6, (2), 291-295.

99. Pohl, N. L., Functional proteomics for the discovery of carbohydrate-related enzyme activities *Current Opinion in Chemical Biology* **2005,** 9, (1), 76-81.